TECHNICAL REPORT STANDARD TITLE PAGE

1. Report No.	2. Government Accession No.	3. Recipient's Catalog No.
FHWA/TX-91+556-4F		

4. Title and Subtitle	5. Report Date
THE PERFORMANCE OF A PRESTRESSED CONCRETE PAVEMENT	November 1989
	6. Performing Organization Code

7. Author(s)	8. Performing Organization Report No.
Elliott Mandell, Jose Tena-Colunga, Kenneth Hankins, Ned H. Burns, and B. Frank McCullough	Research Report 556-4F

9. Performing Organization Name and Address	10. Work Unit No.
Center for Transportation Research The University of Texas at Austin Austin, Texas 78712-1075	11. Contract or Grant No. Research Study 3-10-88/9-556
	13. Type of Report and Period Covered Final
12. Sponsoring Agency Name and Address Texas State Department of Highways and Public Transportation; Transportation Planning Division P. O. Box 5051 Austin, Texas 78763-5051	14. Sponsoring Agency Code

15. Supplementary Notes

Study conducted in cooperation with the U. S. Department of Transportation, Federal Highway Administration. Research Study Title: "Prestressed Concrete Pavement (PCP) Overlay on IH35 in McLennan County"

16. Abstract

Concrete pavements are in constant motion due to daily and seasonal thermal cycles. These thermal cycles cause concrete pavement slab ends to undergo both horizontal and vertical movement. This movement is subjected to wheel and gravity loads, and this develops stresses in the concrete. The amount of movement and stress determines the ultimate serviceability of the concrete pavement. Since PCP slabs are relatively long, the longitudinal and vertical movement are significant and must be considered in design. In 1985 approximately one mile of PCP pavement, consisting of a group of sixteen test slabs, was placed to verify the design by collecting and studying the performance data on these test slabs.

This report describes in detail the instrumentation techniques used in the collection of the horizontal and vertical displacements, the associated climatic changes, non-destructive deflection tests and analyses, the background and theory of the analytical models, and the calibration of the models.

17. Key Words	18. Distribution Statement
concrete, prestressed concrete, pavements, instrumentation, vertical thermal movement, horizontal thermal movement, deflection test	No restrictions. This document is available to the public through the National Technical Information Service, Springfield, Virginia 22161.

19. Security Classif. (of this report)	20. Security Classif. (of this page)	21. No. of Pages	22. Price
Unclassified	Unclassified	100	

Form DOT F 1700.7 (8-65

THE PERFORMANCE OF A PRESTRESSED CONCRETE PAVEMENT

by

Elliott Mandel
Jose Tena-Colunga
Kenneth Hankins
Ned H. Burns
B. Frank McCullough

Research Report Number 556-4F

Research Project 3-10-88/9-556

Prestressed Concrete Pavement (PCP) Overlay on IH35 in McLennan County

conducted for

Texas State Department of Highways and Public Transportation

in cooperation with the

**U. S. Department of Transportation
Federal Highway Administration**

by the

CENTER FOR TRANSPORTATION RESEARCH

Bureau of Engineering Research

THE UNIVERSITY OF TEXAS AT AUSTIN

November 1989

The contents of this report reflect the views of the authors, who are responsible for the facts and the accuracy of the data presented herein. The contents do not necessarily reflect the official views or policies of the Federal Highway Administration or the State Department of Highways and Public Transportation. This report does not constitute a standard, specification, or regulation.

There was no invention or discovery conceived or first actually reduced to practice in the course of or under this contract, including any art, method, process, machine, manufacture, design or composition of matter, or any new and useful improvement thereof, or any variety of plant which is or may be patentable under the patent laws of the United States of America or any foreign country.

PREFACE

This report is concerned with the performance of Prestressed Concrete Pavement (PCP) placed on IH 35 in McLennan County, Texas, in 1985. The report reviews the design, layout, and construction of the PCP sections originally treated in Research Project 3-8-84-401, "Prestressed Concrete Pavement Design". The report then explains the instrumentation and techniques used in the collection of performance information, describes and evaluates the data collected, examines the background and theory of analytical models for PCP, and calibrates the PCP model. Design recommendations are offered and discussed, along with recommendations for further study.

This work is the final report for Research Project 3-10-88-556, entitled "Prestressed Concrete Pavement Overlay." The research was conducted using the resources and facilities of the Center for Transportation Research at The University of Texas at Austin. The research was sponsored jointly by the Texas State Department of Highways and Public Transportation and the Federal Highway Administration under an agreement with The University of Texas at Austin and the Texas State Department of Highways and Public Transportation.

The authors express thanks to District 9 personnel (Waco), particularly Mr. Bill Wiese, and to the Transportation Planning Division personnel, especially Mr. Steve Golding, all with the Texas State Department of Highways and Public Transportation.

Thanks are given to the Center for Transportation Research personnel who processed and produced this report.

LIST OF REPORTS

Report No. 556-1, "Performance Tests On a Prestressed Concrete Pavement—Presentation of Data," by Elliott Mandel, Jose Tena-Colunga, and Kenneth Hankins, presents information found in the the literature search, reviews the parent project, and presents the volumetric, thermal, and deflection data collected in the subject project.

Report No. 556-2, "Prestressed Concrete Pavement: Instrumentation, In-Situ Behavior, and Analysis," by Elliott David Mandel, Ned H. Burns, and B. Frank McCullough, presents the instrumentation techniques used to collect field data, presents the final results of the horizontal displacement data, and addresses the accuracy and consistency of the data. The report then presents an analytical model for horizontal displacements and stresses, describes the calibration of the model, and shows the results of a parametric study using the model.

Report No. 556-3, "Analysis of Curling Movements and Calibration of PCP Program," by Jose Antonio Tena-Colunga, B. Frank McCullough, and Ned H. Burns, presents the final results of a vertical displacement data, reviews the analytical model PSCP-1, and describes the calibration of the model with the collected field data.

Report No. 556-4F, "The Performance of a Prestressed Concrete Pavement," by Elliott Mandel, Jose Tena-Colunga, Kenneth Hankins, Ned H. Burns, and B. Frank McCullough, reviews the design layout and construction of the PCP sections, explains the instrumentation and techniques used in the collection of performance information, describes and evaluates the data collected, reviews the background, theory, and calibration of the analytical models, and describes the deflection analysis.

ABSTRACT

Concrete pavements are in constant motion due to daily and seasonal thermal cycles. These thermal cycles cause concrete pavement slab ends to undergo both horizontal and vertical movement. This movement is subjected to wheel and gravity loads, and this develops stresses in the concrete. The amount of movement and stress determines the ultimate serviceability of the concrete pavement. Since PCP slabs are relatively long, the longitudinal and vertical movement are significant and must be considered in design. In 1985 approximately one mile of PCP pavement, consisting of a group of sixteen test slabs, placed to verify the design by collecting and studying the performance data on these test slabs

This report describes in detail the instrumentation techniques used in the collection of the horizontal and vertical displacements, the associated climatic changes, non-destructive deflection tests and analyses, the background and theory of the analytical models, and the calibration of the models.

KEY WORDS: Concrete, prestressed concrete, pavements, instrumentation, vertical thermal movement, horizontal thermal movement, deflection test

SUMMARY

This the fourth and final report of Research Project 3-10-88-556, "Prestressed Concrete Pavement Overlay." The first report, 556-1, presented the data collected on the project and explained the collection techniques. The second report, 556-2, described the instrumentation, treated the horizontal thermal movement, and used an analytical model to study the PCP. The third report, 556-3, treated the vertical movement (curl) and calibrated the analytical model, PSCP-1. This report reviews the design and construction, and previous associated studies. This report also assimilates and summarizes the information included in the previous reports, performs additional analyses, reports the pavement deflection studies, and makes recommendations.

An examination of the PCP shows the pavement is performing very well. A few longitudinal cracks have formed, but only two transverse cracks were found after about four years of service. The joints appear to be performing very well and almost no cracking or distress has occurred at the joints.

IMPLEMENTATION STATEMENT

The initial design and construction recommended for the PCP near Waco was based on previous work and reports from others in the nation. It is believed that the work in this project has shown the benefits and deficiencies of new design and construction techniques that will assist future PCP projects. The collection of data in this study, and the resulting calibration of the previously developed computer model, was used to determine the behavior and expected performance of prestressed concrete overlays. The monitoring of the test sections permitted a calibration of models, resulting in the verification and development of design procedures. The investigations also assisted in the identification of the most effective construction procedures.

TABLE OF CONTENTS

CHAPTER 1. INTRODUCTION

The efforts of Research Project 3-10-88-556, "Prestressed Concrete Pavement Overlay," have been recorded in four reports. This report is the fourth and final report for the project. In addition to providing additional data and analysis, this report summarizes several tasks performed as a part of the project. This report is also directly related to previous work in Texas. Because of the multiplicity of the effort, the flow chart on page 2 was prepared to permit a ready reference to the work performed in this project and past projects. Report 556-1 contains the data collected in the subject project (Ref 1); Report 556-2 has a detailed analysis of the horizontal movements of the slabs (Ref 2); Report 556-3 has the detailed analysis of the vertical (curl) movements (Ref 3); and this subject report, 556-4F, has a pavement deflection analysis and a synopsis of the previous reports. Reports from previous related projects are discussed in the following chapters.

BACKGROUND

A proposed report of ACI Committee 325 (Ref 4) defines prestressed concrete pavement as follows:

> Prestressed concrete pavements are those which compressive forces have been introduced on the concrete sections during construction, to prevent or decrease tensile stresses in the concrete during service.

Prestressed pavements have several advantages over other more conventional types of reinforced pavements, including the following (Ref 5):

(1) Important savings in materials. Stresses in rigid pavements are produced mainly by the combined effect of wheel loads, warping, thermal curling, and frictional drag produced by thermal contraction. The thickness of conventional reinforced pavements is designed based on the maximum flexural stress produced by wheel loads. For this reason, conventional pavements must be relatively thick to resist flexural tension failure. Additional demands on the tensile strength resulting from friction stresses, warping, and curling are met by constructing shorter slabs.

In prestressed pavements, advantage is taken of the fact that concrete is much stronger in compression than in tension. Therefore, precompression is introduced in the pavement to reduce the tension levels. Research on PCP has shown that moisture gradients through the pavement cross section also produce a favorable prestress distribution. This gradient induces higher precompression at the bottom of the slabs (Ref 6). This higher precompression in the bottom is cumulative with the inherent flexural strength of the concrete. The result is an increase in stress range in the flexural zone. These factors taken together make possible the design of a thinner pavement, and the result is a reduction in the amount of concrete and reinforcing steel.

(2) Improved performance. The thickness of conventional reinforced pavements is designed with little regard for crack prevention. Enough section thickness is allowed only for performance during the design period. To reduce tensile stresses caused by friction, warping, and curling, and to minimize cracking, joints are built relatively close together.

With prestressed pavements, cracking is minimized by prestressing. Longer slabs can then be built and the number of transverse joints is reduced. Cracking and joints are major causes of distress and failure of the rigid pavements. The reduction of cracks and joints leads to a pavement with high potential for providing a low-maintenance, improved-performance, and longer-lasting roadway, as compared with conventional concrete pavements.

(3) Increased load-carrying capacity. The remarkable increase in load resistance, as proved by prestressed pavements on load tests (Ref 7), supported with results from actual highway and airport projects (Ref 8), has attracted attention. This increase in load resistance is explained largely by a favorable prestress distribution. This distribution is a product of the naturally existing moisture differentials between the tops and the bottoms of the pavement slabs (Ref 6).

(4) Improved protection to the supporting layers. The elimination of a large percentage of transverse joints and the reduction of cracking in the road surface has two results. First, there is a reduction in moisture below the slab due to rainwater flowing down the cracks and joints. Second, there is generally better protection of the road foundation.

Past prestressed projects have included two types of slabs: continuous and separate. In the continuous type the stress is applied by using hydraulic jacks between abutments and the slabs being stressed. An option is to do the prestressing between the slabs themselves. Therefore, the slabs are continuous in the sense that expansion joints are not supplied. The use of jacks results in gaps that are subsequently filled. Pavements built under this system are also called post-stressed pavements. With the separate type of slab, the prestress is applied in each slab independent of the other slabs. The stressing is accomplished with high tensile strength cables post-tensioned after the concrete has hardened. The post-tensioning operations can be conveniently done at the slab ends in short gaps left between the long prestressed elements. Next, the gaps are filled with a short filler slab. A individual joint at each end of the filler slab is supplied. A version of the separate type of slab uses interior jacking pockets. The

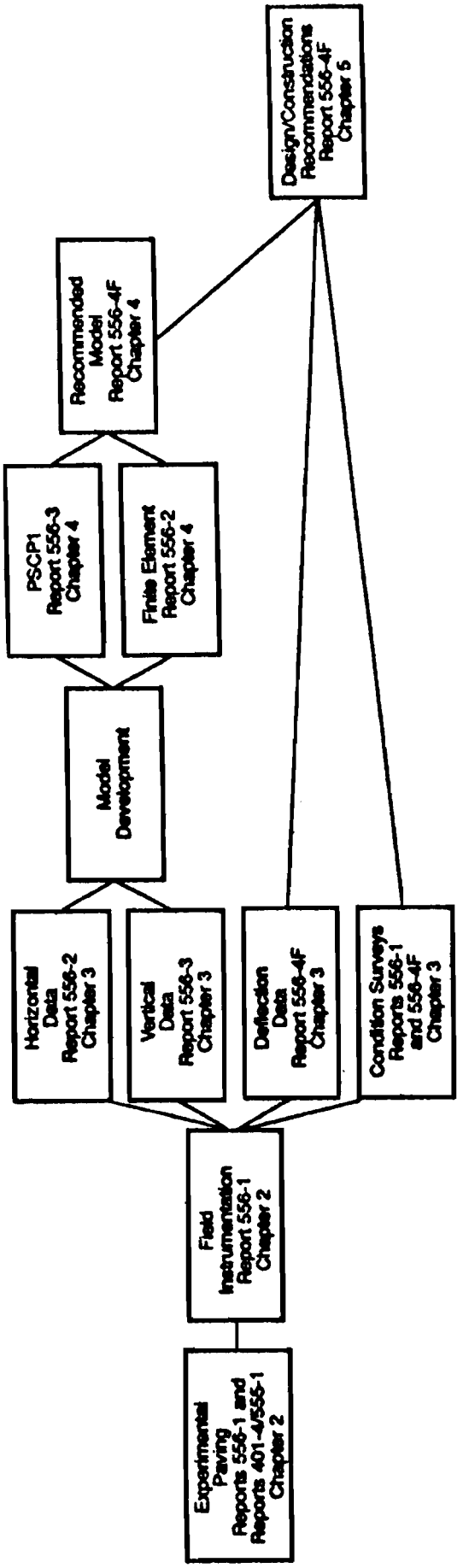
Experimental Paving
Reports 556-1 and
Reports 401-4/555-1
Chapter 2
Field
Instrumentation
Report 556-1
Chapter 2
Horizontal
Data
Report 556-2
Chapter 3
Vertical
Data
Report 556-3
Chapter 3
Deflection
Data
Report 556-4F
Chapter 3
Condition Surveys
Reports 556-1
and 556-4F
Chapter 3
Model
Development
PSCP1
Report 556-3
Chapter 4
Finite Element
Report 556-2
Chapter 4
Recommended
Model
Report 556-4F
Chapter 4
Design/Construction
Recommendations
Report 556-4F
Chapter 5

post-tensioning of cables can be conveniently done at the center of the slabs in jacking pockets (Ref 7). This was shown by the construction of a nearly one-mile-long experimental highway section in Texas (Ref 1).

With either type of slab, the pavement may be prestressed, whether only in the longitudinal or in the longitudinal and transverse directions. In the individual type, cables for prestressing have been used in a variety of patterns: longitudinal, transverse, and at angles with respect to the centerline. The use of transverse prestressing is of importance to the resisting of applied wheel loads, the preventing of longitudinal pavement cracking, and the widening of the longitudinal construction joint between lanes. The use of prestressing in both directions is very convenient in highway pavements, though conventional reinforcement may be sufficient in the transverse direction. Airport pavements are typically prestressed in both directions. The reason for this two-dimensional prestress is that traffic load stresses are of the same magnitude in both directions.

PREVIOUS HISTORY OF PRESTRESSED PAVEMENT

The concept of prestressed pavement originated in Europe over 40 years ago, where it found applications in airfields and highways. Prestressed pavements have been researched in England and France since 1943 (Ref 9). Before 1960, nearly 60 prestressed projects were built, most of them having experimental sections. These projects completed a total of 13 miles of prestressed pavement in highways and 20 miles in airports (Ref 10). One highway and six airport pavements were built in the United States. Slab lengths ranged from 170 feet to 700 feet, with an average of 400 feet. The prestressing technique included the continuous and the individual types of slab. Longitudinally applied prestress in individual slabs ranged from 190 to over 700 psi. Transverse prestress was used in one-half of the highway and on all of the airport projects, ranging from 0 to over 400 psi in the various slabs. The pavement thicknesses averaged 5-3/4 inches for highways and 6-1/2 inches for airports. During the 1960's, very few prestressed pavements were built in the U.S. In contrast, substantial mileage comprised of prestressed runways and taxiways was placed in Europe and resulted in excellent performance. Until the 1960's, achieving a relatively high magnitude of prestress was difficult and expensive. Both facts discouraged the widespread construction of PCP for highways. Design methods were of a mainly empirical nature.

Since the 1960's, several hardware developments and construction practices have favored the use of PCP in the United States. Among these developments are:

(1) The use of plastic-encased, grease-protected, high-strength 7-wire strands in structural prestressing.

(2) The use of combined bearings and strand chucks, which permits easy placement of the post-tensioned strand anchors that firmly grip the strand.

(3) The development of low-friction mediums between the subbase and the pavement. A reduction in friction between the subbase and pavement has permitted slabs to be constructed in lengths up to 800 feet. Simultaneously, the low-friction medium diminishes the prestress reductions resulting from frictional resistance. Double layers of thin plastic membranes have resulted in friction coefficients of less than 0.2, although these values are difficult to get in normal construction.

During the 1970's, new ideas were incorporated on several experimental projects conducted in the USA. These projects include a service road at the Dulles International Airport in Virginia (Ref 11) and three full-scale highway projects in Pennsylvania (Ref 12), Mississippi (Ref 13), and Arizona (Ref 14). Table 1.1 summarizes some features of these demonstration programs. The research report FHWA/RD-82/169 describes the performance of prestressed pavements as observed in four states (Ref 15).

The Portland Cement Association in 1983 developed a computer program called PCP, as described in the report FHWA/RD-82/091 (Ref 16). PCP differs in several respects from the program which was calibrated in the present study. The program calibrated herein is called PSCP1 to avoid confusion with the PCA program.

TABLE 1.1. MOST RECENT PRESTRESSED PROJECTS IN THE USA

	Location			
Description	**Dulles (Virginia)**	**Harrisburg (Pennsylvania)**	**Brookhaven (Mississippi)**	**Tempe (Arizona)**
Length (ft)	400-760 sections	600 sections	450 sections	400 sections
Year built	1972	1973	1976	1977
Slab thickness (in.)	6	6	6	6
Subbase thickness (in.) and Material type	6; cement treated aggregate	6; Aggregate bituminous base coarse	4; Hot mix bituminous concrete	4; Lean concrete

PCP CONSTRUCTION AND RESEARCH IN TEXAS

Because of interest in the potential of prestressed pavements, the Texas State Department of Highways and Public Transportation (SDHPT) and the Federal Highway Administration (FHWA) sponsored two Demonstration Projects of prestressed concrete pavement overlays. Each demonstration project was planned to result in a construction project on Interstate Highway 35, one mile each in Cooke and McLennan Counties, Texas. The projects were conducted by the Center for Transportation Research (CTR), The University of Texas at Austin, and were designated Projects 1-3D-84-555, "Prestressed Concrete Pavement on IH35, Cooke County," and 1-9D-84-556, "Design of the Texas Prestressed Concrete Pavement, McLennan County," respectively. The work plan for both demonstration projects had four distinct phases: (1) design, (2) construction, (3) monitoring, and (4) reporting. The design step was to include the latest procedures in pavement design and technology. The PCP in McLennan County was built between September and November 1985; however, the construction of the Cooke County project was cancelled because it was considered not to be cost-effective. It was believed that the Cooke County project would not provide additional information, given its similarity with the McLennan County project. However, one report was prepared, "Design of the Texas Prestressed Concrete Pavement Overlays in Cooke and McLennan Counties and Construction of the McLennan County Project" (Ref 7).

Soon after that, the SDHPT and FHWA sponsored an HPR project on the planning and design of prestressed concrete pavement overlays. The activities called for the research and trial of new procedures for PCP design and construction. This work was performed by CTR under Research Project 3-8-84-401, "Prestressed Concrete Pavement Design—Design and Construction of Overlay Applications." Its results are documented in Reports 401-1 to 401-8F (Refs 17 to 23). They encompass the activities from laboratory investigation of fatigue of prestressed concrete to the design recommendations obtained from the first field measurements.

OBJECTIVE

The objective of this report is to summarize the findings of Research Project 3-10-88-556, reported in three separate reports. In addition, this report includes the analysis of deflection information collected on the PCP slabs and presents the latest condition survey data.

SCOPE

Chapter 2 of this report offers a discussion of the factors affecting the performance of PCP. Factors such as environment, materials, ageing, and the interactions of these factors are treated. Chapter 3 provides a description of the experimental sections, the instrumentation, and the field measurement program. Chapter 4 includes the data analysis performed using the measurements collected in the field studies. Chapter 5 describes the mechanistic analysis and the modeling performed on the PCP. Chapter 6 provides a discussion of results. Chapter 7 discusses the input data for the models and contains an example application of the models. Finally, Chapter 8 presents the conclusions and recommendations.

CHAPTER 2. FACTORS AFFECTING THE PERFORMANCE OF PCP

In this chapter, a conceptual review is made of the factors that affect the performance of PCP. For purposes of clarity, the more general factors are discussed first. They are followed by the primary factors in design and the interactions produced. Then, the effect of factors such as environment, materials, and losses in prestress are related to loads. In the final part, the interactions of concrete with steel and of slab with subgrade are discussed.

ENVIRONMENT

The majority of engineering structures, in order to fulfill their purpose, must withstand the aggressive action of nature. Pavement slabs are not an exception. All this action of the environment imposes stresses on the pavement. These stresses add to the external load stresses supported by the structure.

The fact that pavements may crack before any external load occurs shows the important effect that these "secondary," environmental, stresses can impose on the slab. Stresses produced by changes in temperature and by changes in moisture add to those for which the pavement was designed to carry in service. These forces raise the level of stress; therefore they shorten, to different degrees, the fatigue life of the slab. In some occasions, environmental stresses can surpass the strength of the paving concrete, and the result is the cracking of the slab. These cracks can induce a loss in load transfer to different degrees if corrective factors are not included in the design.

The environment can be characterized in terms of moisture and temperature as its principal agents. They induce changes in materials slowly. The continuous actions of moisture and temperature transmit the gradients of the climatic change of the region to the pavement. Then, the slab is affected because of the physical and chemical changes being reflected gradually in the volumetric and mechanical stability of the pavement. The soil is also affected by physical and chemical changes. However, its morphology allows the measurement of variations only in the mechanical behavior. These changes follow a cyclical pattern. The combination of pavement and soil changes produces a set of conditions which could be somewhat different from those assumed for the pavement design.

MOISTURE

Moisture can be considered as the main environmental description for each climate considered in pavement design. Water is present in the yearly cycle in its three states: liquid, vapor, and ice. Liquid and ice are the forms of water that have a major effect on pavement performance. Concrete slabs are subjected to a water transient cycle, and they expand or contract as a result. The amount and state of water present varies throughout the year. Clay soils harden or soften when water leaves or enters them. Heave results when water freezes in the soil layers or expansive soils are encountered. The softening or movement of the soil and the contraction of the slab usually introduce higher stresses in the pavement. Conditions for pavement performance improve when the subgrade soil hardens and the slab expands. The phenomena derived from the presence of water in pavements are curling and warping. In the case of soils, the effects are frost heave and thawing. These problems are discussed later in this chapter.

TEMPERATURE

Sun is the main source of heat for our planet. At any location, the effect of temperature is proportional to two factors: the area exposed to the heat source and the coefficient of heat transfer of the material. Highway structures have large surfaces exposed to the environment. The structure is subjected to temperature variations and solar radiation by absorbing heat energy from the sun. Soils are, likewise, subjected to sun rays and temperature exchange. In this way, a system for heat exchange is formed. The active source of energy is the sun, and a second (passive) source is the soil. Soil plays the role of a "thermic battery" and the pavement constitutes the interface for the exchange of heat with the environment. An illustration of this system is in Fig 2.1. A general statement could be that radiation absorption causes the expansion of materials. Similarly, the transfer of this heat to the environment has the opposite effect. Since temperature changes follow a cyclic pattern, pavement slabs are subjected to daily and seasonal variations. Generally, the principles of thermodynamics apply to the rate of heat exchange.

Concrete and steel have similar coefficients of expansion, which makes it possible to use steel as a reinforcement of concrete. However, some stresses are introduced. An increase in the slab temperature has different effects in PCP. A temperature increase causes concrete and steel to expand, and the first effect is the strain of concrete resulting from subbase friction. This strain is detrimental for concretes because the concrete cracks when the stress exceeds the strength of the material. This is true especially at early ages when concrete has not developed its full strength.

For prestressed slabs, a second effect is an increase in the prestress. This expansion raises the level of stresses that pavement can bear, but this gain is somewhat diminished by the give in the prestressing due to expansion of the strands.

Soil is affected by temperature, too. It is important not because of its direct effect but because of the changes it introduces in soil moisture. Temperature modifies the moisture content in soils. This modification changes the mechanical properties of the soil and the level of stress developed in the pavement.

The combined result of an increase in temperature is an improvement of the bearing capacity, but, because of differences in expansion between the materials, the result is internal stresses and losses in efficiency. Mainly, these effects are due to friction.

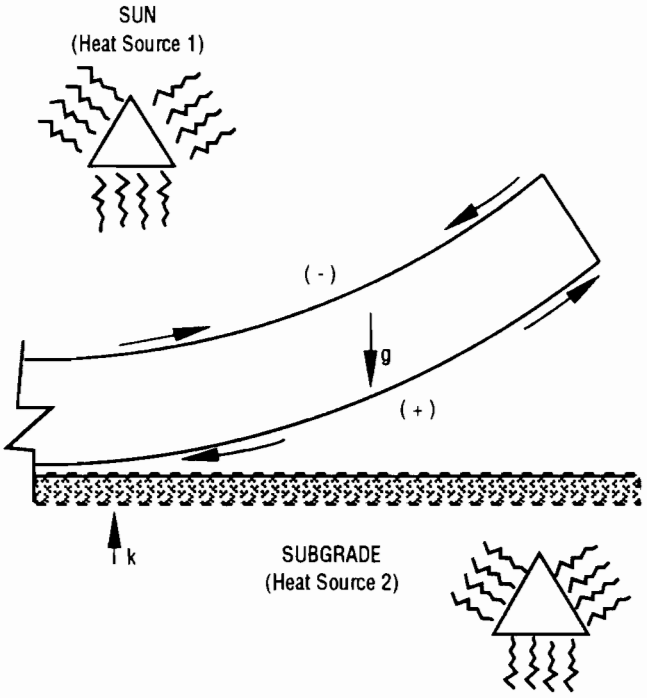

(a) Slab representation.

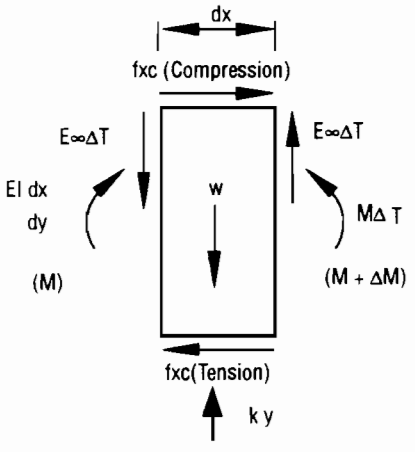

(b) Free-body diagram of forces.

Fig 2.1. Schematic representation of warping and curling.

DAILY VARIATIONS PATTERN

As noted earlier, the daily temperature variations in the pavement are determined by heat gained and lost, plus other climatic conditions. This imposes a pattern for the daily changes in pavement slabs. In this pattern, the temperature rises after sunrise and reaches its peak in midafternoon. Then, it decreases to reach its low at dawn. This is illustrated in Fig 2.2. This cyclical behavior produces periods of expansion and contraction under different service periods of the structure. In terms of the bearing conditions for the structure, we see that (a) expansion happens during the hours of major traffic volume and (b) contraction takes place at night, with a lesser volume of vehicles. Therefore, these conditions are generally favorable for portland cement concrete pavements.

SEASONAL VARIATIONS PATTERN

Besides the number of hours of solar energy, the other prevailing factor is the amount of sunrays received in that interval. This is a function of the relative position of and distance to the sun. The former relates to the location of the pavement with respect to earth latitudes. Both hours and intensity of sunrays determine the seasons, and peaks in temperature vary for each season. Lower temperatures and ranges in temperature occur during winter, and higher values are found in the summer. This is depicted in Fig 2.2.

In summary, environment can be characterized in terms of moisture and temperature. Moisture and temperature are affected by the daily and seasonal cycles of our planet. All these factors produce a new set of conditions for pavements in a repetitive fashion. In this way, environment affects the behavior of the pavement.

CHARACTERISTICS OF THE MATERIALS

Description of the relative characteristics and properties of materials is a necessary step in engineering. In this study a review of the materials' characteristics was necessary for the delineation and review of a model. Therefore, a brief analysis of materials used in PCP is offered to enable a better comprehension of the materials interaction in this study.

Prestressed Concrete Pavements are composite materials. That is, the behavior of the structural unit varies from the behavior of the materials of which the pavement is composed. Nonetheless, composite materials reflect in part the behavior of each one of the structure's components. The influences of one constituent can be predominant over those of the others within a certain range. In this way, the change in one constituent can modify the behavior of PCP in that range. Thus, separate reviews of the concrete and steel are important.

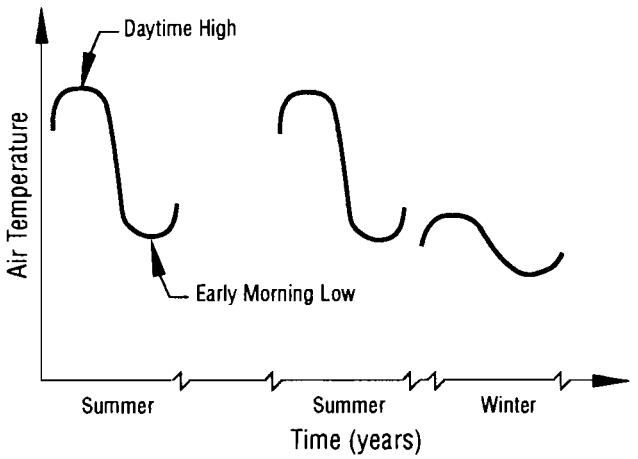

Fig 2.2. Conceptual scheme – daily temperature cycles for various seasons.

CONCRETE

It is well known that concrete has a good set of mechanical properties. These properties are diminished only by poor performance in tension and flexure. It is worthwhile to note that flexural behavior of concrete is important for pavements and slabs. Another characteristic of concrete is that it does not have high strength at early ages and there is a strength gain with time.

For this study, the structural behavior of concrete is reviewed. The focus is on the mechanical properties that are of importance in modeling. Also, comments are made on porosity, warping, curling, shrinkage, and ageing.

The hardening process of the cement matrix is important. The strength of the matrix is the final result. The principal factors in the hardening process are porosity, chemical composition, fineness of the cement, moisture, and temperature. These factors establish the difference between a well-developed homogeneous matrix and a poor matrix, that is, a matrix with poor hydration, fiber length, excessive porosity, etc.

Structural Behavior. The main function of concrete as a paving material is to provide a smooth-riding, durable surface in all weather. The concrete should be capable of bearing the loads to which it is subjected and dissipating the loads to the soil of the roadbed. Concrete has a brittle structure; that is, it can not undergo large deformations. Consequently, it accomplishes the dissipation of the stresses by means of the rigidity of its microstructural limits. Knowledge of the development of the modulus of elasticity and the strength with time is necessary for the analysis of concrete performance.

Strength Development. Many of the strength properties of concrete normally develop in a period of 28 days; the rate of strength gain after it has reached 28 days is slower. The gain in strength practically never stops, and so concrete is stronger and more brittle with time.

The development of the strength in concrete has been studied and is well documented. Curves have been determined for the strength gain at different ages up to its design age. The most widely known are the curves published by the portland cement concrete service organizations. However, the job curve is different from the theoretical curve in each case. Factors such as type, composition, and fineness for cement, as well as the design, admixtures, and curing of the mix, affect the rate of strength development.

For example, the rate of strength gain is higher the finer the cement grind. Other results of higher fineness in cements are higher shrinkage and lower level of hydration.

Moisture is of prime importance in the first stage of the hardening of the cement. It provides the water for the continuous hydration process, and the hydration hardening of the cement ends when it dries. When the dimensions of the specimen are regular, this effect is of no consequence: the water in the mix gives the surface a certain "replenishing." However, where there are layers of concrete, such as in slabs, this effect does not take place, and the degree of hydraulic hardening developed is limited.

Modulus of Elasticity. The gain in the modulus of elasticity is parallel to the gain in strength, but the modulus is also affected by the factors already mentioned. The determination of the modulus is not as simple as the determination of the compressive stress. Therefore, several related items have been studied in the determination of the modulus of elasticity.

The compressive strength and modulus of concrete have been related to the values of flexural strength. Parameters such as porosity, creep, and shrinkage do not have an experimentally measured relationship with flexural strength. However, they can be associated in terms of the common trends observed.

There are strong indications that the tensile strength of concrete is not limited by compressive stress. It appears that a tensile strain determines the strength of concrete. Under static loading this strength is usually assumed to be between 10,000 and 20,000 psi. It has been found that at the point of initial cracking the strains in beams and cylinders correlate. The strains on the tension face of a beam in flexure are of the same magnitude as the lateral tensile strains in a cylinder in uniaxial compression.

Therefore, the relationship between flexural strength and the modulus of elasticity is direct. It follows that relatively higher values of flexural strength occur when values of the modulus of elasticity increase.

Neville (Ref 24) says,

> Poisson's ratio varies generally between about 0.11 for high strength concrete and 0.21 for

weak mixes, and it is significant that the ratio of the normal tensile and compressive strengths for different concretes varies in a similar manner and between about the same limits. There is a possibility of a connection between the ratio of nominal strength and Poisson's ratio, and there are good grounds for suggesting that the mechanism producing the early cracks in uniaxial compression and in flexure tension is the same.

Porosity. Porosity affects concrete in two aspects: strength and permeability. In turn, these variables affect the flexural capacity reliability and the occurrence of warping in the slab.

Porosity has a direct relationship with the water/cement ratio. The total amount of pores is the sum of gel pores and capillary pores. Recent studies (Ref 25) indicate the relationship between the final stress in the cement and the pores is:

$$f = f_o \exp(-B_s P) \quad \text{for low porosities,} \qquad (2.1.a)$$

$$f = f_o (1 - P)^A \quad \text{for high porosities, and} \qquad (2.1.b)$$

$$E = E_o \exp(-b_E P) \quad \text{for the modulus of elasticity} \qquad (2.2)$$

where f_o and E_o are the stress and modulus of elasticity value for zero porosity, P is the value of porosity, and A, B_S, and b_E are constants.

Finally, the compressive strength is higher with a low-porosity, better-crystallized structure. This structure must exhibit good linkage, forming a mat. At the microstructural level, flexural strength seems to be a function of the development of interlocking between and within the mats. Then, flexural strength will improve with the better development of the crystalline needles and the reduction of weak planes.

Shrinkage and Creep. The interaction between flexural strength and the related properties has not been researched deeply. At this point, only general observations have been reported by investigators. They cover properties as diverse as porosity, impact strength, creep, and shrinkage. However, this meager information is useful when we think of concrete as an integral unit, a unit that must fulfill a series of different purposes.

The most important quality of a dense, plastic mix is a good, long-lasting concrete or a concrete with good durability and structural serviceability. Shrinkage and creep in concrete are closely related. Studies of the effect of accelerators in concrete (Ref 25) have linked these admixtures to changes in the microstructure and to higher susceptibility to moisture conditions. The effect of microcracking on the creep rate has also been addressed. Studies point out that creep happens with a mechanism of shear slippage along the microcrystalline sheets in the presence of interlayer water, viz., microcracking, bond breaking, and reforming. Therefore, there is a direct link between tensile strength, shrinkage, and creep. Then, good tensile and flexural levels in concrete are accompanied by low shrinkage and creep.

WARPING AND CURLING

Curling and warping are similar phenomena. They produce similar effects in the slab. They are originated by the environment. The main difference between them is the driving force. Curling is caused by a temperature differential, and warping is mainly the result of a moisture differential.

Concrete is a permeable material, and this permeability increases with a higher water/cement ratio. Water can get in through the material from external sources and then leave through evaporation. In pavements, water can be evaporating from the top surface while the bottom stays almost saturated. This effect was observed by Fridberg in tests with short pavement slabs at Rolla (Ref 26). In these experiments, the bottom parts of the slabs were near full saturation, whereas the top portions showed lower contents most of the time. This moisture differential tends to induce warping deformation that is restrained to different degrees by the forces induced by the slab's own weight. This restraining effect is higher towards the slab interior. This is illustrated in Fig 2.3.

The warping stresses toward the center of the slab produce compressive stresses along the bottom of the slab, introducing factors beneficial for the pavement in resisting wheel loads. The difference in moisture within the slab depends on local environmental conditions and the characteristics of the concrete.

Curling is produced by the difference in temperature between the top and the bottom of the slab, because of the relatively poor heat conductivity of the concrete. Curling in slabs has been recognized since 1935 when Teller and Sutherland (Ref 27) measured the deflections at pavement ends, edges, and corners that were induced by temperature gradients between the top and bottom of a concrete slab. A difference in temperature could cause the slab to be cooler on the surface and warmer at the bottom. This effect happens when the subgrade is the source for heat and the air temperature is cold. With this, curl would result because the top of the slab has less volume than the bottom of the slab. The contrary effect could occur when the sun rays supply the source of heat to the slab surface.

Along with the cement matrix, aggregates are a major contributor to the physical properties of concrete. As a result, curling is affected by the insulating characteristics of the aggregate in the mix. The curling effect is more pronounced as these insulating characteristics increase. In pavements, the temperature differential between the top and the bottom of the slab is important. A low rate of

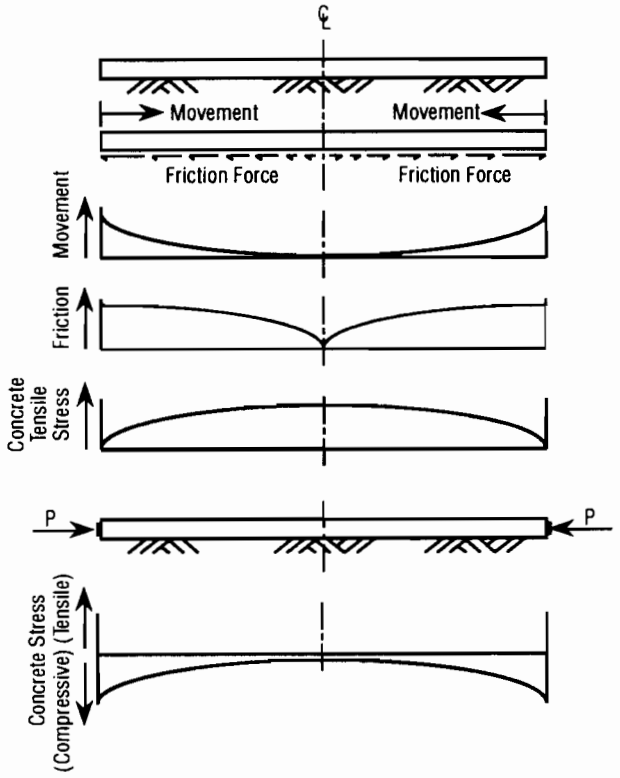

Fig 2.3. Effect of frictional resistance on movements and stresses in the slab for temperature decreases.

thermal change happens in the subgrade, while fast changes occur on the surface.

Therefore, forces induced by curling and warping of pavement slabs depend mainly on the moisture and temperature differentials developed between the top and the bottom of the pavement.

Ageing. The term "ageing" is usually related to decay. However, a well-designed structure should fulfill the necessary requirements of durability throughout the design life without showing excessive deterioration. Modifications can result from weathering of the material in the structure. In this section, we include all the effects that occur during the normal life of a pavement.

A characteristic of concrete is a continuing strength gain with age, which is produced by chemical changes in the solid phase of the microstructure. This phenomenon occurs in the solid phase and is known as silica polymerization. This change also affects the flexural/compression strength ratio. Thus, it is reasonable to believe the behavior registered in a new PCP is different from that registered years later. In summary, the polymerization of silica occurs at even old ages. Its effects are higher strength and less creep.

Fatigue. When a material fails due to the cumulative action of stress smaller than the elastic limit, the failure is termed a "fatigue" failure. Fatigue happens in concrete as in other materials. Studies have found that this type of failure does not take place if the level of stresses is kept below one-half of the elastic limit. Otherwise, if the applied loads are higher than the established threshold, the number of applications to failure decreases logarithmically. For a given level of stress, the number of applications to failure is smaller the higher the ratio between loading and unloading. The effect of ageing in concrete has not been covered by research in this field of study.

The following statements summarize this review on concrete:

(1) Concrete is a material that keeps developing strength with time.
(2) The gain in strength is at high rates soon after casting but the strength gain decreases with time.
(3) Concrete is unable to withstand environment stresses in its first days.
(4) Factors such as water/cement ratio plus porosity, etc., determine final strength in concrete.
(5) Studies suggest that it is a limiting tensile strength that governs concrete failure.
(6) Under working stress conditions, failure can happen by fatigue of the material.
(7) The different mechanical properties of concrete can be correlated.

STEEL

Steel has been used to assist concrete where tensile stresses occur. In prestressed concrete, the role of steel is even more important. The steel in prestressing allows concrete to withstand higher tensile stresses placing the concrete in compression. Steel reinforcing bars are produced under controlled conditions. Nonetheless, steel also has some peculiarities that need to be reviewed for a better understanding of this material.

The mechanical behavior of steel has two aspects: one shows an elastic behavior, and the second shows an elastoplastic behavior. For PCP, steel is subjected to stresses within its elastic range. Thus, in theory, the prestressing steel will never affect the elastoplastic portion, and the steel will keep its deformation proportional to the stresses. Therefore, if the steel is maintained in the elastic region, the material keeps its properties throughout time. However, there are other factors, such as fatigue, corrosion, and ageing, that affect steel. These factors change the properties of steel, including its level of elastic stress. These factors are discussed later in this chapter.

Steel undergoes creep in the same fashion as concrete. Creep is a time-dependent deformation of a material subjected to a constant stress or load. Creep in steels is a function of the material and the conditions of stress and temperature. Therefore, as time passes, creep must be expected in the steel strands of PCP slabs. Relaxation of steel is another effect caused by the applied prestressing

loads with time. Relaxation is more properly associated with polymers. For steel, relaxation is closely related to creep. However, there is not an elastic recovery of the relaxed portion once the load is no longer applied. Thus, for PCP, a small loss in prestress will occur eventually, resulting from creep and relaxation in the steel.

Three factors that can shorten the life of the prestressed steel in PCP are corrosion, fatigue, and ageing. They are somewhat interrelated. Corrosion in steel has different forms. The form that is best known is corrosion by oxidation of steel. A different type of corrosion is the embrittlement of steel by hydrogen. This happens in steels with a solubility limit above one part per million when the steel is subjected to a constant load for a given period of time. Ageing can also produce embrittlement of steel. In the case of ageing, the embrittlement is due to strain hardening, changes in the microstructure of the material between its grain boundaries, or diffusion of other elements in the structure. Hydrogen embrittlement is a good example of embrittlement due to diffusion. Both ageing and corrosion have measurable effects when combined with fatigue.

For PCP, an elastic procedure, rather than a fatigue approach, has been recommended for designing thickness and the prestress level. Considering the fact that PCP is designed for no cracking, the net tensile stress resulting from wheel loads is relatively small (Refs 28, 29, and 30). Hence, it is argued that fatigue is not a major factor in the design. Since an elastic design method is not sensitive to wheel load repetitions, this method is not considered in this study. Moreover, fatigue is not considered in the elastic criteria. The magnitude of the wheel load stresses over the precompression of prestress is relatively low. However, the cumulative effect of wheel loads may cause an eventual fatigue failure. Failure, as discussed previously, can be accelerated by a combination of corrosion and ageing of steel. It is worth noting that the most innovative design procedures are fatigue-oriented, among them the revised AASHTO method (Ref 31) and the PCA method of design (Ref 32). Finally, these criteria follow the conception of Research Report 401-3 (Ref 17).

SUBBASE

Subbase and base are structural layers in pavements. Their functions are to improve the mechanical and drainage characteristics of the roadbed soil. Because of this, soils with better mechanical properties should be used. Yet, soils are also subjected to seasonal variations in their levels of performance. As stated previously, soil is affected by temperature and rainfall. Temperature modifies moisture and in this way changes the mechanical characteristics of soil. This, in turn, changes the stresses the pavement has to undergo.

The climatic changes introduced by the seasonal pattern affect mainly the soil conditions and, therefore, the pavement. The pavement is affected not only in the range of stresses resulting from cyclical variations but in the actual level of stress applied to the structure. Generally, soils with high contents of clay and very fine soils will be more affected by seasonal changes. The characteristic problems of seasonal climatic changes are expansive soil swelling during the rainy season, frost heave in the cold season, and thawing after the cold season. All of them reduce the performance life of the pavement.

LOSSES IN PRESTRESS DEVICES

During the prestressing operations, losses in prestress take place due to three factors: stressing devices, slippage, and corrosion. The latter refers not to corrosion in the steel strands but in the devices. The other two causes result from the efficiency of the devices and the operations involved in prestressing. These losses must be considered in the design of PCP. Nevertheless, the seatings that occur in lock-couplers in PCP slabs are insignificant and can be ignored. These aspects have been previously considered in Research Project 401 (Ref 22).

The lock-couplers which are available at present permit a loss in prestress before effectively gripping the steel strand. This loss is caused by friction and, as reported in Research Project 401 (Ref 22), was measured to be between 2.5 and 4.2 kips (5 to 10 percent of the total prestress). Depending on the presence of rust and the curling of the strands, these values can be higher.

Therefore, losses in prestress devices must be checked in design and performance models. In this way, the danger of using values which are under-designed is prevented.

TYPE OF PCP LAYOUT

Another important source of prestress losses is in the layout of the slab. The configuration of strands, the type of anchorage, and slab geometry play an important part in design.

STRAND CONFIGURATION

Prestress losses happen because of friction between the strands and the encasing conduit. Friction increases with the strands' length and curvature. The values and other results of the study carried out on this topic are found in Research Report 401-6 (Ref 22). Good practices are (1) the use of central stressing to reduce the effective length and (2) the use of simultaneous stressing. These practices provide a maximum level of stresses in the central portion of the slabs. This is where the stresses are needed. In addition, the strand spacing also has an effect. Smaller strand spacing allows higher stressing levels at early ages.

ANCHORAGE TYPE

Anchorage is critical at the early stages of the pavement life. Strands must be stressed to keep them in position, and stressing should be applied immediately after the concrete is capable of withstanding the forces. This early stressing of PCP is needed to prevent the cracking of concrete during curing. Otherwise, cracks appear on the surface because of slab contraction. The temperature of concrete rises during its early curing. A drop in temperature follows the first hydration reactions of the mix, and the tensile cracking occurs.

The anchorage must be capable of distributing this early stress and the final stress in an effective way. Otherwise, stress concentration will take place. This concentration of stresses will lead to an early failure. The opposite effect comes with good anchorage. Less cracking will be observed when a wider anchorage area is achieved. A more detailed discussion on anchorage and strand losses is given in Research Report 401-6 (Ref 22).

GEOMETRY OF SLAB

The properties derived from the geometry of the structure determine to a large extent the effective use of the materials. The main dimensions of pavement slabs are length, width, and thickness. The latter dimension is determined by the characteristics of subgrade, service, and economy. Width is usually governed by the type of facility and the number and type of vehicles. The length of the slab is limited only by the performance properties of the type of pavement.

In the prestressed pavements, the length is usually limited by the capabilities of effective prestressing and joint width of the slabs. A joint is provided for the contraction of the pavement. The size and number of these joint openings must not cause discomfort to the user or put drivers in jeopardy. Consideration of thickness in PCP is also needed to prevent buckling of a slab subjected to high compressive stresses, but a thicker pavement will experience more cracks because of the hydration temperature of concrete. Generally, a balance must be sought in terms of geometric stiffness of the structure.

Therefore, a good design will keep strand stress losses to a minimum. A layout is needed that reduces losses in the strands, optimizes the geometry of the slab, and achieves a good anchorage.

EFFECT OF LOADS

Loads are imposed by the vehicles traveling on the highway. Such loading is of short duration, concentrated, and dynamic and repetitive along the slab.

The life of the slab depends on its ability to transfer the loads to the underlying soilbed. The process can be considered as one of stress buildup and dissipation.

STRESS BUILDUP

Stress buildup is the result of vehicle load application. The slab bears this load for an instant. This produces stresses in the structure that can be transferred to a greater or lesser extent to the subgrade beneath the point of application. The higher the stress dissipation, the less stress the pavement must bear. That is the importance of this "discharge" or dissipation of stresses.

STRESS DISSIPATION

Materials can dissipate loads in two ways: through stresses and through deformations. Elastic and plastic materials dissipate stress mainly by means of deformation. Meanwhile, rigid materials achieve dissipation, to a major extent, through stress buildup. When additional load cannot be dissipated in these two ways, the material undergoes a third type of liberation; that is, the material ruptures, releasing the stored energy.

PCP and rigid pavements dissipate stresses in both ways. The more advantageous method of dissipating stress is through transmission of load to the layers underneath the point of load application. In this way, the stress buildup in the slab is minor. The stresses are applied to and distributed by the layers beneath it. When the stress is higher than the stress the layer can undergo, deformation occurs. This deformation reduces or eliminates the support for the slab. The slab then deforms, and the stresses are redistributed among the adjacent areas. However, in this process the slab must undergo higher stresses. The stress cycles also add to the fatigue life of the pavement.

STRUCTURAL UNITY

From the preceding discussion, a concept can be formed. The structure of the pavement must be designed to work as a unity. The roadbed soil, subbase, base, and bearing surface layer must be considered together. A design focusing on any individual part will not permit an effective transfer and dissipation of the stresses. If one component fails, the others will undergo higher stresses. Ultimately, they too will fail before the end of the service life of the pavement.

CONCRETE-STEEL INTERACTIONS

Steel and concrete work together in PCP slabs. Steel is put in tension, and it transfers this stress as compression to concrete. In this way, both materials bear the loads, and tensile stresses are lower for concrete. Both concrete contraction and expansion affect prestress. Expansion stretches the steel strands and increases the prestress tension. Contraction has the opposite effect. Tension in the strands is relaxed, and concrete is affected because of the development of friction that takes place in the structural unit.

STRUCTURAL UNIT

The composite formed by PCP is designed to work as a structural unit capable of transmitting the action of loads to the underlying soil. Concrete offers a rigid surface for the rolling vehicles and stiffness for the even distribution of stresses. Steel helps concrete in this task and relieves concrete of tensile stresses to a certain extent. The more advantageous conditions for this type of structure occur when steel is allowed completely to take the tensile stresses. For this purpose, concrete must be allowed to break. This translates to the working of the steel and concrete beyond the elastic range. However, in practice, the majority of PCP designs do not exceed the elastic range.

FRICTION

Friction between steel and concrete was mentioned before. The result of this friction is a loss in the efficiency of the prestress. The degree of friction varies with the strand layout, encasing of the strands, etc. In CRCP slabs, friction induces tensile stresses on concrete. In PCP, friction between steel and concrete is not known to induce tensile stresses. In any event, friction is detrimental to the concrete.

Concrete and steel interact. The action of one affects the performance of the other; i.e., loss in efficiency of steel shortens the life of the concrete. Therefore, the achievement of a working unit must be assured in the design and construction of the PCP.

SLAB-SUBBASE INTERACTION

Slab and subbase are in extensive contact. They interact in both planes, vertical and horizontal. In the vertical plane, the slab stresses are dissipated to the roadbed soil. In the horizontal plane, friction develops between the slab and the subbase. Both phenomena vary with seasonal and daily cycles.

SEASONAL CHANGES

The environmental changes occurring in the soil affect the interaction of the slab-subgrade structure. Depending on the type of subgrade, these variations are larger or smaller. During the dry season, the support value of the subgrade is higher. This means more transmission of stresses to the roadbed. It also implies less deformation and fewer stresses in the pavement layers. As discussed in the first part of this chapter, a change of environment brings a change in moisture. Moisture, especially in clays, reduces the stiffness or the bearing capacity of the soil. This reduced stiffness forces the pavement slab to undergo higher stresses. At the same time, there is a larger contact area, and a deeper substratum of soils is affected.

FRICTION

Variations in moisture and temperature cause minute volume changes in the pavement. However, this expansion is different from the expansion that might occur in the subbase. Therefore, movement develops with friction occurring between slab and subbase. In classical mechanics, the friction force is defined as the tangential force that develops when two surfaces which are in contact tend to move with respect to each other. The nature of the friction force is not completely known; however, it is assumed to be produced by two factors: (1) molecular attraction and the nature of the surfaces in contact, and (2) the irregularities between the surfaces in contact.

For PCP, the development of friction has a beneficial and a detrimental effect. The type of effect depends on the direction of movement in relation to the prestressing as the friction develops. A detrimental effect results during the contraction of the slab. Friction introduces tensile stresses on the bottom of the slab. After the temperature reaches its minimum, generally during the early morning hours, expansion begins in the pavement. A beneficial effect is produced because of the compressive stresses that develop with slab expansion, again due to friction at the slab/subbase interface.

Research at the Bureau of Public Roads (Ref 33) established the fact that frictional resistance is not constant. Instead, it increases with slab movement, rapidly at first and then at a decreasing rate until a maximum value is reached. This maximum value corresponds to the force needed to produce free sliding (Ref 34). For pavement slabs, the magnitude of the movements produced by a daily temperature cycle depends on the location along the slab length. The movements normally vary from a maximum at the edge to the smallest at the center of the slab. Therefore, the maximum friction forces develop at the ends and decrease toward the center. Concrete stresses resulting from the accumulation of friction forces grow from zero at the end to a maximum at the center. Figure 2.3 shows the profiles of movements, friction forces, and concrete stresses which are characteristic of temperature related movements.

Studies by Fridberg and Stott (Refs 35 and 36) clearly show the inelastic nature of the friction forces developing beneath long pavement slabs. Reversals of movements lead to reversals of friction forces and corresponding concrete stresses. Characteristically in a daily cycle, two movement and friction resistance reversals happen. The reversals are triggered within a few degrees of temperature change after the maximum or the minimum slab temperatures occur. For example, tensile stresses, as shown in Fig 2.3, develop several hours after the afternoon peak. As a counterpart, compressive stresses with profiles opposite to those of Fig 2.3 develop

after the morning minimum temperature. The magnitude of the friction restraint stresses depends primarily on three factors. The factors are (1) the concrete coefficients of contraction and expansion, (2) the concrete modulus of elasticity, and (3) the friction force versus movement relationship. The tensile stresses are the most important, since they result in two unfavorable conditions for the PCP.

(1) Before application of prestress forces, the tensile stresses produced on long slabs may cause premature cracking of the slabs. This is critical, especially during the first night, the slabs are constructed at high temperatures. For this reason, the recommended practice is to apply an initial amount of prestress during the first night. This keeps tensile stresses below the concrete tensile strength. In this way the first night cracking is avoided.

(2) After the application of the prestressing forces, the friction forces occurring with temperature drops diminish the prestress at the ends of the slab. After the application of a certain amount of force, the stress level at any section of the PCP slab is the summation of the external prestress force and the restraint stresses resulting from daily temperature changes. The final stresses on the concrete are the mirror image of the friction restraint stresses before the prestress force is superimposed. Therefore, when the temperature drops, the frictional restraint reduces the effectiveness of the external prestressing. This effectiveness will be less at the center of the slabs.

Therefore, the interaction between the slab and the subbase affects the level and distribution of stresses and prestress in PCP.

CHAPTER 3. FIELD INSTRUMENTATION AND DATA COLLECTION

This chapter provides a short description of the experimental pavement sections, the instrumentation used on the in-service pavement, and the field measurement program.

DESCRIPTION OF EXPERIMENTAL SECTIONS

The experimental prestressed concrete overlay in Waco is on the southbound lane of Interstate Highway 35 (IH35) between stations 696+00 and 749+00. Between September 17 and November 20, 1985, eighteen 240-foot and fourteen 440-foot PCP slabs were cast. The roadway is a typical rural depressed median of an interstate section, having two southbound lanes, each 12 feet in width, an inside shoulder of 4 feet, and an outside shoulder of 10 feet. The paving was accomplished in two passes of the paver. The first pass had a paving width of 17 feet and the second pass had a width of 21 feet. The prestressed overlay consists of the following slabs:

9 slabs @ 240 feet x 21 feet,
7 slabs @ 440 feet x 21 feet,
9 slabs @ 240 feet x 17 feet, and
7 slabs @ 440 feet x 17 feet.

The arrangement of the slabs in each of the southbound lanes of IH35 is presented in Fig 3.1. The joints are numbered from north to south. The original pavement consisted of 12 inches of jointed concrete pavement over 5 inches of select material over 8 inches of lime-treated subgrade. The old jointed pavement was 24 feet wide with a 4-foot inside shoulder and a 10-foot outside shoulder, for a total width of 38 feet. During the PCP overlay, the jointed pavement was sealed and overlaid with approximately 2 inches of asphalt concrete pavement (ACP). Subsequently a single polyethylene sheet was placed as a bond breaker and a 6-inch-thick PCP slab was constructed. The aggregate materials used in the paving concrete were obtained locally from the Neelley Sand and Gravel Company. The concrete conformed to the Texas SDHPT Standard Specification Item 360, except that a six-sack mix was used and a minimum compressive strength of 3600 psi at 28 days was required. The PCP overlay in Waco was opened to traffic in December 1985. The design and construction of the overlay are reported by Mendoza et al in Ref 7.

DESCRIPTION OF THE INSTRUMENTATION

An instrumentation program for the McLennan County PCP was carried out in order to monitor movements of the slabs after changes in the material properties of the concrete had stabilized and after shrinkage and creep effects were essentially complete. Information collected in this instrumentation program was to be used to characterize the long-term behavior of the PCP. The descriptive information in the following sections is based on Refs 33, 34, and 35.

OBJECTIVES AND SCOPE

The purpose of the instrumentation program for the present investigation was to evaluate the response of the McLennan County PCP to daily temperature cycles for a variety of extreme seasonal conditions. Information about daily horizontal and vertical slab movements was used to calibrate both the computer model presented in Ref 2 and the model presented in Ref 3. Information collected during extreme seasonal conditions was used to compare the behavior of the slabs under different moisture conditions and to establish boundaries on the joint movements of the slabs for a large range of temperatures.

The following are the basic objectives of the instrumentation program:

(1) to determine the magnitude of longitudinal slab movements due to daily temperature cycles, for different moisture conditions, and to correlate them with the mid-depth temperature of the slabs;

(2) to determine the magnitude of curling slab movements due to daily temperature cycles, for different moisture conditions, and to correlate them with the change in temperature gradient across the slabs thicknesses; and

(3) to determine the magnitude of changes in joint opening between

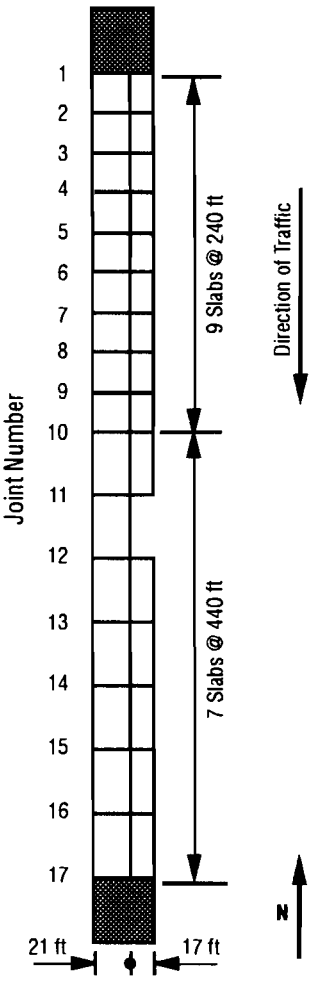

Fig 3.1. Layout of the McLennan County PCP experimental section.

TABLE 3.1. DATA COLLECTION FIELD VISITS

Field Visit	Date	Maximum Ambient Temperature (°F)	Minimum Ambient Temperature (°F)	Weather Condition
2	July 26, 1988	107.13	74.80	Hot, dry
3	August 6, 1988	104.00	75.85	Hot, dry
4	August 26, 1988	107.87	71.28	Hot, dry
5	November 5, 1988	84.00	41.72	Mild, dry
6	January 21, 1989	64.22	27.39	Cold, wet
Additional	February 4, 1989	—	17.60	Cold
7	February 9, 1989	62.87	30.90	Cold, wet

Note: Visit 1 was a site survey and performance data was not collected.

slabs for a maximum range of mid-depth slab temperatures.

FIELD VISITS

Work performed at the McLennan County PCP site included site surveys, preliminary measurements, installation of instrumentation equipment, and data collection. Data collection took place from July 1988 to February 1989. During that time, six field visits were made to the PCP. The field visits took place under different conditions of moisture and ambient temperature: three during hot and dry conditions, one during mild and dry conditions, and two during cold and wet conditions. Also, one additional trip to the PCP was made during extremely cold conditions for the purpose of measuring maximum joint openings. Table 3.1 outlines the data collection field visits and the additional trip. A site survey (Ref 1) was conducted during the first field visit, so it is not included on the table. The duration of each data collection was 24 hours, with the exception of the sixth field visit, which lasted 48 hours.

This array of weather conditions covers approximately the maximum range of temperatures expected at the site. It is difficult to evaluate whether the wet moisture conditions can be considered as the extreme conditions; 1988 was a drought year with almost no precipitation from July to December. The conditions described as "wet" in Table 3.1 were wet from rains that occurred one to two days prior to data collection.

INSTRUMENTATION SET-UP

Concrete "dead-man" anchors were used to support the dial gages and linear voltage-distance transducers (LVDT's) used to measure slab movements. The anchors consisted of typical 6-inch x 12-inch concrete cylinders with embedded threaded inserts that receive 7/8-inch threaded dowels. The anchors were inserted into the soil, levelled, and secured into place with concrete about 18 inches from the west edge of the slabs. Then, for each field visit, a vertical dowel with a threaded end was screwed into each anchor, and horizontal dowels, onto which dial gages or LVDT's were secured, were attached to the verticals with 90° dowel clamps. Insulation was placed around all support dowels to reduce warping and expansion from radiant solar heat. This type of set-up allowed for the temporary fabrication of instrumentation supports at the work site and for their removal after data collection was completed for each field visit.

Steel angles (3 inches x 3 inches x 3/8 inch) were bolted onto lead inserts that were drilled and epoxied onto the edge of the slabs; the angles served as reaction stops for the dial gage or LVDT plunger-pins. Plastic receptacles were used to provide a smooth and level surface for the plunger pins of the dial gages or LVDT's that were measuring curling slab movements. These receptacles consisted of a 3-inch x 3/8-inch x 3/4-inch polyvinylchloride pipe that was epoxied to the top surface of the slab and filled with hot (liquid) sulphur mortar. The liquid was allowed to cool and solidify, creating a level top surface onto which a 1-1/2-inch x 1-1/2-inch x 1/4-inch plastic square was epoxied. The typical set-up of the instrumentation is shown in Fig 3.2. Components of the instrumentation set-up are labelled in Fig 3.3 (this figure shows dial gages, but the set-up for LVDT's is identical).

Concrete temperatures at three depths in the slabs were measured using thermocouples that were drilled and grouted into the slabs near joint 10. The top and bottom thermocouples were used to determine temperature gradients across the thickness of the slabs (so that they could be correlated with curling slab movements), and the middle thermocouple was used to determine slab temperatures to be correlated with horizontal slab movements. The layout of the thermocouples is shown in Fig 3.4.

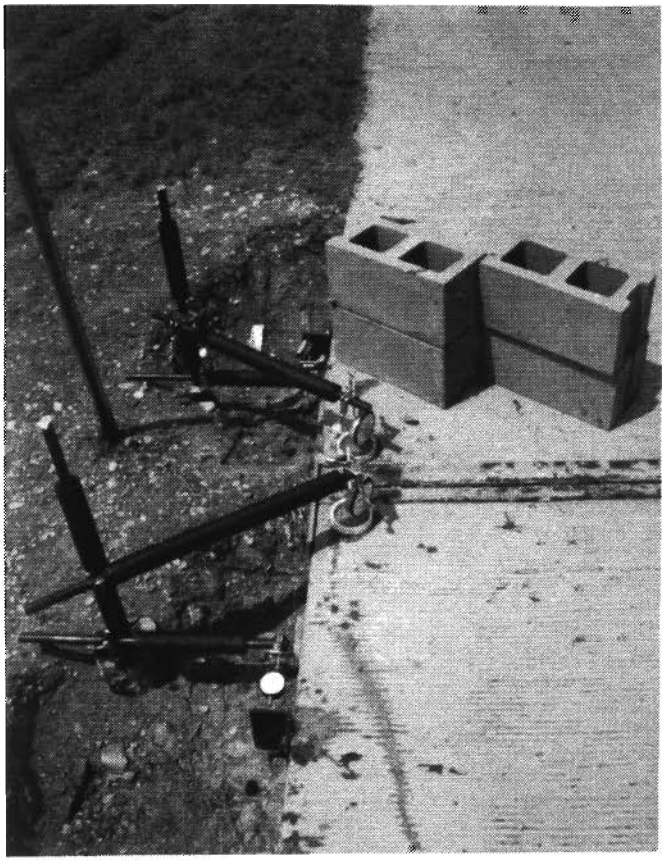

Fig 3.2. Instrumentation set-up.

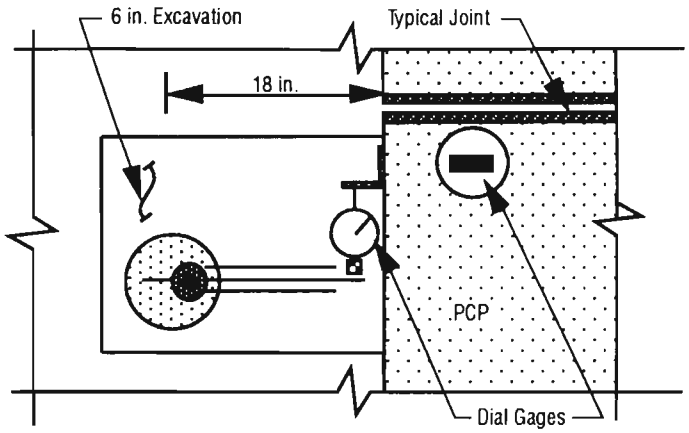

Plan
(Upper Horizontal Dowel Not Shown)

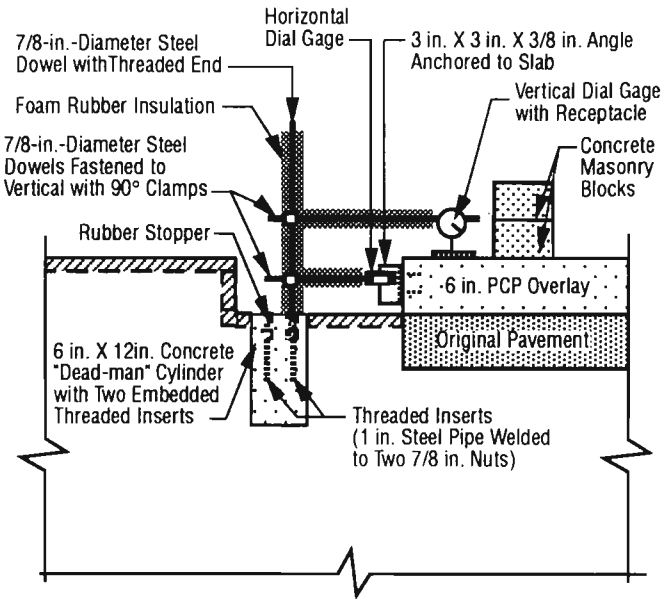

Elevation

Fig 3.3. Components of instrumentation set-up.

MEASUREMENT

The number of locations on the slabs that could be instrumented simultaneously was limited by the number of available dial gages. Figure 3.5 shows a plan view of the slabs that were instrumented for this project, along with instrumentation locations. Instrument locations labelled with "/3" or "/6" respectively indicate third or sixth points along the slab length. Figure 3.6 shows a more detailed plan of instrumentation locations for slabs that were instrumented along their length as well as at their ends. During the first three data collection periods, data were collected from joint locations only so that joint displacement data could be based on the largest possible sample for a portion of the field visits. For the remainder of the data collection periods, displacement data were collected at locations along slab lengths so that the

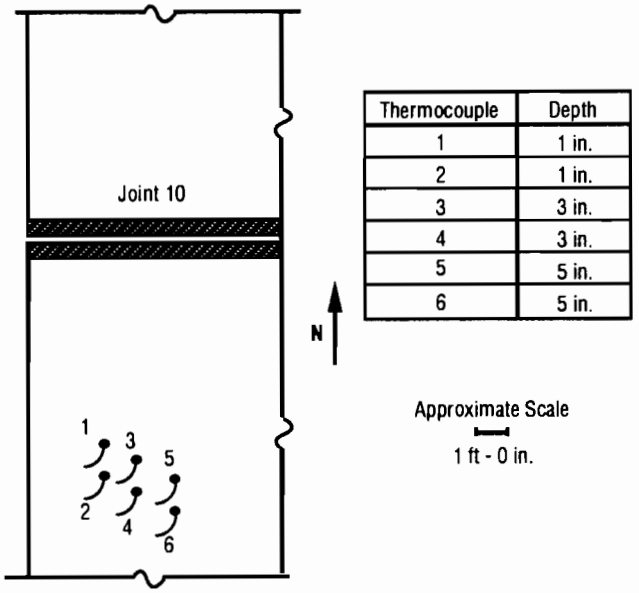

Thermocouple	Depth
1	1 in.
2	1 in.
3	3 in.
4	3 in.
5	5 in.
6	5 in.

Fig 3.4. Thermocouple locations at Joint 10.

computer models could be calibrated to displacements of the entire slabs. Table 3.2 shows a compilation of the instrumentation schemes that were carried out for each field visit. It outlines the type of instrument used at each instrumentation location for the measurement of both horizontal and vertical slab movements. The dial gages had an accuracy of 0.001 inch and the LVDT's had an accuracy of 0.0001 inch. Joint 10 was the only joint instrumented with LVDT's. The redundant readings of horizontal movements at location 10S and 10N (using both LVDT's and dial gages) provided a verification of data readings. The combined dial gage and LVDT instrumentation is shown in Fig 3.7.

The instrumentation set-up allowed for the relative measurement of horizontal and vertical slab movements with respect to an arbitrary datum. The collected data for these movements give displacements measured from the first data reading at each location for each field visit. The displacements for a daily temperature cycle determined in this manner are in direct parallel with the displacement output from the computer models.

Joint widths were measured with a dial-caliper by inserting the legs of the calipers into the joint, flush with the joint edges. Measurements took place at scribe marks on the joint hardware so that readings would reflect joint movements at one location for each joint. The method of joint width measurement is shown in Fig 3.8.

Data were collected both manually and automatically. Dial gage data and joint width readings were recorded manually onto data sheets at two-hour intervals. LVDT measurements and thermocouple readings were recorded automatically every 10 minutes by a programmed data acquisition system. A schematic diagram of the data acquisition system is shown in Fig 3.9 (Ref 38).

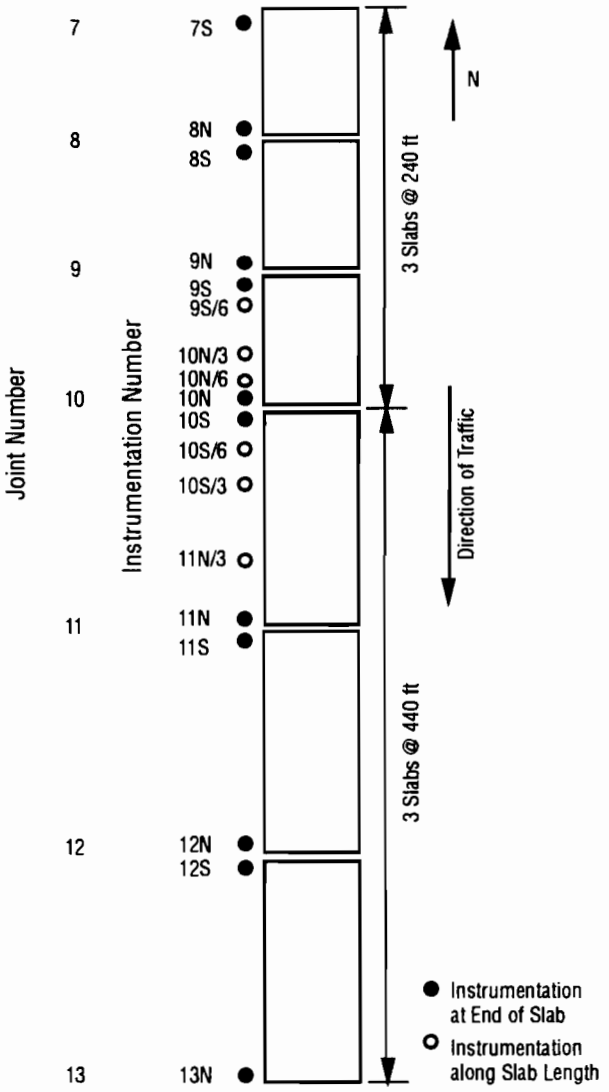

Fig 3.5. Instrumented slabs and instrumentation locations.

A more complete description of the instrumentation may be found in Ref 2.

DATA PRESENTATION

Original and final data on horizontal and vertical slab displacements, joint widths, ambient temperatures, and concrete temperatures at three depths in the pavement were presented in Report 556-1 (Ref 1), and a detailed explanation of their corrections and handling for analysis was made in Report 556-2 (Ref 2) for the horizontal displacements and in Report 556-3 (Ref 3) for the vertical displacements.

In general, the data were first carefully screened to insure that all obvious blunders were removed. This was accomplished by plotting the data as a function of time. This step resulted in a file of edited data, and this file was used in all regression and other statistical analysis.

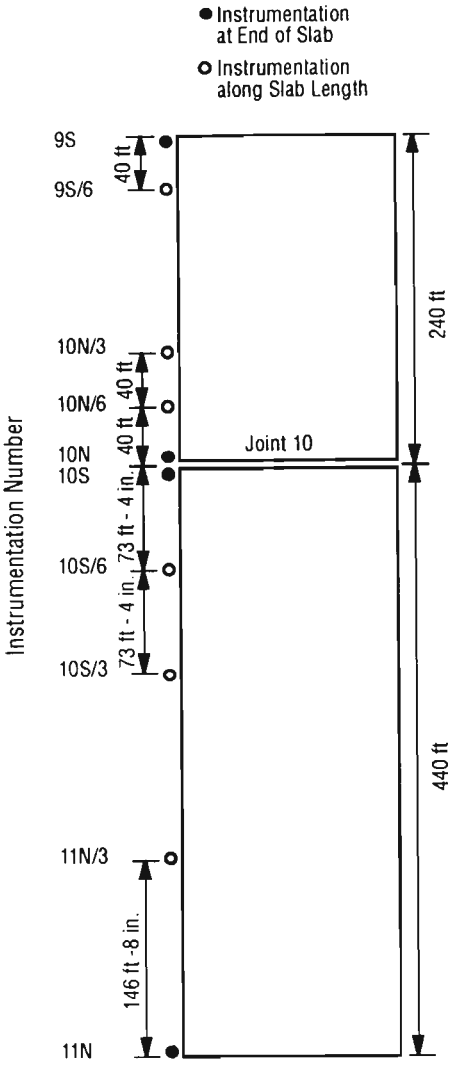

Fig 3.6. Instrumentation locations between Joints 9 and 11.

Fig 3.8. Joint width measurement using dial-caliper.

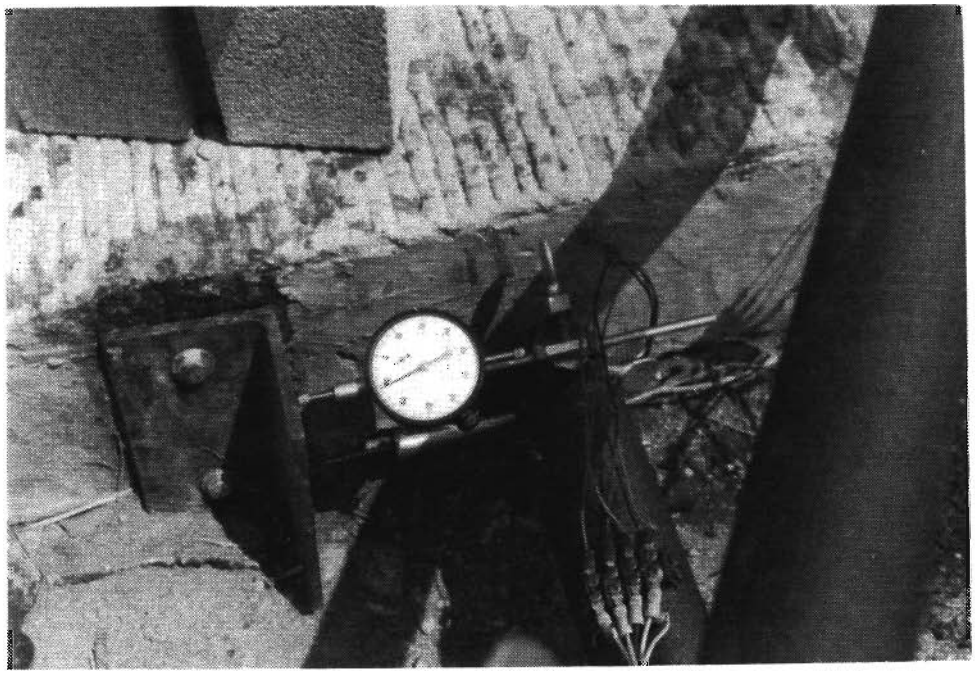

Fig 3.7. Combined dial-gage and LVDT instrumentation.

TABLE 3.2. INSTRUMENTATION SCHEMES FOR EACH FIELD VISIT

Location	Field Visit 2 7/26/88		Field Visit 3 8/6/88		Field Visit 4 8/26/88		Field Visit 5 11/5/88		Field Visit 6 1/21/89		Field Visit 7 2/9/89	
	Horiz	Vert	Horiz	Vert	Horiz	Vert	Horiz	Vert	Horiz	Vert	Horiz	Vert
7S	Dial Gauge	Dial Gauge	Dial Gauge	Dial Gauge	Dial Gauge	Dial Gauge						
8N	Dial Gauge	Dial Gauge	Dial Gauge	Dial Gauge	Dial Gauge	Dial Gauge						
8S	Dial Gauge	Dial Gauge	Dial Gauge	Dial Gauge	Dial Gauge	Dial Gauge	Dial Gauge	Dial Gauge	Dial Gauge	Dial Gauge	Dial Gauge	Dial Gauge
9N	Dial Gauge	Dial Gauge	Dial Gauge	Dial Gauge	Dial Gauge	Dial Gauge	Dial Gauge	Dial Gauge	Dial Gauge	Dial Gauge	Dial Gauge	Dial Gauge
9S	Dial Gauge	Dial Gauge	Dial Gauge	Dial Gauge	Dial Gauge	Dial Gauge	Dial Gauge	Dial Gauge	Dial Gauge	Dial Gauge	Dial Gauge	Dial Gauge
9S/6							Dial Gauge	Dial Gauge	Dial Gauge	Dial Gauge	Dial Gauge	Dial Gauge
10N/3							Dial Gauge	Dial Gauge	Dial Gauge	Dial Gauge	Dial Gauge	Dial Gauge
10N/6							Dial Gauge	Dial Gauge	Dial Gauge	Dial Gauge	Dial Gauge	Dial Gauge
10N	LVDT & Dial Gage	LVDT	LVDT & Dial Gage	LVDT	LVDT & Dial Gage	LVDT	LVDT & Dial Gage	LVDT	LVDT & Dial Gage	LVDT	LVDT & Dial Gage	LVDT
10S	LVDT & Dial Gage	LVDT	LVDT & Dial Gage	LVDT	LVDT & Dial Gage	LVDT	LVDT & Dial Gage	LVDT	LVDT & Dial Gage	LVDT	LVDT & Dial Gage	LVDT
10S/6							Dial Gauge	Dial Gauge	Dial Gauge	Dial Gauge	Dial Gauge	Dial Gauge
10S/3							Dial Gauge	Dial Gauge	Dial Gauge	Dial Gauge	Dial Gauge	Dial Gauge
11N/3							Dial Gauge	Dial Gauge	Dial Gauge	Dial Gauge	Dial Gauge	Dial Gauge
11N	Dial Gauge	Dial Gauge	Dial Gauge	Dial Gauge	Dial Gauge	Dial Gauge	Dial Gauge	Dial Gauge	Dial Gauge	Dial Gauge	Dial Gauge	Dial Gauge
11S	Dial Gauge	Dial Gauge	Dial Gauge	Dial Gauge	Dial Gauge	Dial Gauge	Dial Gauge	Dial Gauge	Dial Gauge	Dial Gauge	Dial Gauge	Dial Gauge
12N	Dial Gauge	Dial Gauge	Dial Gauge	Dial Gauge	Dial Gauge	Dial Gauge	Dial Gauge	Dial Gauge	Dial Gauge	Dial Gauge	Dial Gauge	Dial Gauge
12S	Dial Gauge	Dial Gauge	Dial Gauge	Dial Gauge	Dial Gauge	Dial Gauge						
13N	Dial Gauge	Dial Gauge	Dial Gauge	Dial Gauge	Dial Gauge	Dial Gauge						

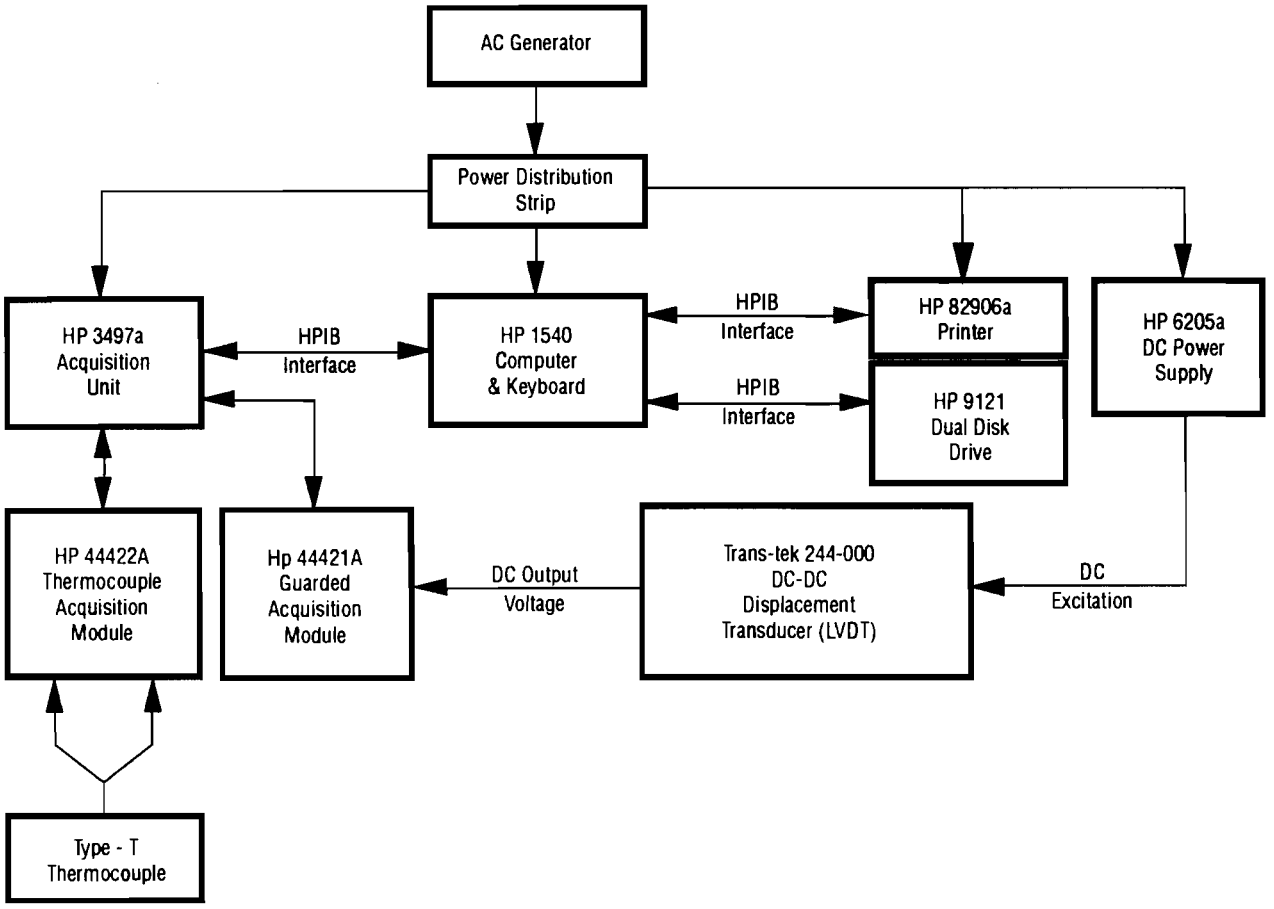

Fig 3.9. Schematic diagram of the data acquisition system.

CHAPTER 4. DATA ANALYSIS

This chapter describes the analysis of the field data that were collected at the McLennan County PCP. The data include measurements of horizontal and vertical slab displacements, joint widths, ambient temperatures, concrete temperatures at three depths in the pavement, and slab deflection. The condition survey data are also discussed. This chapter presents an overview of the data analysis that was performed; a complete discussion of data analysis can be found in Refs 1, 2, and 3.

HORIZONTAL SLAB MOVEMENTS

The design of a PCP involves the evaluation of two major aspects of the horizontal slab movements: the character of slab activity during temperature changes and the range of joint widths between slabs. The former is of interest because stresses in the slab are a direct function of displacements. The latter affects the placement of slabs (where the design criteria is to avoid extremely wide joint widths, or complete closure of the joints). Of course, slab activity affects the range of joint widths; that is, slabs with more active horizontal movements will cause a larger range of joint widths.

REGRESSION ANALYSIS OF HORIZONTAL DISPLACEMENTS

Analysis of slab activity for temperature changes was performed by calculating a series of regression equations for horizontal displacements. The equations are linear, where the abscissa, X, is the concrete temperature at mid-depth of a slab in degrees Fahrenheit, and the ordinate, Y, is the horizontal displacement from the initial data reading for a field visit. Table 4.1 shows a compilation of the regression equations for all field visits, along with the coefficient of partial determination statistic, R^2. The R^2 value indicates how well the data fit the regression equation, where a value of 1.0 is a perfect fit.

All R^2 values are high; most are greater than 0.95, and the lowest value is 0.854. This indicates the linear equations can predict horizontal displacements with a high degree of accuracy. As expected, the slopes (coefficients of the abscissas) in the equations increase for the longer slabs. The ratio of slab lengths between the 440-foot and the 240-foot slabs is 1.835, and the ratio between the average values of the slopes in the equations for the slabs is 2.024, or 10.31 percent higher. This

TABLE 4.1. REGRESSION EQUATIONS FOR HORIZONTAL DISPLACEMENTS

Field Visit	Measurement Location	Regression Equation	Coefficient of Partial Determination
2	240 ft slab (joint)	$Y = (5.374 \times 10^{-3})T - 0.586$	$R^2 = 0.854$
	440 ft slab (joint)	$Y = (1.281 \times 10^{-2})T - 1.422$	$R^2 = 0.951$
3	240 ft slab (joint)	$Y = (5.148 \times 10^{-3})T - 0.558$	$R^2 = 0.884$
	440 ft slab (joint)	$Y = (1.212 \times 10^{-2})T - 1.323$	$R^2 = 0.970$
4	240 ft slab (joint)	$Y = (6.076 \times 10^{-3})T - 0.653$	$R^2 = 0.931$
	440 ft slab (joint)	$Y = (1.270 \times 10^{-2})T - 1.371$	$R^2 = 0.854$
5	240 ft slab (joint)	$Y = (6.792 \times 10^{-3})T - 0.542$	$R^2 = 0.991$
	240 ft slab (sixth point)	$Y = (4.206 \times 10^{-2})T - 0.335$	$R^2 = 0.982$
	240 ft slab (third point)	$Y = (2.344 \times 10^{-3})T - 0.186$	$R^2 = 0.993$
	440 ft slab (joint)	$Y = (1.217 \times 10^{-2})T - 0.970$	$R^2 = 0.983$
	440 ft slab (sixth point)	$Y = (7.697 \times 10^{-3})T - 0.611$	$R^2 = 0.970$
	440 ft slab (third point)	$Y = (3.717 \times 10^{-3})T - 0.295$	$R^2 = 0.932$
6	240 ft slab (joint)	$Y = (6.089 \times 10^{-3})T - 0.358$	$R^2 = 0.991$
	240 ft slab (sixth point)	$Y = (3.738 \times 10^{-3})T - 0.219$	$R^2 = 0.971$
	240 ft slab (third point)	$Y = (1.887 \times 10^{-3})T - 0.112$	$R^2 = 0.988$
	440 ft slab (Joint)	$Y = (1.106 \times 10^{-2})T - 0.649$	$R^2 = 0.980$
	440 ft slab (sixth point)	$Y = (6.948 \times 10^{-3})T - 0.402$	$R^2 = 0.964$
	440 ft slab (third point)	$Y = (3.138 \times 10^{-3})T - 0.182$	$R^2 = 0.920$
7	240 ft slab (joint)	$Y = (5.864 \times 10^{-3})T - 0.542$	$R^2 = 0.985$
	240 ft slab (sixth point)	$Y = (3.706 \times 10^{-3})T - 0.335$	$R^2 = 0.966$
	240 ft slab (third point)	$Y = (1.738 \times 10^{-3})T - 0.186$	$R^2 = 0.984$
	440 ft slab (joint)	$Y = (1.074 \times 10^{-2})T - 0.970$	$R^2 = 0.981$
	440 ft slab (sixth point)	$Y = (6.287 \times 10^{-3})T - 0.611$	$R^2 = 0.947$
	440 ft slab (third point)	$Y = (2.855 \times 10^{-3})T - 0.295$	$R^2 = 0.904$

suggests that the increase in horizontal activity with increased slab length is not linear.

The slopes follow logical trends for the different measurement locations. The average slopes for displacements at the joints are 5.890×10^{-3} and 1.193×10^{-2} inch/°F for the 240-foot and 440-foot slabs respectively. At the sixth points, the average slopes are 3.883×10^{-3} and 6.977×10^{-3} inch/°F, 65.93 percent and 58.48 percent of the slopes at the joints. At the third points the average slopes are 1.990×10^{-3} and 3.237×10^{-3} inch/°F, 33.78 percent and 27.13 percent of the slopes at the joints, and 51.25 percent and 46.40 percent of the slopes at the sixth points. The horizontal activity varies approximately linearly with respect to the geometry of the slabs. In addition, it appears that for both 240 and 440-foot lengths, almost the entire slab is moving. Figure 4.1 shows a graph of the slopes of the regression equations as a function of the distance from the centerlines of the slabs.

The regression equations do not show a strong trend for different moisture levels. Field visits 6 and 7 took place under moist conditions; the 440-foot slabs have slightly smaller slopes for these visits, and there is no definitive trend for the 240-foot slabs. One explanation for their not showing large differences for field visits 6 and 7 is that the slabs might not have been completely saturated, and, therefore, expansion and contraction characteristics of the slabs would not have changed enough to show up in the data. Another explanation is that the horizontal activity is not very sensitive to changes in moisture levels. The reason for this would be that the regression equations relate horizontal movements to the concrete temperature at mid-depth of the slabs. The moisture level might affect the lag time between changes in ambient temperature and changes in concrete temperature, but the expansion and contraction characteristics of the slab would not necessarily change appreciably for the same concrete temperatures.

ANALYSIS OF JOINT WIDTHS

The determination of an initial joint width for construction of PCP depends on

(1) the projected amount of creep and shrinkage that will occur during the early life of the pavement,
(2) the projected amount of elastic shortening a slab will undergo during stressing operations,
(3) the width requirements for inserting a protective neoprene seal into the joint, and
(4) the expected range of temperatures and subsequent horizontal displacements that the slabs will experience throughout their service life.

For the current study, a sample range of maximum and minimum joint widths was determined; Fig 4.2 summarizes the results. These maximums and minimums represent a range of ambient temperatures from 17.6° to 107.13°F.

The joint widths were measured at scribe marks on the joint hardware so that the readings could be compared consistently. The joint edges are not perfectly parallel, so the reported maximum and minimum widths are not necessarily the absolute maximum and minimum widths for the entire length of a joint. In fact, several of the joints between 240-foot slabs were observed to be completely closed during hot weather measurements. In addition, debris in the joints between these slabs often prevented slab

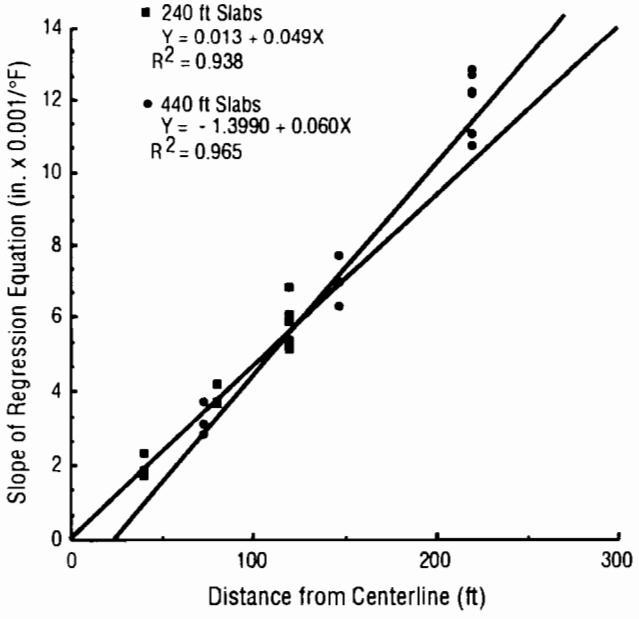

Fig 4.1. Slopes of the regression equations as a function of distance from slab centerline.

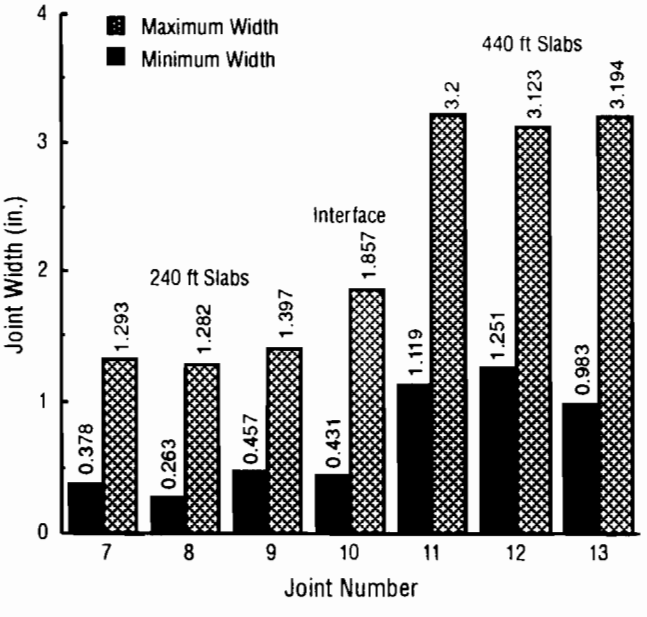

Fig 4.2. Maximum and minimum joint widths for all field visits.

movement for temperature increases during hot weather. However, joints between the 440-foot slabs never completely closed.

Regression equations were calculated for the joint width data for joints between the slabs. The equations describe the joint width behavior (ordinate, Y) as a function of concrete temperature at mid-depth of a slab in degrees Fahrenheit (abscissa, X). Figures 4.3 and 4.4 show graphs of the joint width data for the two slab lengths along with the corresponding regression equations.

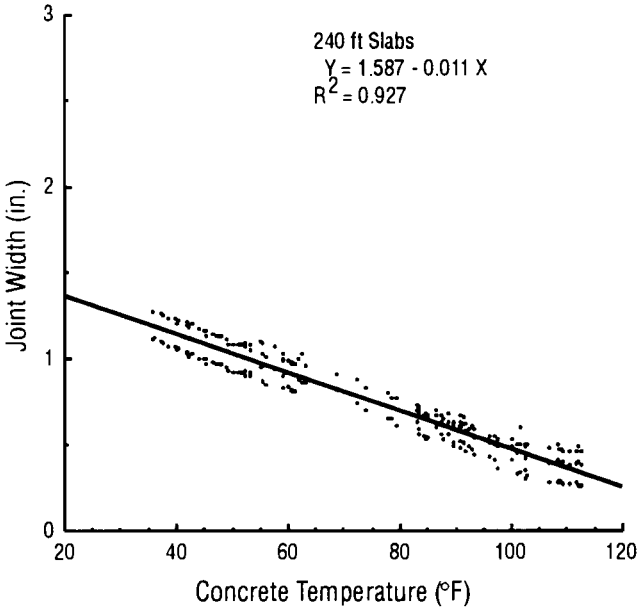

Fig 4.3. Regression equation for joint widths between 240-foot slabs.

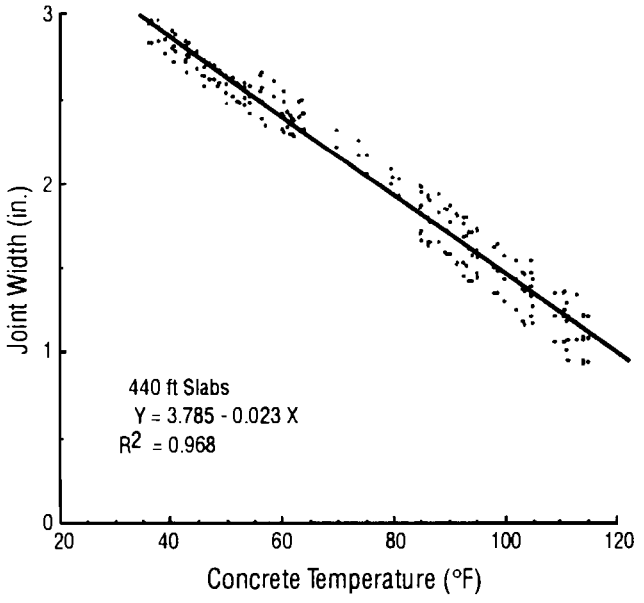

Fig 4.4. Regression equation for joint widths between 440-foot slabs.

SEASONAL SLAB OPERATION

Overall seasonal behavior of horizontal movements of the slabs is a function of daily temperature cycles superimposed over seasonal temperature cycles. This superposition causes slabs to operate, on a daily basis, at different seasonal datum values. During the summer season, the joint widths are small; horizontal displacements occur over a range of small joint widths. Similarly, during the winter season, horizontal displacements occur over a range of wide joint widths. Figure 4.5 shows the ambient and concrete temperatures that were measured for all field visits.

SUMMARY

Horizontal slab movements are significant. Measurements indicate entire slabs are moving. The resulting maximum joint widths range from about 1.5 inches to 5 inches. Additionally, slab movements correlate well with concrete temperatures at mid-depth of the slabs. The techniques used for measuring slab movements work well.

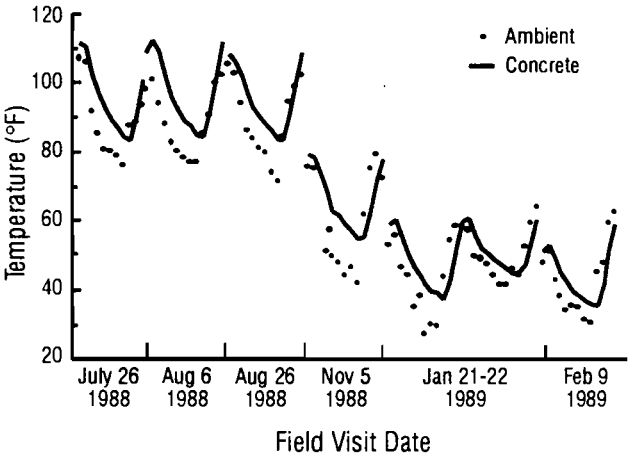

Fig 4.5. Seasonal variation of ambient and concrete temperatures for all field visits.

This study investigated slab movements that occur after shrinkage and creep of the concrete have already occurred. The regression equations that result from these horizontal movements are basically the same for all data samples. However, regression equations for the 240-foot slabs have flatter slopes than the 440-foot slabs. When the slab temperature rises above about 107° F joints between 240-foot slabs may close.

Figure 4.6 shows the average horizontal displacements for the 240-foot and 440-foot slabs superimposed over a curve of the first joint width measurement for each field visit. This plot illustrates the actual measured seasonal variation of slab movements.

VERTICAL MOVEMENT

The analysis of the vertical movement data was made by comparing the movement with time and temperature measurements collected during each visit. Report 556-3 (Ref 3) indicated the vertical movement activity was best associated with the difference in the temperatures collected at the top and the bottom of the PCP slab (Delta t). The vertical movement data for both the 240-foot and 440-foot slabs were corrected for temperature effects in the bars supporting the instrumentation as well as the LVDT's. For this purpose data were used from a monitoring bar which recorded the movement of an insulated metal bar similar to that used for the instrumentation supports. It should be noted that, beginning with the November 1988 visits data were collected at the PCP edge at the 1/6 and 1/3 points along the length of the slab

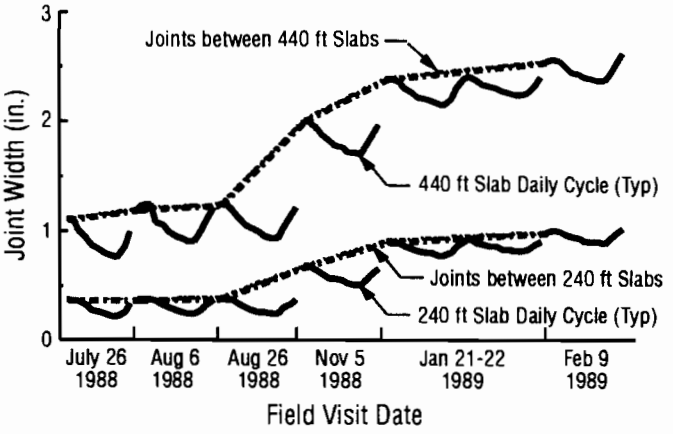

Fig 4.6. Seasonal variation of joint widths with horizontal slab displacements superimposed.

ANALYSIS OF VERTICAL MOVEMENTS

The vertical movement data were collected during each visit at approximate two-hour intervals. The vertical movement was recorded in inches and the temperature in degrees F. Figures 4.7 and 4.8 show typical plots of the vertical movement in a 24-hour period. The data used in the figures were collected on July 25-26,1988, and the data represent the summer season. Figure 4.7 reflects the 240-foot slabs and Fig 4.8 represents the 440-foot slabs. Note that the overall vertical movement or curl was about 0.2 inch. The curl at the corner of the 440-foot slabs could be slightly greater than the corner curl of the 240-foot slabs. However, statistically, the "T Test" indicated the difference between the two slab lengths was not significant.

Figures 4.9 and 4.10 also show the vertical movement at the corner during a 24-hour period. The data used in these plots represent the winter season and consist of the average values for the November, January, and February visits. Figure 4.9 shows the 240-foot slabs and Fig 4.10 shows the 440-foot slabs. The effects of temperature on vertical movement are obvious since the winter months in Texas have less variation in temperature and therefore less vertical movement.

Figures 4.11 and 4.12 are plots of vertical movement with time, where the average movement at the corner, the 1/6 point, and the 1/3 point have been shown. The data for November 5-6, 1988, were used. The vertical movements at the corners were larger than the movements at the 1//6 or 1/3 points. Also, the movements at the 1/6 point seem larger than at the 1/3 point on the 240-foot slabs, but the difference between the movements at the 1/6 and 1/3 points seem less on the 440-foot slabs. Note that the lengths from the 1/6 or 1/3 points to the corner of a 240-foot slab are different from similar points on a 440-foot slab. This could mean the vertical movement (at any instant in time) is maximum at the corner, becomes less as measured from the corner, and along the pavement edge, but becomes asymptotic or relatively constant at a given length from the corner. This effect is revealed in Fig 4.13. In this figure, the vertical movements for 10N, 10 N/3, 10N/6, 10S, 10S/6, and 10S/3 are shown at three measurement intervals on November 5-6, 1988. There is little comparative difference in vertical movement between the 240 and 440-foot slabs. The vertical movement appears to become asymptotic at about 60 to 80 feet from the corner.

In curling theory, when the temperature in the top of the slab is cooler than that in the bottom, the volume of the concrete in the top will be less and the slab will be concave at the surface. Therefore, it is of interest to observe the vertical movement with respect to differential slab temperature. Again, the differential temperature is the difference in temperature from the top of the slab to the bottom of the slab. Figure 4.14 shows the relationship between the vertical movement and differential temperature at a corner of a PCP slab on July 25-26, 1988. Vertical movement information began to be recorded at about 3:30 PM (zero movement). As time increased, the differential temperature became less and the vertical movement increased. This information is shown using the open boxes in Fig 4.14. At about 6:30 AM the vertical movement peaked at about 0.22 inch and the surface of the slab began to warm. The differential temperature then began to increase and the slab elevation at the corner became less. However, Fig 4.14 shows a loop formed and the vertical movement did not have the same relationship with the differential temperature on the return trip. The cause for this loop is not known. It is possible that the effect may be in the instrumentation or the concrete slab may react differently when heating as compared to cooling. Dial gages normally have some gap in the gears and do not respond instantaneously to change in direction, but two types of instrumentation were used in this work. Both dial gages and LVDT's were used, and data from both show the same loop. Therefore, both paths were

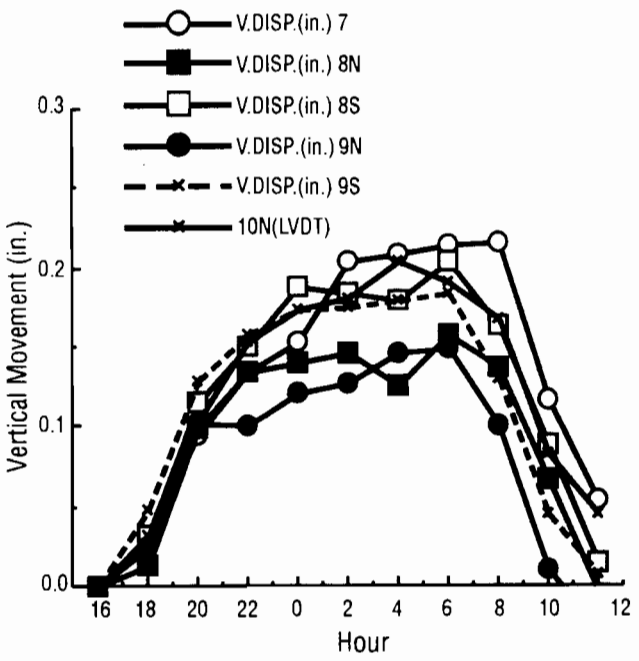

Fig 4.7. Vertical movement of 240-foot slab.

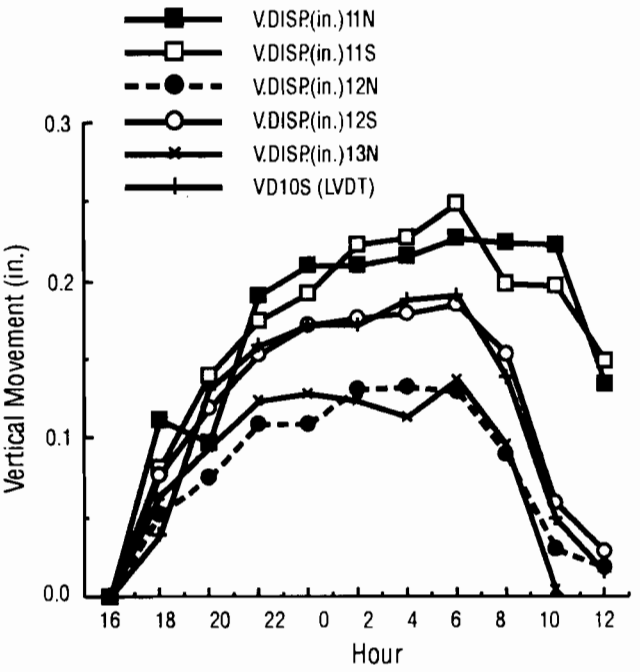

Fig 4.8. Vertical movement of 440-foot slab.

studied and a loss in temperature on the surface of the slab was termed a "cooling cycle" (open boxes, Fig 4.14). The increased warming of the surface was termed a "warming cycle"(closed diamonds in Fig 4.14).

In order to study the effect of vertical movement with differential temperature, plots were developed where all the corner positions were considered. Figure 4.15 shows this relationship during the cooling cycle, and Fig 4.16 shows the warming cycle. Figures 4.17 and 4.18 contain similar information for the 1/6 points, and Figs 4.19 and 4.20 reveal the relationships for the 1/3 points. An exponential type curve seemed to provide better data fits.

DEFLECTION INFORMATION

The pavement deflection data included in this study were obtained for four different time periods. Two of these time periods occurred prior to the prestressed concrete overlay, and two were after the overlay. The latter were planned and conducted as a part of the subject project. The collection periods and the structure occurring during that period are as follows.

SEPTEMBER 1983

The 1983 deflection information was collected on the original pavement structure prior to the prestressed concrete overlay. The original pavement structure consisted of:

(1) a variable depth asphaltic concrete overlay (generally 4 inches),
(2) 12 inches of jointed portland cement concrete pavement,
(3) 5 inches of select material,
(4) 6 inches of lime-treated subgrade.

AUGUST 1985

The 1985 deflection data were collected after work on a construction job was initiated in the area. The original asphaltic concrete overlay had been removed and replaced with a new 2-inch asphaltic concrete designed to provide a level up prior to the prestressed concrete overlay. Therefore, the pavement structure at the time of the 1985 deflection data collection was

(1) 2-in. new asphaltic concrete level-up,
(2) 12-in. jointed PC concrete pavement,
(3) 5-in. foundation course,
(4) 6-in. lime-treated subgrade.

AUGUST 1988

During the subject project, a portion of the work was directed toward collecting deflection information to (1) study changes or improvements in the structural strength and (2) observe the effect of seasonal or environmental changes in the pavement strength. Therefore, the 1988 deflection data were collected during the hot-dry season, or in August. The pavement consisted of

(1) 6-in. prestressed concrete,
(2) 2-in. asphaltic concrete level-up,
(3) 12-in. jointed PC concrete pavement,
(4) 5-in. foundation course,
(5) 6-in. lime treated subgrade.

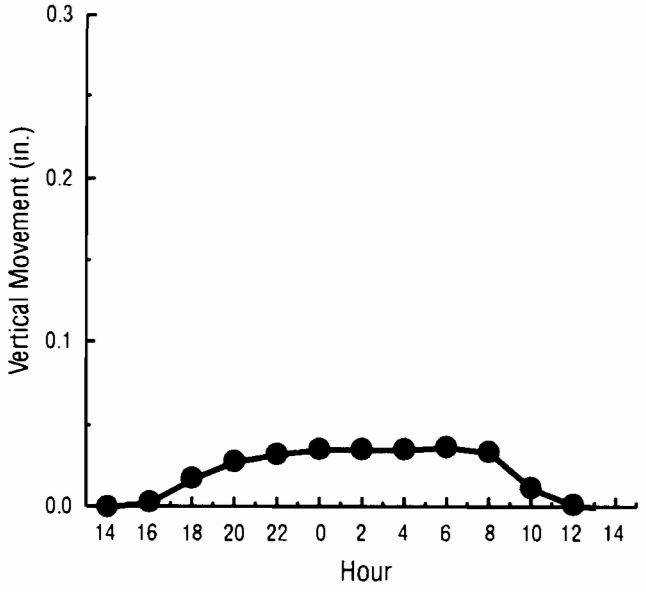

Fig 4.9. Vertical movement of 240-foot slabs—winter.

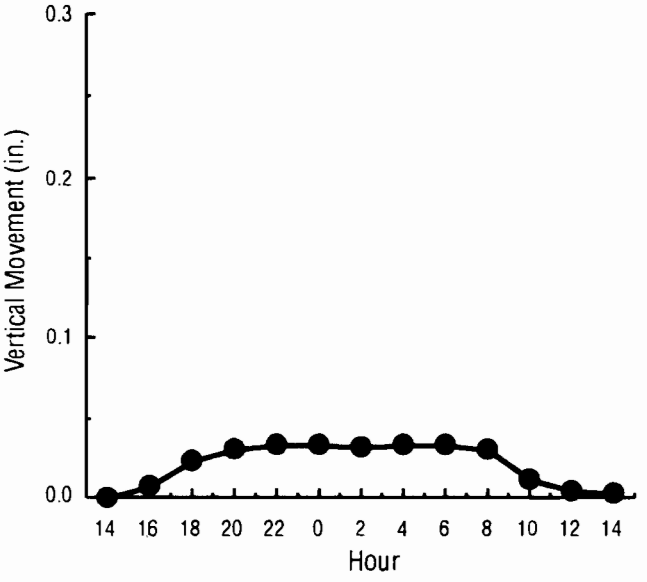

Fig 4.10. Vertical movement of 440-foot slabs—winter.

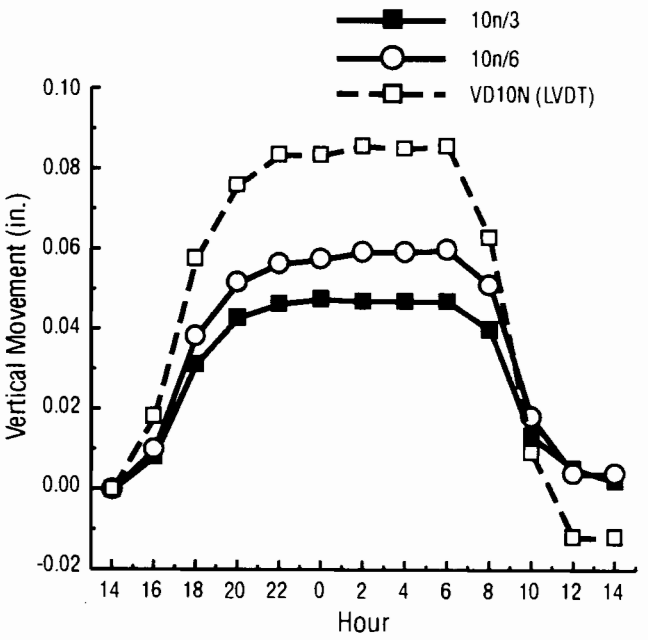

Fig 4.11. Vertical movement at corner, 1/6, and 1/3 points.

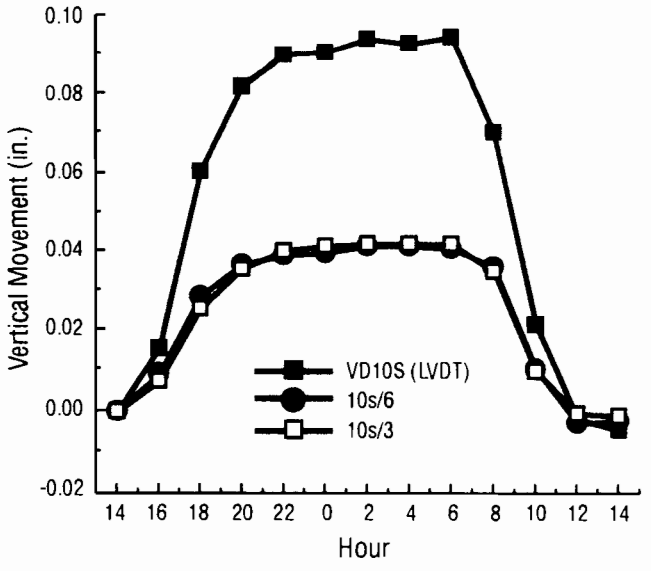

Fig 4.12. Vertical movement at corner, 1/6, and 1/3 points.

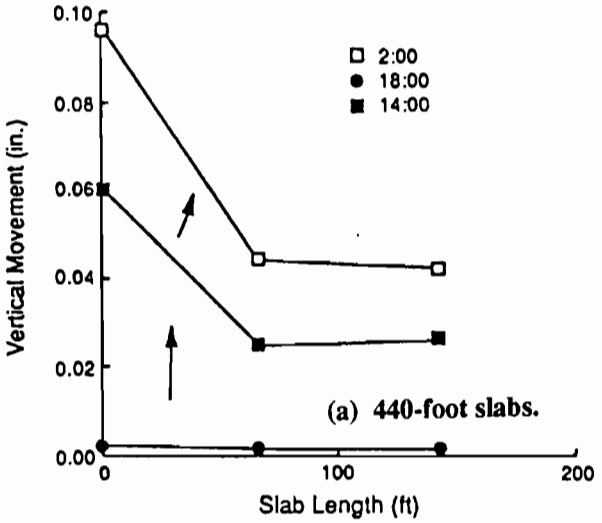

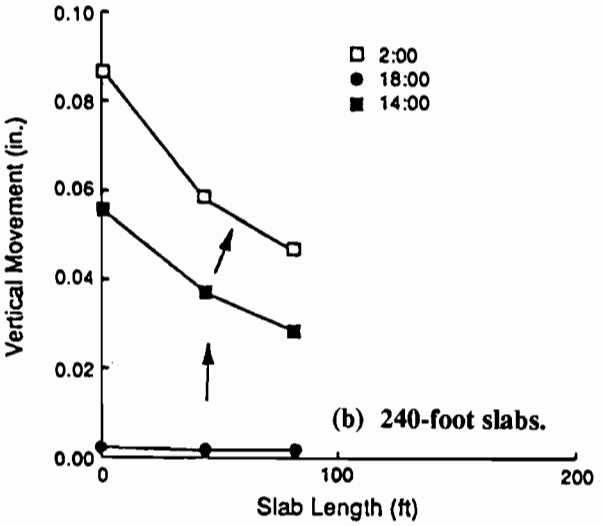

Fig 4.13. Components of vertical movement with length.

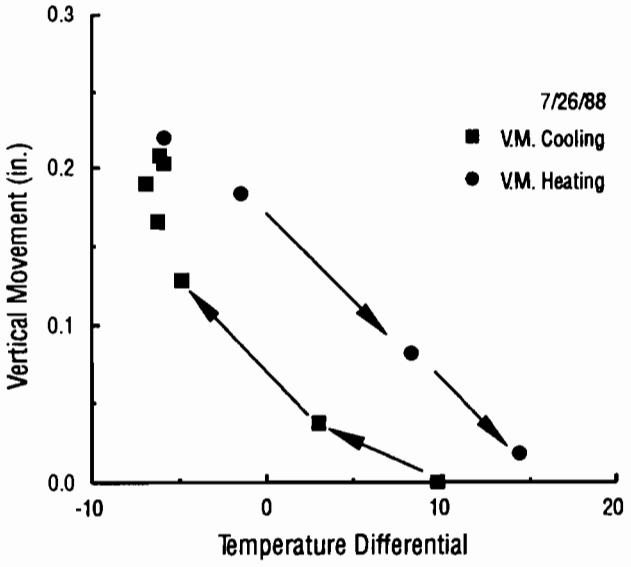

Fig 4.14. Vertical movement heating and cooling cycles.

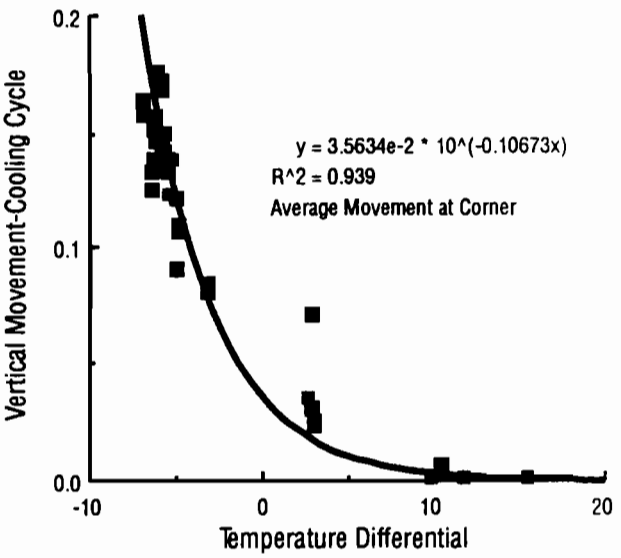

Fig 4.15. Vertical movement—cooling cycle, corners.

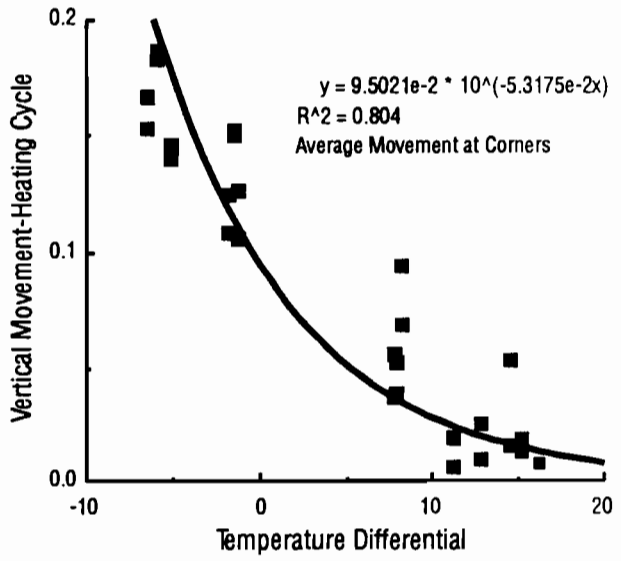

Fig 4.16. Vertical movement—heating cycle, corners.

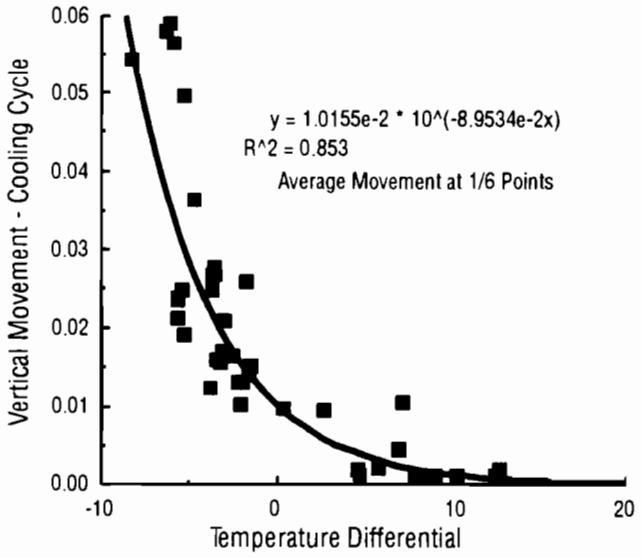

Fig 4.17. Vertical movement—cooling cycle, 1/6 points.

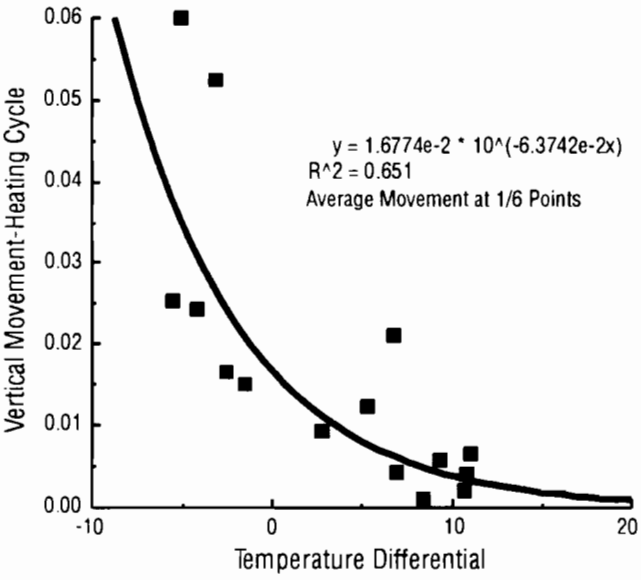

Fig 4.18. Vertical movement—heating cycle, 1/6 points.

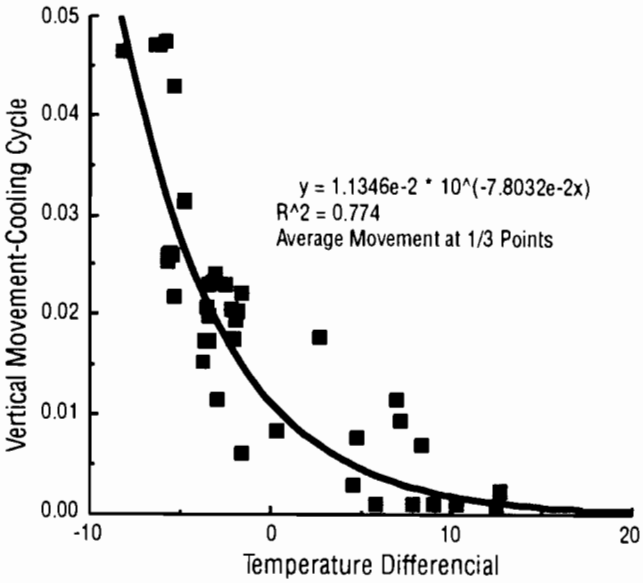

Fig 4.19. Vertical movement—cooling cycle, 1/3 points.

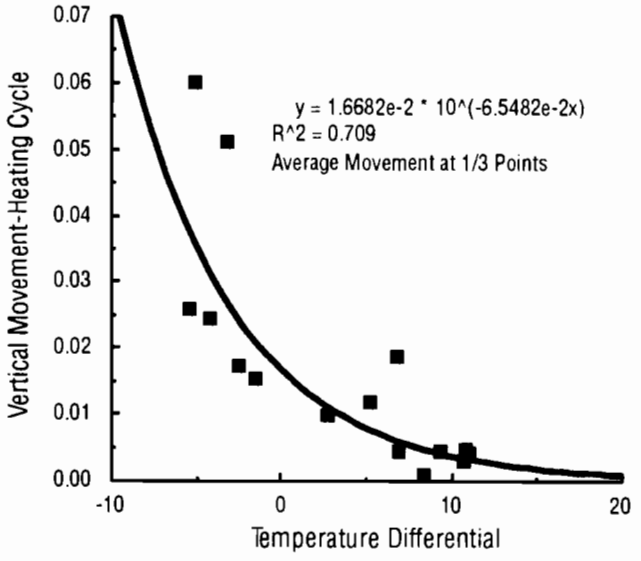

Fig 4.20. Vertical movement—heating cycle, 1/3 points.

JANUARY 1989

The 1989 data were collected in January, or the cold-wet season. The pavement structure was the same as that August 1988, given above.

The parent soil is a dark clay which tends to have expansive properties. The select material is an untreated gravel.

On each occasion, the deflection data were collected using a Dynaflect operated by the Texas SDHPT. It is believed the same Dynaflect unit was used during each collection period. During each collection period, the deflection information was obtained with the Dynaflect centered in the right wheel path of the outside southbound lane of IH 35 and moving south. The longitudinal location was established by engineering stations and the same numerical sequence was used throughout the study period. However, the longitudinal positioning of the Dynaflect varied between the 1983, 1985, and 1988 periods. For example, the 1983 data were obtained at the even station and at a point ten feet downstream (to the traffic flow direction) from the even station number. The 1985 data were collected at intervals of 50 feet, beginning at the even station. The 1988 data were collected with the load wheels positioned just upstream of a joint, just downstream of the joint, and at midspan positions between the joints. The 1988 and 1989 data were obtained at the same longitudinal positions.

Because of the variation in longitudinal positioning and since it was desired to study the changes in pavement strength, a decision was made to study the deflection values at only the midspan locations, as denoted in the 1988 and 1989 collection periods. Therefore, the data which were collected between the joints at the midspan positions were separated and studied. This procedure was pursued for each collection period by using the locations established by the engineering stationing. A detailed description of the data collection and a listing of the data may be found in Research Report 556-1 (Ref 1). It should be noted that the 1988 and 1989 deflection information obtained near the joints was generally greater than the midspan values. This difference could be associated with the vertical movement of the PCP slab at the joints. In 1988 and 1989, deflection information was also collected on the shoulders formed by the PCP. Since deflection data were not obtained at this transverse position in 1983 and 1985, little comparison could be developed and no conclusions were formed.

ANALYSIS OF DEFLECTION DATA

The technique for analyzing the deflection information was to (1) edit the data, (2) determine if differences in deflection could be associated with slab length (that is, the 240 and the 440-foot slabs), (3) study the seasonal effects, and (4) study changes in pavement strength using the Surface Curvature Index (SCI), the Base Curvature Index (BCI), and the Basin Slope (BS). The SCI is the difference in the deflection sensor (geophone) values considering the sensor nearest the load wheel (W1) and the next sensor (W2), which is one foot from the sensor nearest the load. The SCI value is indicative of the strength in the upper layers of the pavement structure. The BCI is the difference in sensor values of the fourth (W4) and fifth (W5) sensors where W4 is about 3 feet from W1 and W5 is about 4 feet from W1. The BCI value is more indicative of the strength of the lower layers of the pavement structure. The BS value is generally associated with the strength of the upper layers of the pavement; however, the value can be influenced by soil or subgrade strengths.

DATA EDIT

The data were edited by plotting the five sensor values obtained at each location. Typically a plot of the five geophone values forms a reverse curve, which is termed a "deflection basin." Generally, outlying plot points or points not fitting the basin are often found to be in error. In the case of the four sets of data considered in this report, outlying deflection values were not found. The deflection basins for the midspan locations were then developed and the basins for each data collection period were observed by considering each PCP slab. That is, for any one slab, the basins for each overlay period were overlaid. These observations indicated two things. First, there is very little difference in deflection between the data collection periods. The W1 value is generally about 0.50 mil, with the maximum about 0.57 mil and the minimum about 0.27 mil. The W5 value is a maximum at about 0.46 mil and minimum at about 0.2 mil. The variation in deflection values between slabs is greater than the variation between measurement periods. Second, even though the difference is small, the deflection values obtained in 1989 are consistently less than the deflection measurements obtained during the other periods. This is particularly true of W4 and W5 values.

EFFECTS OF SLAB LENGTH

Little difference in the midspan deflection values was found when the 240-foot data were compared with the 440-foot values. Therefore, rather than treat the data individually by slab length it was decided to combine the midspan deflection data and disregard slab length as a variable.

EFFECTS OF SEASON

In the Waco area there is probably little seasonal weather difference between August and September. In the fall of the year the summer drought is broken around the later part of September to October. The drought may be broken earlier if rainfall from a hurricane occurs. Generally, the winter is considered to be wet, with periodic

rainfall. The winter season is mild with the lowest temperatures, around 10 to 20°F, occurring during cool fronts of short duration. Roadway damage due to low temperatures is normally confined to the loss of thin lift ACP, because of the daily freeze/thaw moisture just below the surface of the ACP. Freezing of the soil is only a few inches in depth.

Because of these seasonal weather conditions, it was decided to study the seasonal effects of deflection measurements using the August 1988 and the January 1989 data. The weather during August 1988 had been dry and hot, with daily temperatures (°F) consistently between the 70's at night and the high 90's to low 100's during the day. The January 1989 weather was cool and the measurements were purposely delayed until there was periodic rainfall with three days of rain just prior to data collection. The morning that the deflection measurements were collected had a temperature of 17°F. Small quantities of water in the ditches had turned to ice but it is doubtful that the material below the concrete pavement had frozen.

Figure 4.21 shows a comparison of the SCI values of the 1988 (summer) and the 1989 (winter) periods for each slab. Note that the pavement structure is the same for each period. Except for slabs 13 and 14, the data in Fig 4.21 indicate lower SCI (stiffer or stronger upper layers) values during the summer. Figure 4.22 shows a similar comparison of the BCI values. The BCI should be indicative of the strength of the lower layers of the pavement structure, including the subgrade. The comparison shows a randomness, with the BCI of some slabs larger in the winter and of some larger in the summer. Figure 4.23 shows a comparison of summer and winter BS values. Again, with the exception of slabs 1 and 14, the summer values tend to be less.

The data in Figs 4.21 through 4.23 are inconclusive but tend to show the PCP to be stiffer during the daylight hours of the summer, with little seasonal effect in the subbase and subgrade. Since the results were inconclusive, it was decided to use only the data collected during the same season to study the strengths with the addition of PCP.

CHANGES IN PAVEMENT STRENGTH

Figure 4.24 shows a comparison of the SCI before and after the PCP construction. The plot shows the SCI values were smaller in 1988. This indicates the PCP or upper layers of the pavement structure were stronger as compared to the "before" condition. The decrease in SCI varies from zero to about 4.5 times the "before" values.

Figure 4.25 is similar to Fig 4.24 but shows a comparison of the BCI values before and after the PCP placement. These data are varied, with some slabs having lower BCI values before PCP overlay and some slabs having higher BCI values. This information shows that there is little change in subbase or soil conditions due to PCP placement.

Figure 4.26 shows a plot of the BS values before and after the PCP construction. Again, a randomness occurs in the comparison, with some slabs having larger BS values before PCP construction and some slabs having smaller BS values.

CONDITION SURVEYS

The condition surveys performed in this project were visual observations of the pavement condition. The pavement condition was collected in terms of the extent of distress or types of failure modes. For the purposes of this report the condition surveys have been subdivided into (1) the distress occurring in the pavement slab and (2) the general condition observations, which include the joints and seals.

SLAB CONDITION

Condition surveys were obtained at the prestressed concrete locations on two occasions. The first survey was conducted in April 1988. A small amount of longitudinal cracking was noted along with a small pot hole in the outside lane of slab 11. The longitudinal cracking was very tight with only a small crack width. This cracking normally occurred near the outside edge of the outside lane and at times in the right wheel path. In addition, one transverse crack was observed in the inside lane of slab 5.

The second condition survey was obtained on February 9, 1989, near the end of the data collection phase of the project. The pavement was found to be in very good condition. The results of the survey are shown in Figs 4.27(a, b, c, and d). It should be noted that the plots shown are not to scale and that the longitudinal crack lengths shown are relatively short as compared to the slab lengths of 240 or 440-foot. This survey revealed two pot holes. One of these pot holes was in the outside lane of slab 11, as observed in the first survey, and the second pot hole was in the outside lane of slab 16. Both pot holes were small, approximately 1 to 1 1/2 feet in diameter, and appeared to be formed as the result of disintegration of debris, or "clay balls", which was inadvertently introduced into the concrete during mixing. Two transverse cracks were also found. One transverse crack was in the inside lane of slab 5, as noted in the first survey and the second transverse crack was in the outside lane of slab 15. Again the transverse cracks were very tight, with small crack width. The only other distress noted was the longitudinal cracking. The longitudinal cracking seemed to be initiated at the "leave-out pockets" where the stressing was applied to the steel strands during construction. There appeared to be more longitudinal cracking in the shorter length (240-foot) slabs. The longitudinal cracking seemed more dominant near the outside edge of the outside lane and tended to be near the right wheel path.

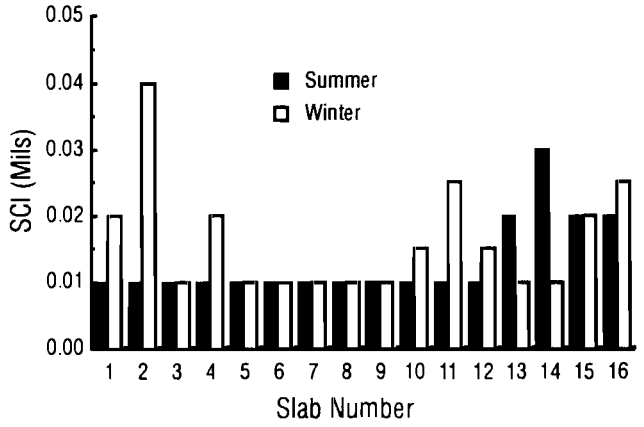

Fig 4.21. Comparison of SCI in summer and winter.

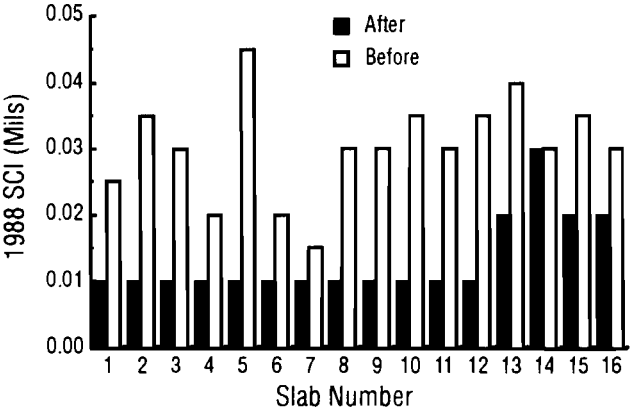

Fig 4.24. SCI comparison—before and after PCP overlay.

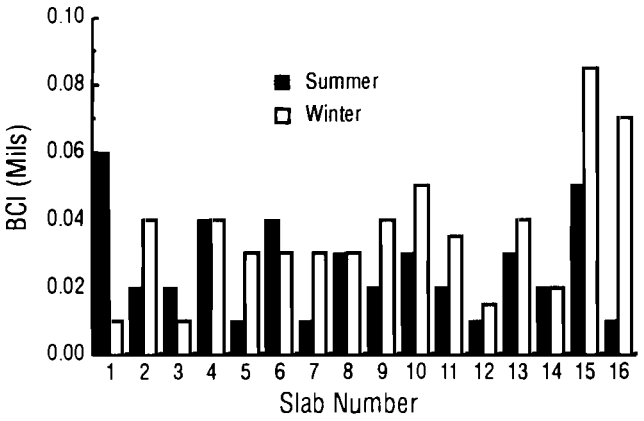

Fig 4.22. Comparison of BCI in summer and winter.

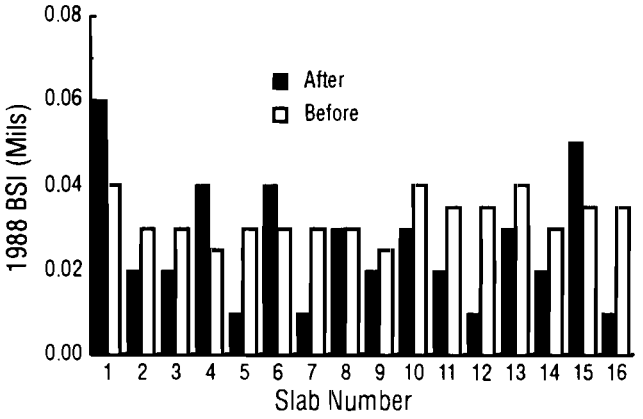

Fig 4.25. BCI comparison—before and after PCP overlay.

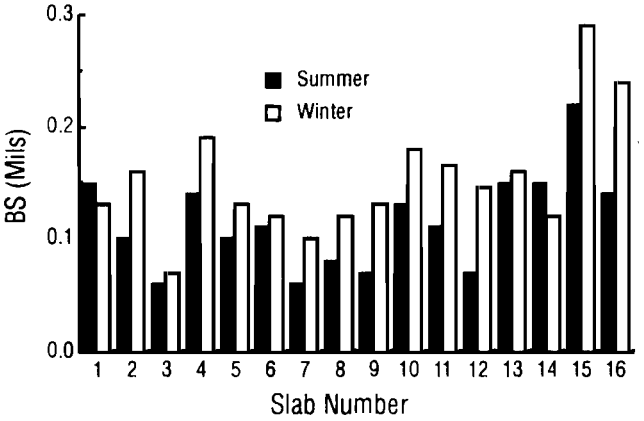

Fig 4.23. Comparison of BS in summer and winter.

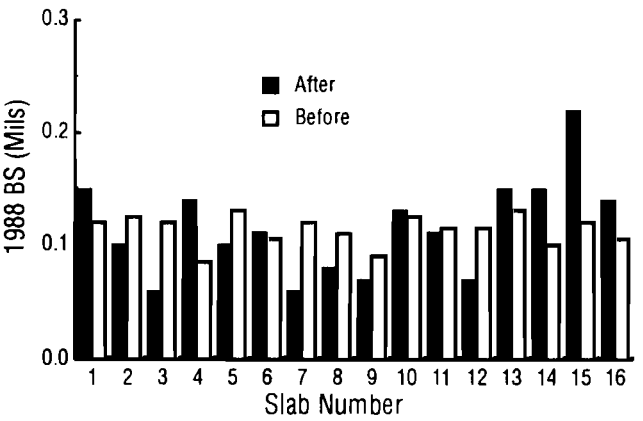

Fig 4.26. BS comparison—before and after PCP overlay.

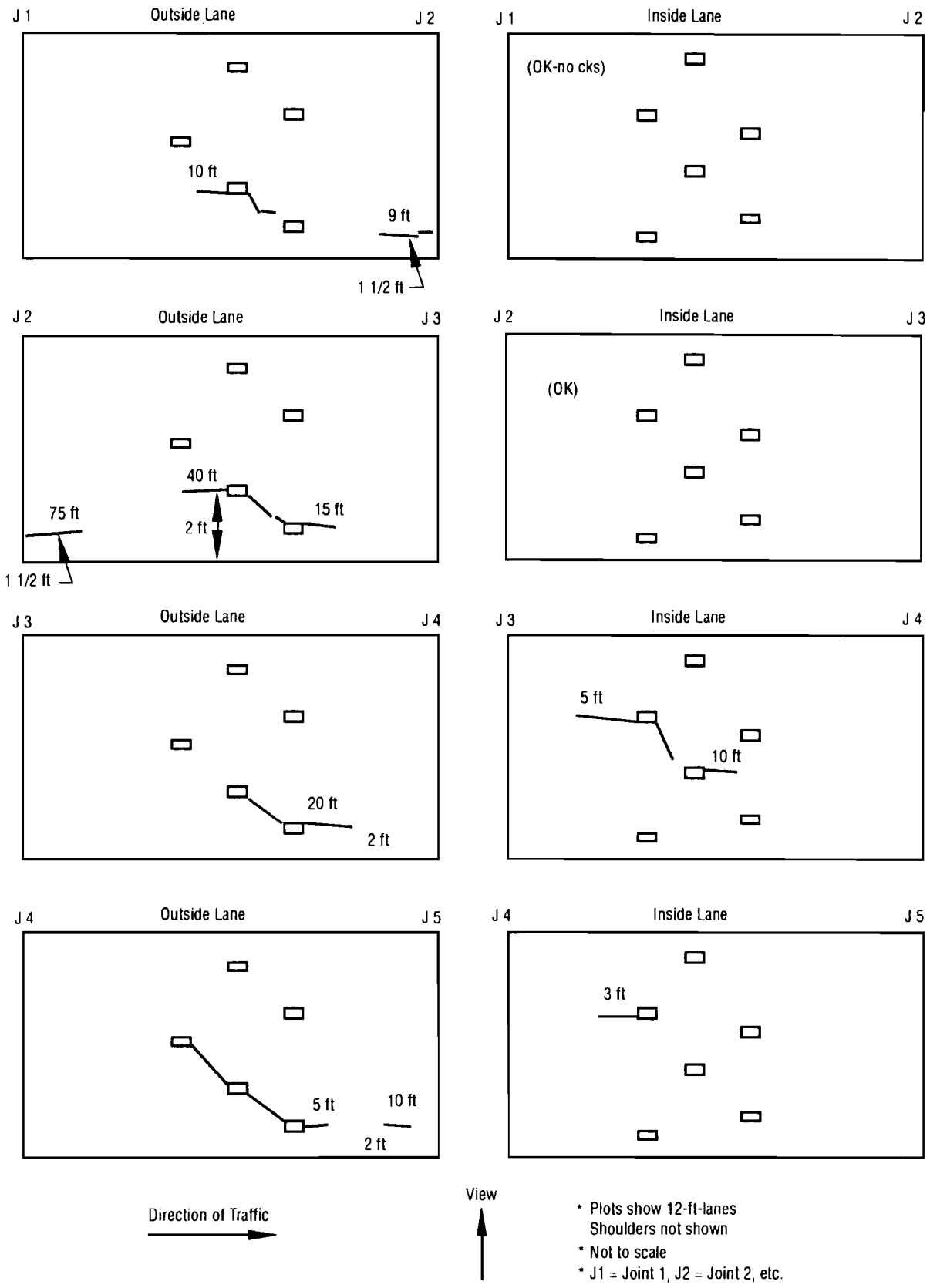

Fig 4.27(a). Condition survey—slabs 1 to 4.

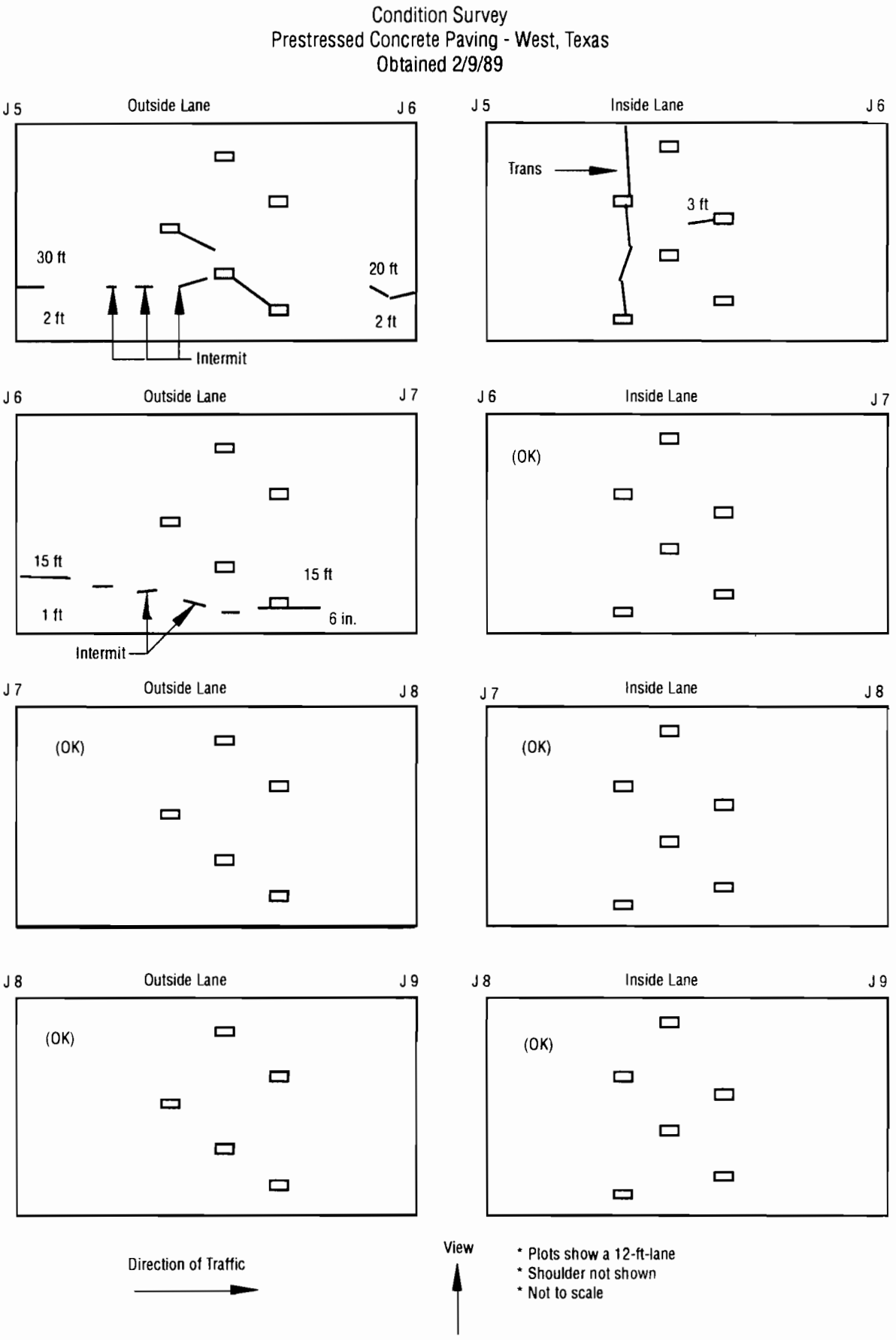

Fig 4.27(b). Condition survey—slabs 5 to 8.

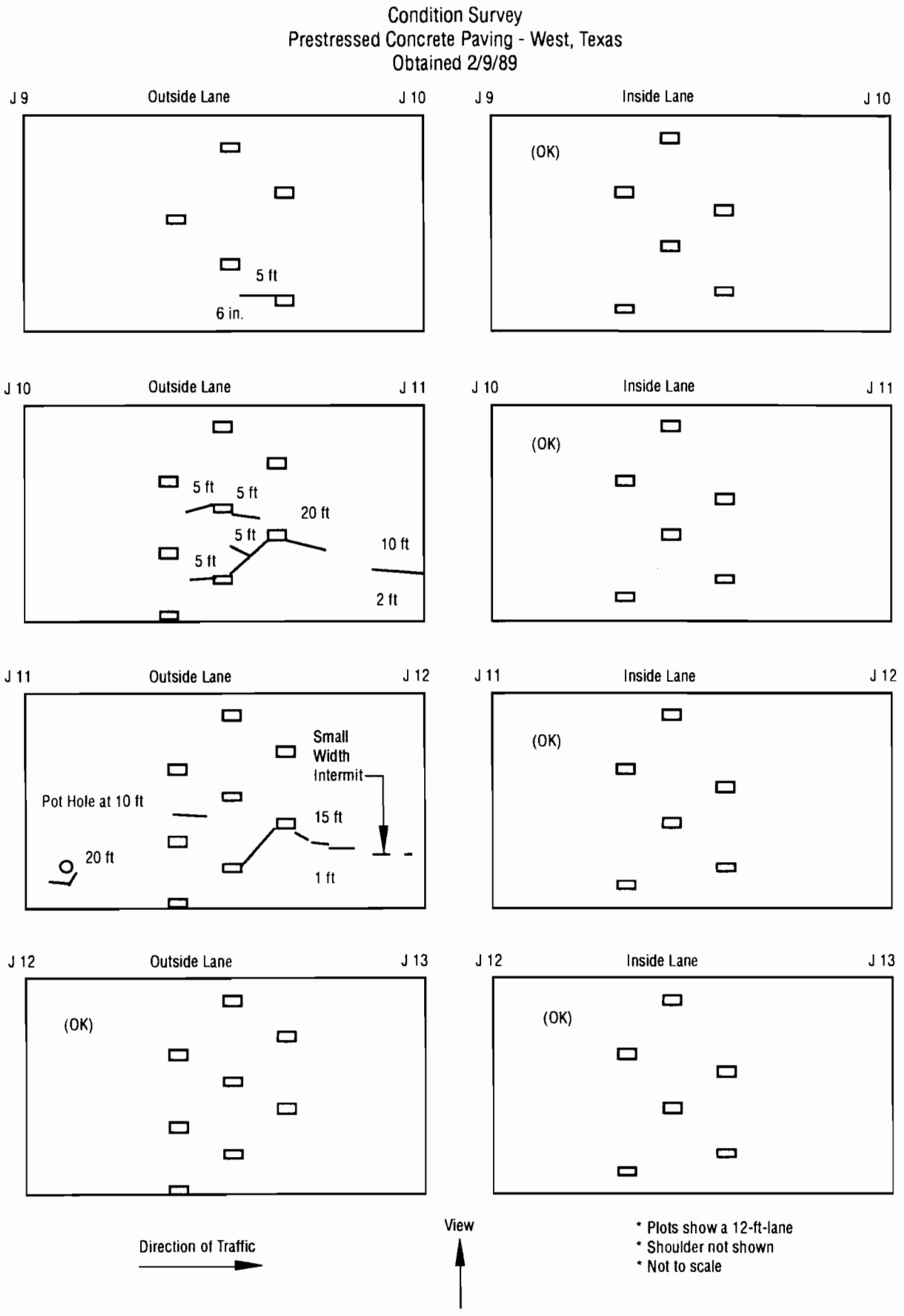

Fig 4.27(c). Condition survey—slabs 9 to 12.

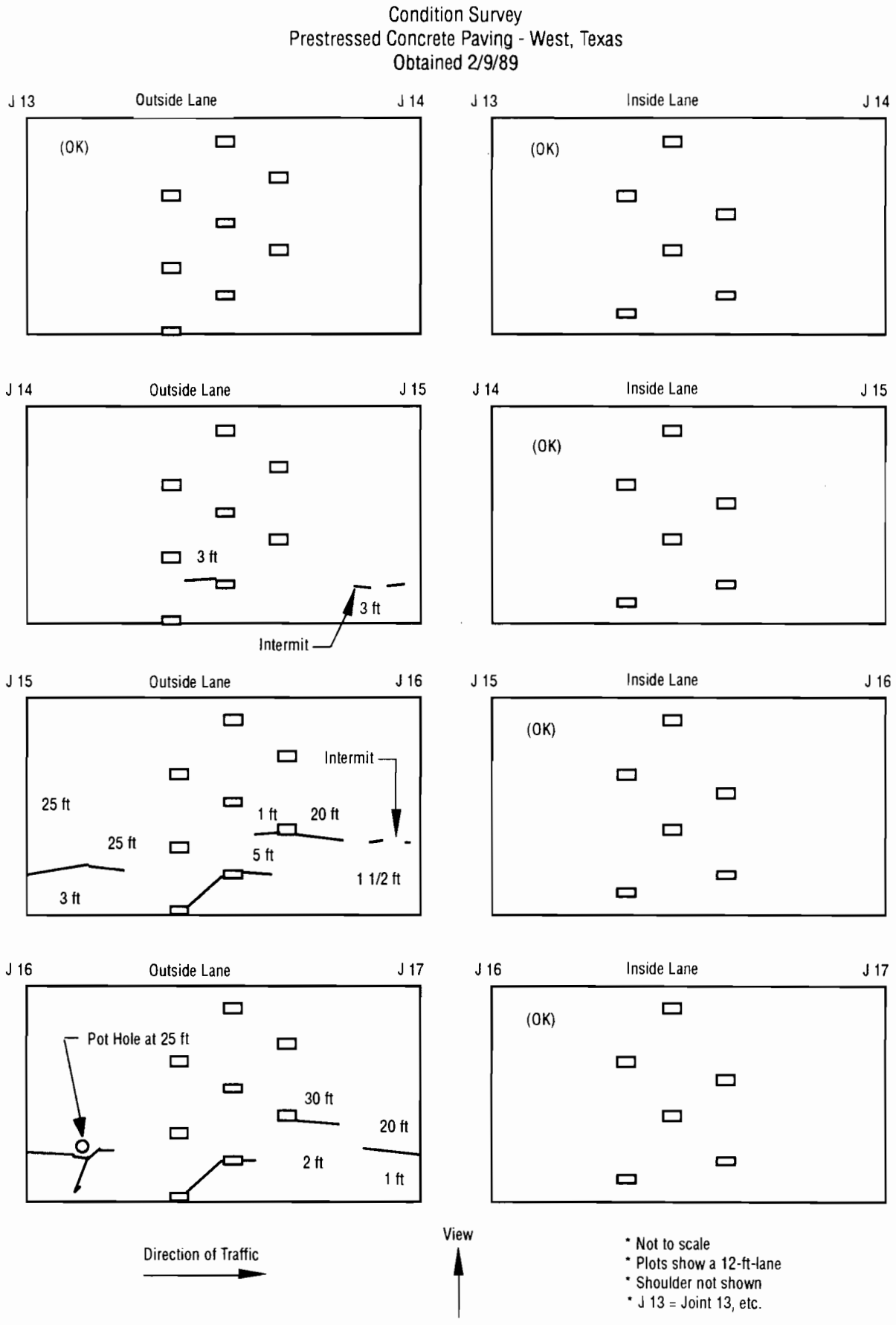

Fig 4.27(d). Condition survey—slabs 13 to 16.

GENERAL OBSERVATIONS

Observations of the paving near the joints show very little distress. There is no spalling or transverse cracking near the joints. Where there is longitudinal cracking that intersects a transverse joint, the crack does not "Y" or deviate near the joint. That is, the longitudinal crack approaches and intersects the joint in a perpendicular manner. The joint design included a thick neoprene diaphragm which attached to the joint edges on each slab to cover the joint opening. Debris was found to lodge in the cavity formed by the neoprene. These debris has cut the neoprene when the slabs have expanded, in warmer temperatures, but, the damage is not excessive and the diaphragms are performing well.

CHAPTER 5. MECHANISTIC MODELING OF PCP

This chapter discusses two types of mechanistic models that were developed to assist in the design and analysis of PCP. The first model, PSCP2, is a revision of a design model, PSCP1, which was prepared in Research Project 3-8-84-401, "Prestressed Concrete Pavement Design—Design and Construction of Overlay Applications." The environmental and performance information collected in the subject project was used to calibrate PSCP1, and PSCP2 is the result. The second mechanistic model developed used a two dimensional finite element technique to develop a specialized analysis of the performance trends noted on the PCP test sections.

PSCP2

Program PSCP2 constitutes the upgraded version of program PSCP1. In program PSCP1, the model of inelastic friction for the prediction of horizontal displacements was introduced and it renders reasonable results. For a more thorough discussion of the former program, PSCP1, the reader should refer to Research Project 3-8-84-401. The calibration of PSCP1 was discussed in Research Report 556-3 (Ref 3).

A REVIEW OF MECHANISTIC MODELING AS RELATED TO PSCP1

The properties of concrete and steel were reviewed in earlier chapters of this report. It was stated that some of the mechanical and physical properties change with time. Strength development, shrinkage and creep of concrete, and the relaxation of steel are among the principal properties that change with time. A presentation of the models used in the PSCP1 program has been included in the following information.

STRENGTH DEVELOPMENT IN CONCRETE

Several studies offer a mathematical description of the development of strength in concrete. In general use are the equations from the Portland Cement Association (PCA) and the American Concrete Institute. These formulas describe an exponential function of strength development. Estimates of concrete modulus of elasticity and strength as a function of time are needed for predicting PCP behavior. The models adopted from the literature for evaluating these concrete properties in PSCP1 are included here.

STRENGTH

Generally, the value of the final strength is assumed in design and used during construction. At times the practice is to take samples of the mix and test the specimens at 3, 7, 14, and 28 days of age. Next, the strength development is checked against the standards. Variation in strength can be expected for different reasons, such as type of cement or cement admixtures. But, for design purposes, values from strength curves generated from this type of information are generally considered to be close to reality. However, these values must be updated to represent the development achieved with new cements and admixtures.

Provision has been made in the PSCP1 program to input the relationship of the time-strength of the mix. However, If the compressive strength as a function of time is not known, the prediction of the modulus of elasticity is made possible through the use of typical values developed from the percentage of the 28-day compressive strength for various intermediate ages tested by the US Bureau of Reclamation (Ref 40). A plot of this data may be found in Report 401-3 (Ref 19). If this procedure is to be used, the only information required is the compressive strength at 28 days. However, it is recommended that users develop a typical plot of data which is representative of the material to be included in construction.

Modulus of Elasticity

The following relationship specified by the ACI (Ref 41) was selected for the computation of the modulus of elasticity. This formula is useful in those cases when the time relationship is known and the aggregates are close to the gradation standards:

$$E_c = \gamma^{1.5} \sqrt[33]{f'_c} \qquad (5.1)$$

where

E_c = modulus of elasticity of concrete, psi;
g = unit weight of concrete, pcf; and
f'_c = compressive strength, psi.

Some research has been undertaken by CTR on the aspects of the development of strength and modulus of elasticity. This work has been assigned to Research Project 3-8-86-422, "Evaluation of Pavement Concrete Using Texas Coarse Aggregates." The determination of representative values for Texas is discussed later in this report.

CONCRETE SHRINKAGE

In the determination of the shrinkage, program PSCP1 makes use of the following expression suggested by Hansen and Mattock (Ref 42):

$$\frac{Z_t}{Z^{\infty}_t} = \frac{t}{M + t} \qquad (5.2)$$

where

$M = 26\, e^{0.36(V/S)}$,
V = volume of the member in inches,
S = exposed surface area in inches,
t = time in days after concrete is set,
Z_t = drying shrinkage strain at time t, and
Z_t^{∞} = final value of shrinkage strain.

For pavement slabs, where drying occurs from the top surface, the ratio of volume to surface area is the thickness of the concrete slab.

Therefore,

V/S = pavement thickness D in inches.

While other models have been proposed (Ref 25), general agreement between researchers has not been reached.

CREEP

Creep magnitude in portland cement concrete varies with gradation of concrete aggregate, particle shape, aggregate type, cement content, water-cement ratio, concrete density, curing, age at loading, load intensity, etc. Several researchers have studied creep in concrete. Creep and shrinkage have been expressed as a function of time. Among these expressions are those proposed by Wittman and Lucas (Ref 43) and Gamble (Ref 44). Other researchers have proposed qualitative models. Neville (Ref 45) and Feldman (Ref 46) are among them. However, PSCP1 does not use a model for creep. Instead, it uses an initial value to compute the final creep. Here, creep strain is nearly proportional to the initial strain in the concrete upon loading. Therefore, it is possible to define a creep coefficient C_u as

$$C_u = \frac{\varepsilon_{cu}}{\varepsilon_{ci}} \tag{5.3}$$

where e_{ci} is the initial or elastic strain in the concrete and e_{cu} is the additional or creep strain.

Creep at any time t in days can be estimated (Ref 47) as

$$\varepsilon_{ct} = \frac{t^{0.60}}{10 + t^{0.60}} \cdot C_u \tag{5.4}$$

Correspondingly, the creep strain at time t as a function of the ultimate concrete creep strain is

$$\varepsilon_{ct} = \frac{t^{0.60}}{10 + t^{0.60}} \cdot \frac{\varepsilon_{cu}}{\varepsilon_{ci}} \tag{5.5}$$

An ultimate creep coefficient between 2.3 and 2.5 is suggested for computing creep associated strains of PCP slabs (Ref 24). In PSCP1 a default value of 2.35 is assumed by the program if this term is not provided by the user.

STEEL RELAXATION

Steel relaxation is defined as the loss in steel stress when it is held at a constant strain level. The expression adopted for PSCP1, is an equation commonly used by designers of PCP slabs (Refs 30 and 48). Equation 5.6 provides a reasonable estimate of the steel relaxation after t hours of stress (Ref 48):

$$f_{pt} = 1 - \frac{\log t}{10}\left(\frac{f_{pi}}{f_{yi}} - 0.55\right) f_{pi} \tag{5.6}$$

where

f_{pt} = prestress level in the steel after t hours,
f_{pi} = initial prestress level in the steel,
t = time in hours after initial prestressing, and
f_{yi} = steel yield stress.

The quality control and homogeneity exhibited by steel make the use of reliable models possible. Thus, little discrepancy exists around this model.

MODELS WITH THE FUNCTION OF ENVIRONMENT AS A PRINCIPAL PARAMETER

As stated previously, environment can be characterized in terms of moisture and temperature. Two principal effects are a result of a changing environment, friction, and curling. Models used in PSCP1 for both phenomena are discussd here.

FRICTION IN SLAB SUBGRADE

Since slab and subgrade are in extensive contact, friction develops between them. For pavement slabs, the magnitude of the movements produced by a daily temperature cycle depends on the location along the slab length. Maximum friction forces develop at the slab ends and decrease toward the center. Concrete stresses resulting from the accumulation of friction forces grow from the end to the center. There are two theories predicting these phenomena, elastic and inelastic. These theories are depicted in Fig 5.1. They are discussed below because of the importance of friction in the output of PSCP1.

THE ELASTIC MODEL

The elastic model has been discussed extensively in the available literature. It assumes friction forces may be considered elastic if sliding does not occur along the slab.

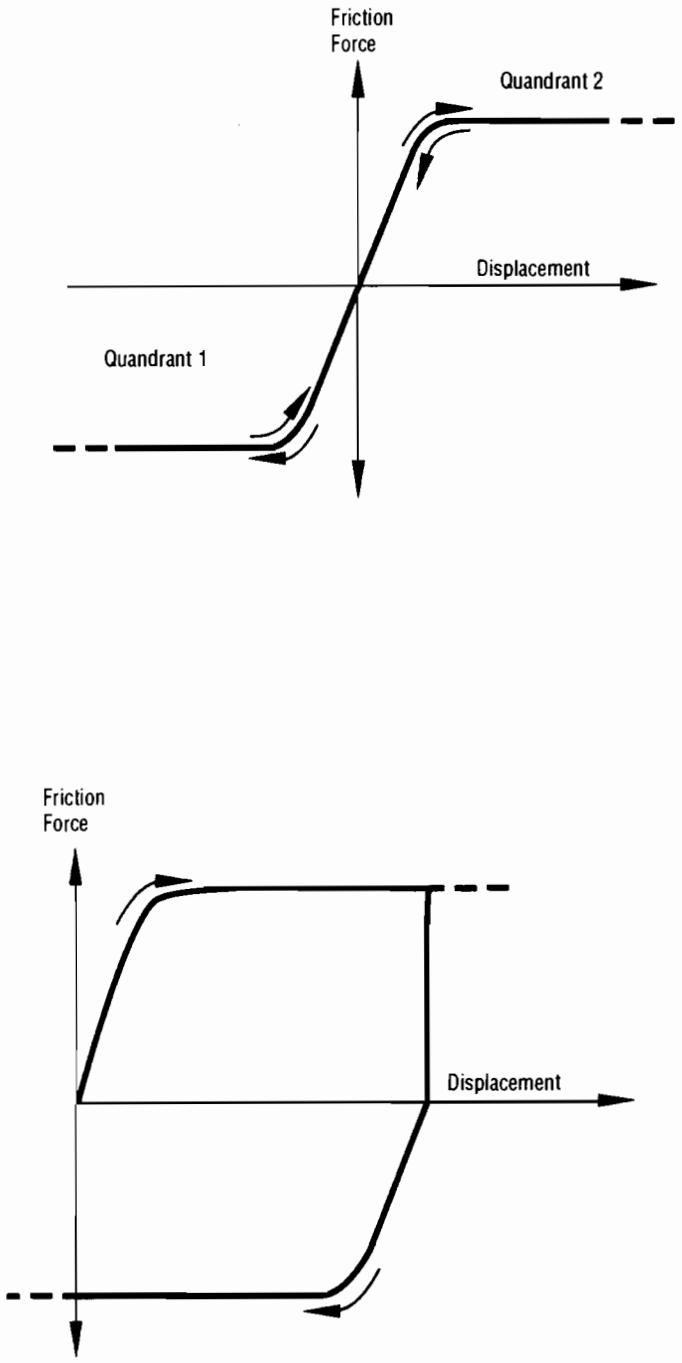

Fig 5.1. Elastic and inelastic models of friction curves (Ref 19).

This is the case for plain concrete and conventional reinforced concrete pavements typically shorter than 40 feet. Here, stresses will be proportional to the expansion or contraction force of the slab. An elastic system of friction forces, following a force versus movement curve, is shown in Fig 5.1. This model was assumed by McCullough et al. (Ref 49) and Rivero-Vallejo and McCullough (Ref 50) in the development of design models for CRCP and JRCP pavements. The reader should refer to them for an indepth discussion. These are some relevant implications of this theory:

(1) The slab will develop compressive stresses whenever the temperature exceeds an initial reference temperature.
(2) Equal stresses are obtained for other temperatures representing equal temperature changes with respect to the reference temperature.
(3) Shrinkage and other sources of long-term longitudinal movement do not occur without frictional resistance but accumulate on a daily rate basis, resulting, eventually, in the maximum friction forces and concrete restraint stresses.

Another result is that tensile stresses produced by movement reversals cannot be predicted if the friction forces are used in the elastic model.

THE INELASTIC MODEL

When inelastic friction forces are assumed, reversals of slab movement can take place as a result of slab contraction or expansion. The elasticity leads to reversals of the direction of the friction forces. Accordingly, a slab cast at the minimum temperature of the day will develop compressive stresses when the temperature is above this minimum temperature. A few hours after the slab reaches peak temperature, the slab movement reversal causes a friction force reversal. Then tensile stresses build up in the slab. Reversals of movements exceeding 0.01 to 0.02 inch, result in reversals of frictional resistance. These amounts of movement are particularly true if friction reducing materials are used beneath the slab.

Some results from assuming an inelastic system of friction forces beneath the slab (Ref 19) are:

(1) Slabs cast at the minimum temperature of the day will develop compressive stresses during the part of the temperature cycle at which the temperature increases above the set temperature. A few hours after the peak temperature, the reversal of frictional resistance causes the build-up of slab tensile stresses.
(2) The long-term sources of longitudinal movement, occurring at small daily rates in comparison with the daily contraction and expansion, takes place without frictional resistance and, practically, does not cause stresses in the concrete slab.

This behavior can be explained based on the mechanism shown in Fig 5.2. If the slab starts contracting from the maximum temperature of the day, point A in Fig 5.2 will move from its initial position Z_{A0} to Z_{A1} for the maximum contraction of the day. The part of the movement Z_{A1} due to the temperature drop is Z_{AT1}; the rest of it is produced by the small portion of

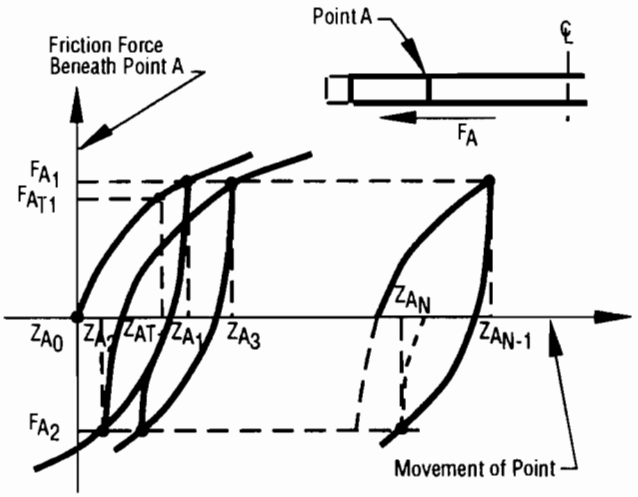

Fig 5.2. Shifting of point A without frictional resistance for long-term movements if an inelastic system of friction forces is assumed (Ref 2).

long-term movement occurring during the day. This portion of movement does not cause a significant increment in the friction force (from F_{AT1} to F_{A1}). If the temperature rises to the maximum again, point A moves to position Z_{A2}, reducing the force F_{A1} and increasing the friction force F_{A2} in the opposite direction. The point does not come back to Z_{A0} because a portion of long-term contraction has occurred. Z_{A2} is the new initial position for the movement of the next cycle. For the next day cycle, the portion of long-term movement occurring during the day causes a small increment of friction force again, but the effect is not cumulative with the force increment of the previous cycle, which had already dissipated when the slab movements reversed. Therefore, Point A like the rest of the points of the slab will shift following this mechanism without significant build-up of friction forces from the long-term movements. Another implication of assuming inelastic friction forces is that the long-term sources of longitudinal movement (shrinkage, creep, etc.), occurring at small daily rates (as opposed to the contraction and expansion movements of the daily cycle, which are fairly substantial), occur practically without frictional resistance and do not cause concrete stresses. This behavior could not be predicted if the friction forces were assumed elastic. If elastic friction forces are assumed, the long-term movements, usually representing contractions, accumulate on a daily rate basis, resulting in an eventual build-up of maximum friction forces and slab stresses.

Figure 5.1(b) illustrates the type of friction force versus movement curve assumed in PSCP1. A few hours after reaching the peak temperature, the slab movement reversal causes a friction force reversal and the build-up of tensile stresses in the slab. This behavior cannot be predicted with elastic models.

The inelastic nature of the friction forces developing beneath long pavement slabs was denoted in studies by Fridberg and Stott (Refs 35 and 36). This type of friction was assumed for PSCP1. A more thorough discussion of the basis and development of this theory is presented by Mendoza-Diaz et al. in Research Report 401-3 (Ref 19). Here, we refer only to the assumptions and models produced in this former project Ref 19).

The environmental model is composed of two submodels:

(1) The first is used to simulate the contraction or expansion of the slabs away from maximum or minimum temperatures of the thermal cycle.

(2) The second is required to simulate the stress relief mechanism and reversal of movements of the slabs immediately after maximum or minimum temperatures of the thermal cycle.

ASSUMPTIONS OF THE MODEL

The following assumptions are made in the derivation presented herein:

(1) Concrete is a homogeneous, linearly elastic material. The slab is a solid body without discontinuities, such as cracking.

(2) The frictional resistance produced by dowels, tie bars, and lanes adjacent to the slab longitudinal movements is neglected.

(3) The relationship of the friction coefficient versus displacement under the slab is described in Fig 5.1(b).

(4) The temperature variations considered in this analysis are those occurring at the slab mid-depth. The friction stresses that develop are considered as evenly distributed on the cross section. As a result of this assumption, a one-dimensional analysis of an axial structural member is applicable.

(5) The redistribution of the slab weight due to curling and warping, which affects the friction forces developing beneath the slab, is neglected.

(6) The effect of concrete creep before application of prestress forces is neglected too.

(7) Symmetry of conditions with respect to the geometric center of the slab is assumed. Therefore, the analysis will be limited to the half-slab length, with the geometric center being fixed.

(8) The origin for slab length X in the longitudinal direction is at the midslab. Friction forces are positive in the positive X direction. Movements in the positive X direction are also positive. Friction forces and movements are always of opposite signs. Tensile stresses in the concrete are positive. Mid-depth temperature changes are positive if they represent temperature increments at a given time, for an earlier time considered.

SUBMODEL FOR CONTRACTION AND EXPANSION

The equilibrium of forces in the slab segment to the right of the element considered can be written as

$$F_X = \int_X^{L/2} U_X \, g \, h \, dx \tag{5.7}$$

where

g = concrete unit weight, and
h = slab thickness.

This equation represents the equilibrium condition for a section located a distance X from the center of the slab. The equation is a function of the friction coefficient Ux developed below the elements dx located to the right of section X. Equation 5.7 can be transformed to the stress equation

$$F_X = \int_X^{L/2} U_X \cdot \gamma \cdot dx \tag{5.8}$$

The deformation dZ_X of the length element dX is

$$dZ_X = \underbrace{\alpha \cdot \Delta T \cdot dX}_{\text{free deformation}} + \underbrace{\left(\frac{f_X}{E_c}\right) dX}_{\text{part of deformation restrained by the friction}} \tag{5.9}$$

The unit deformation at point X is

$$\frac{dZ_X}{dX} = \alpha \cdot \Delta T + \frac{f_X}{E_c} \tag{5.10}$$

and

$$\frac{f_X}{E_c} \leq -\alpha \cdot \Delta T \tag{5.11}$$

The movement Z_X is

$$Z_X = \int_0^X \alpha \cdot \Delta T \cdot dx + \left(\frac{f_X}{E_c}\right) dx \tag{5.12}$$

Here, the term f_X represents the resisting frictional stress of the elements to the left of point X . Equation 5.12 gives the movement of the concrete at any point X along the slab.

The coefficient of friction below each element dx is expressed as

$$U_X = F(Z_X) \text{ if } Z_X \geq 0 \tag{5.13a}$$

or

$$U_X = -F(Z_X) \text{ if } Z_X > 0 \tag{5.13b}$$

The profiles of movements, concrete stresses, and friction forces can be determined by solving simultaneously Eqs 5.9, 5.12, and 5.13, subject to the restriction of Eq 5.11. The integrals in Eqs 5.9 and 5.12 are evaluated numerically, with the slab divided into discrete elements. The movements of the nodes and the average restraint stresses of the elements are computed.

SUBMODEL FOR MOVEMENT REVERSAL INTERVALS

Just beyond the end of the cycle, the next temperature variations change from temperature drops to temperature increments. Due to this reversal of temperature variations, the elements of the slab are assumed to relieve the restraint stresses first, and then to experience expansion deformations. Segment 2 is analyzed considering that its elements tend to develop the expansion unit deformation:

$$\varepsilon_X = \left(\alpha \cdot \Delta T_r - \frac{f_{x1}}{E_c}\right) \tag{5.14}$$

The analysis of both segments follows the principles of submodel 1. However, for segment 1, the stress equation includes the internal force Fa acting at the end of the segment:

$$f_x = \frac{F_a}{h} + \int_0^X U_x \, g \, dx \tag{5.15}$$

Equation 5.12 is restated as

$$Z_X = \int_0^X \alpha \cdot \left(\Delta T_1 + \Delta T_r\right) dx + \left(\frac{f_x}{E_c}\right) dx \tag{5.16}$$

For segment 2, Eq 5.12 is redefined as

$$Z_X = Z_{X1} + Z_{Xr} \tag{5.17}$$

where

$$Z_{Xr} = (Z_{Xa} - Z_{X1}) + \int_{Xa}^X \varepsilon_x \, dx + \left(\frac{f_X}{E_c}\right) dx \tag{5.18}$$

and

e_x = expansion strain of the elements between point A and the point X considered within segment 2 (defined by Eq 5.14),

f_x = concrete stress of the points between point A and point X,

Z_{Xa} = movement of end point A of segment 1, evaluated from Eq 5.16,

Z_{X1a} = "initial" contraction movement of end point A of segment 1, and

Z_{Xr} = expansion reversal experienced by the points of segment 2 starting from the initial contraction Z_{X1}.

The term f_x in Eq 5.18 is evaluated from the following expression:

$$f_X = \int_X^{L/2} U_{xr} \cdot \gamma \cdot dx \qquad (5.19)$$

where the friction coefficient U_{xr} is determined from relationship 5.13 as a function of the reversal Z_{xr}:

$$U_{xr} = F(Z_{xr}) \text{ if } Z_{xr} <= 0 \qquad (5.20a)$$

or

$$U_{xr} = -F(Z_{xr}) \text{ IF } Z_{xr} > 0 \qquad (5.20b)$$

Iterative Solution. The solution procedure consists of applying the successive iterative procedure (SAP) proposed in Report 401-3 (Ref 19) for submodel 1 consecutively on both segments. Profiles of movements, friction coefficients, and stresses along the slab are obtained after convergence is reached.

Simulation of Consecutive Cycles. The simulation of consecutive cycles is achieved following the principles described earlier. The position reached by the slab elements at a specific reversal ZXi and the restrained strain of the elements f_{Xi}/E_c, represents the initial condition for computation of further movements and stresses after the reversal. After reversal i, the slab has to experience a relieving process of the restrained strains first, which can be modeled with submodel 2. Once this stage is completed, submodel 1 is applicable until the next reversal occurs. Then, submodel 2 can be applied again for the subsequent cycle.

Slab elements tend to experience unit deformations e_x after a reversal. They are determined for the initial condition defined at the reversal. The unit deformations e_{xi} of the elements after reversal is computed as follows:

$$\varepsilon_{xi} = \alpha \cdot \Delta T_{ri} - \frac{f_{Xi}}{E_c} \qquad (5.21)$$

where

e_{xi} = unit deformation that an element dx located a distance X from midslab tends to develop after the reversal i,

ΔT_{ri} = magnitude of temperature change with respect to peak or to the temperature at reversal i,

f_{Xi} = restrained strain of element dX reached at reversal i.

The unit deformations e_{xi} from Eq 5.21 are the unit deformations input into submodels 2 and 1 consecutively for analyzing the cycle after reversal i. The position reached by the slab elements at the end of this cycle and the restrained strains of the elements represent the initial condition for the subsequent cycle after reversal i+1.

Length changes due to seasonal cycles are computed in PSCP1, as discussed previously.

Profiles for the Coefficients of Friction. Three types of friction relationships can be input into the program: a straight line, an exponential curve, and a multilinear curve. For a straight line, only one point is required to define the curve, the point where sliding occurs. The mirror image of the curve type used for the slab base friction is used for movements reversing direction. Here, the new origin is where the reversing movement starts occurring.

For an exponential curve, the program uses a function of the following form:

$$U = U_{max} \left(\frac{Z}{a}\right)^{1/3} \qquad (5.22)$$

where

U_{max} = maximum friction coefficient,

Z = movement of a given point of the slab,

U = friction coefficient corresponding to movement Z, and

a = movement at sliding point.

For the elastic profile, the straight line equation is generated, and, for the multilinear case, the profile is defined by the user.

FRICTION IN CONCRETE AND STEEL

Interaction between steel and concrete was mentioned before. There are two stresses produced by the interaction between concrete and steel. The first is the friction in the casing while the second is a product of the deformation between steel and concrete.

Friction in the Prestress Casing. There is a difference between friction in CRCP and PCP. In CRCP, steel and concrete are in direct contact, while in PCP this is not the case. In PCP, steel tendons must be free from bonding to be prestressed. To add protection and prevent

a bond between concrete and steel, prestressed steel is encased in a conduit. The conduit is normally greased to reduce friction between the conduit and the strand. However, there are some bends due to the length of the slab or the strand layout. When the steel is prestressed, contact and friction develop between steel and the casing. The result is a loss in the efficiency of the prestress. Its degree varies with the strand layout, encasing of the strands, etc. Friction increases with length and curvature. General values for coefficients of friction range between 0.001 and 0.003 per feet or 0.089 per radian inch, the latter in the case of loops. Besides, the quality and condition of the casing are paramount. Damage in the casing can produce an increase of fifty percent in the friction. The general formula for the calculation of the friction force is

$$Ps = P_x e^{(Klx + \mu y)} \tag{5.23}$$

where

P_x = prestressing tendon force at jacking end, in kips,
K = wobble friction coefficient per foot of prestressing tendon,
lx = length of tendon,
μ = curvature friction coefficient,
y = total angular change of prestressing tendon from jacking end to any point X, in radians.

Values and results of friction tests in steel tendons are included in Research Report 401-6 (Ref 22).

Compatibility Relationship Between Concrete and Steel Deformations. In PSCP1, relative movements between concrete and steel are assumed to occur freely. Then, the model departs from the strain produced from the restriction of movement. That is,

$$\Delta F_c = -\Delta F_s \tag{5.24}$$

where

$$\Delta F_c = \frac{-E_c (Z_e - Z_{re}) A_c}{L/2} \tag{5.25}$$

and

$$\Delta F_s = \frac{E_s \cdot Z_{re} \cdot A_s}{L/2} \tag{5.26}$$

where

E_c = concrete modulus of elasticity,
E_s = steel modulus of elasticity,
Z_e = unrestrained end movement,
Z_{re} = actual end movement,
A_c = transverse area of concrete slab, and
A_s = reinforcing steel area.

The final expression for the stresses induced (Ref 19) is

$$\Delta f_c = \frac{\varepsilon_c \cdot E_c}{1 + 1/\rho n} \tag{5.27}$$

and

$$\Delta f_s = \frac{\varepsilon_c \cdot E_s}{1 + \rho n} \tag{5.28}$$

where

r = reinforcement percentage and
n = ratio of steel to concrete moduli.

Other strains produced by seasonal temperature variations, shrinkage, and creep occurring from post-tensioning until the time of analysis are included in PSCP1 for calculation.

CURLING AND WARPING

On this aspect of pavements, very few investigations have been performed and only a small amount of data has been offered. However, new models of wide acceptance have not been produced. The deflections and stresses for temperature and moisture gradients from the top to the bottom of slabs are determined using the principles of beams on an elastic foundation. The solution for a slab with an infinite edge and extending infinitely in the X direction, perpendicularly to its edge, as presented by Westergaard (Ref 52), is the solution adopted in PSCP1. Because of its importance in the output of PSCP1, the assumptions, general equations and solution of this model are included here.

The assumptions of this model are

(1) The vertical reaction to any section is directly proportional to the deflection Y, the proportionality constant k being the modulus of subgrade reaction.
(2) Zero deflection is at the position of rest on the level subgrade from the initial deflection w/k, w being the weight of the slab.
(3) Concrete is a homogeneous, linearly elastic material.
(4) Temperature or moisture differentials from top to bottom producing upward deflections are negative.
(5) Upward deflections are positive.
(6) Tensile stresses are positive.
(7) The origin of coordinate X is taken as the mid-slab.

General Equations. Assuming the temperature is DT_D degrees higher at the top of the pavement than at

the bottom, the curvature of the middle plane of the pavement in the X direction is

$$\frac{d^2y}{dx^2} = \frac{12\,(1 - n^2)M_x}{E_c \sum h^3} - \frac{(1 + n) \sum a \sum \Delta T_D}{h} \quad (5.29)$$

where

a = concrete thermal coefficient of contraction and expansion,
n = Poisson's ratio of concrete,
M_x = bending moment in x direction per unit width, and h and E_c are as defined above.

The equilibrium of any small element of the slab requires that

$$\frac{d^2\,Mx}{dX^2} = -K \cdot Y \quad (5.30)$$

Solutions. Combining Eqs 5.29 and 5.30 and introducing the radius of relative stiffness,

$$4\frac{d^4Y}{dX^4} + Y = 0 \quad (5.31)$$

where

$$l = \sqrt[4]{\frac{E_c\,h^3}{12\,(1 - \nu^2)\,k}} \quad (5.32)$$

At the edge X = L/2, where L is the slab length, the bending moment M_x and the vertical shear dM_x/dX must be 0. Therefore, the following equations may be used for deflections:

$$Y = Y_e \sqrt{2} \cdot \cos\left(\frac{\frac{L}{2} - X}{l \cdot \sqrt{2}} + \frac{\pi}{4}\right) e^{-\left(\frac{\frac{L}{2} - X}{l\sqrt{2}}\right)} \quad (5.33)$$

where Y_e is the deflection at the edge:

$$Y_e = \frac{(1 + N) \sum a \sum \Delta T_D \sum l^2}{h} \quad (5.34)$$

and, by substituting these expressions in Eq 5.33, the bending moment M_x is obtained. By dividing M_x by the section modulus per unit width, $h^2/6$, the tensile stress at the bottom of the slab at any location X is obtained:

$$f_{cx} = f_{co}\,1 - \sqrt{2} \sin\left(\frac{\frac{L}{2} - X}{l\sqrt{2}} + \frac{\pi}{4}\right) e^{-\left(\frac{\frac{L}{2} - X}{l\sqrt{2}}\right)} \quad (5.35)$$

where f_{co} is the stress for the fully restrained curling deformation differential:

$$f_{co} = \frac{E_c \sum a \sum \Delta T_D}{2(1 - n)} \quad (5.36)$$

The same solutions can be applied to warping deflections and stresses, if the term ΔT_D is exchanged with the warping deformation from top to bottom w_D.

EFFECT OF MODELS IN PCP

In this section, the effects of models and input on PSCP1 are inspected. The input is also considered. The purpose is to outline the best path for the calibration. The criterion that will be followed is that models that have a higher effect will be calibrated first. Next, the calibration will proceed with models of secondary importance to the output. Then, the calibration will be gradual.

The models that have a higher effect on the input are those used for the determination of the stresses and movements due to friction and curling. They are followed by the functions of the prediction of post-tensioning, the functions of steel, and the functions of concrete. The inputs for the k-value for soil, the creep, and the shrinkage follow. Inputs of importance are the strength of concrete, modulus of elasticity, Poisson's ratio, and thermal coefficient of soil.

The friction model is iterative. This can induce roundup or truncation errors. The function of this model is a numeric integration of a polynomial function. The degree of the polynomial is given by the profile of the coefficients of friction. The magnitude of an error due to mismodeling of the friction can be illustrated with part 6 of Fig 5.3(b), which illustrates the difference between two polynomials of different order. For this determination, the employment of the correct coefficients and profiles of friction is necessary.

Curling is an important output item. Temperature gradients, thermal coefficients, modulus of elasticity, Poisson's ratio, and the k-value are considered in curling determination. Because of the architecture of PSCP1, most of these inputs are considered in the program as constants, and the only variable affecting curl is the friction profile. Therefore, this effect is easy to detect once

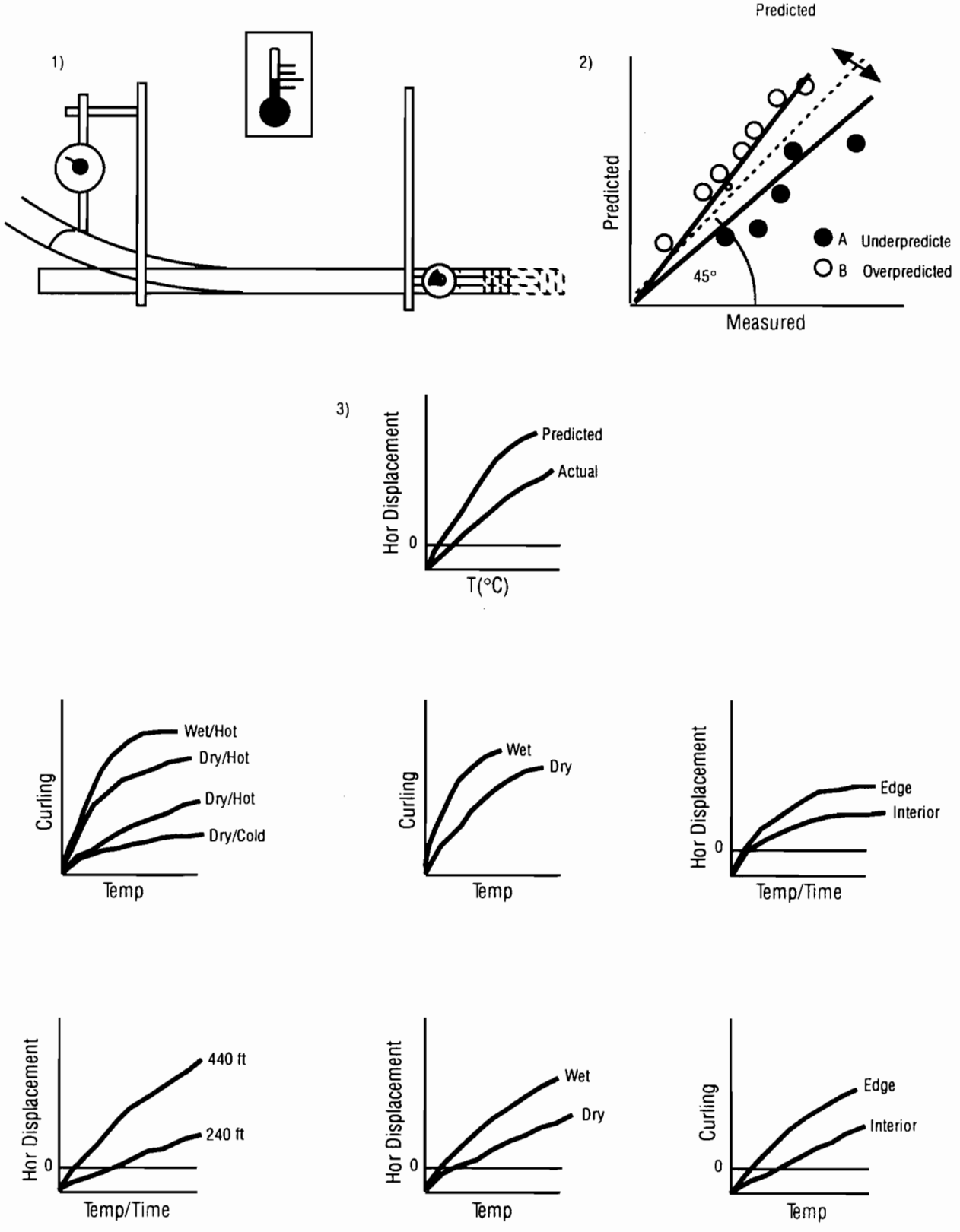

Fig 5.3(a). Graphical description of calibration process.

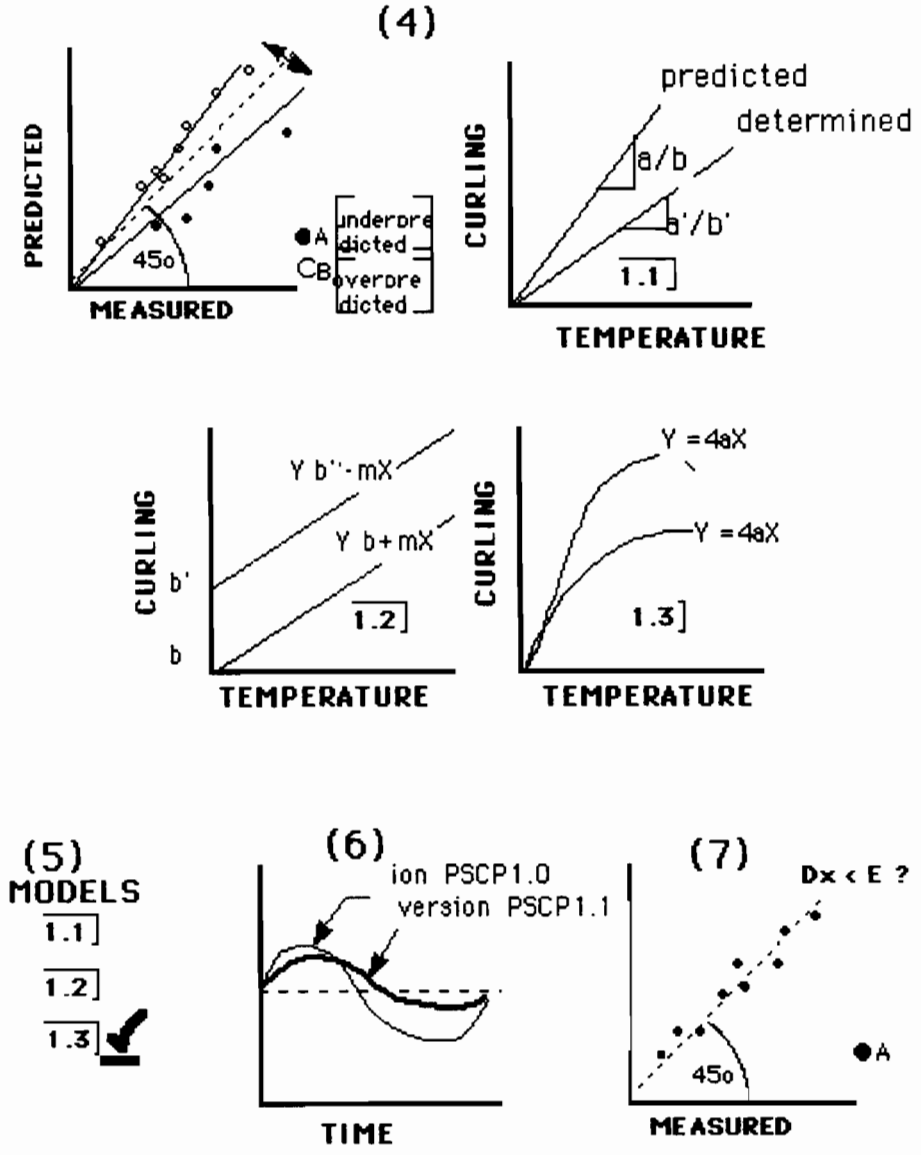

Fig 5.3(b). Graphical description of calibration process.

the friction model can simulate the physical phenomena. Part 3 of Fig 5.3(a) is a schematic representation of the interaction of all the factors that intervene in curling and friction.

The effect of data input was mentioned in the preceding section. The main effect is to modify the rate of change in the values of the output. Some secondary effects are changes in the range of prediction values. Part 4 of Fig 5.3(b) is a schematic representation of this effect. Among these input variables, creep shrinkage and the thermal coefficient can be targeted. The magnitude of error is small for the majority of input variables because of the range and magnitude of their values.

Therefore, the recommended order for the calibration of the program is

(1) Model and coefficients for curling,
(2) Model and coefficients for concrete properties,
(3) Model and coefficients for steel, and
(4) Model and coefficients for post-tensioning.

Because of the time involved and the scope of the project, the decision was made to concentrate on the calibration of the first two items.

CALIBRATION OF PSCP2

Program PSCP2 has the following changes with respect to PSCP1:

(1) There is a new model for curling that allows the prediction of vertical displacements due to curling and/or warping and introduces geometry factors not considered before in the calculation of this type of displacements.
(2) There is an equation for the computation of the modulus of elasticity developed at CTR for concretes made in Texas. It considers the type of aggregate in the computation. The equation was developed under a research project conducted at CTR for the Texas State Department of Highways and Public Transportation (Ref 53).

CURLING MODEL

Different forces act while curling is produced. Therefore, curling is considered to be governed by the following factors:

(1) Strains developed by the temperature gradient between opposite faces of the slab.
(2) Strains developed by friction between subbase and slab that resists the contraction of the slab due to thermal changes.
(3) Stored deformation energy of the slab.
(4) Structural stiffness of the element.

For the development of the model, the general state of forces in the body during curling was analyzed for each one of the governing factors. Once the initial particular expression was produced, the generalization of the model was achieved by the introduction of the parameter developed for the intermediate points along the slab.

Using the previous information related to curling and including the effects of temperature differential, the model that describes the behavior for the edge of the PCP slab as it curls due to temperature differentials is

$$Y = \frac{1}{2}\left[\frac{\left(DT_{D'}\, a + \frac{n\, w\, L^3}{15\, E_c{}^2\, k}\right) x^2\, f\, (B/L)^2\, (1 - n^2)}{h} + \frac{3\left(DT_{M'}\, a + \frac{n\, w\, L^3}{15\, E_c{}^2\, k}\right) x^2\, f\, (B/L)^2\, (1 - n^2)}{h^2}\right] \quad (5.37)$$

where f is a parameter representing a restricting factor affecting the level of displacements along the slab:

$$f = \frac{1}{3}\left[\frac{7x}{L} + \frac{7L}{x\text{-}1} - 11\right] \quad (5.38)$$

and

Y = vertical displacements due to a temperature gradient;
x = distance from the middle of the slab;
L = total length of the slab, inches;
B = width of slab, inches;
h = slab thickness, inches;
a = concrete thermal coefficient of contraction and expansion;
n = Poisson's ratio of concrete;
E_c = concrete modulus of elasticity, psi;
$DT_{D'}$ = effective increment of temperature;
$DT_{M'}$ = the increment in temperature with reference to the original casting temperature;
w = uniform distributed weight of concrete, lb/inch; and
k = relative value of soil support (k-value), psi/inch.

When the temperature gradient experiences a reversal, the slab recovers its former shape. For this transition, Eq 5.39 introduces the model describing this recovery:

$$Y = \left(j - DT_{Di}\right)\left[\frac{Yc_{max}}{\Omega DT_{Dtmax}\Omega + \Omega DT_{Dcmax}\Omega}\right] \quad (5.39)$$

where

j = parameter in function of the history of intensity of the heat radiation and the thermal effective coefficient of the pavement. For the present research, the values ranged between 18.5 for hot weather and 13 and 10 for cold weather;

DT_{Di} = increment of temperature differential for period i;

Yc_{max} = maximum curl experienced by the slab before the transition, inches;

DT_{Dtmax} = maximum positive temperature differential produced during the transition, °F; and

DT_{Dcmax} = maximum negative temperature differential produced during the curling cycle, °F.

The expression for the stresses produced by the temperature differential has the form

$$s = Ec\left[DT_D \cdot a + \frac{n\ w\ L^3}{15\ E_c^2\ k}\right] \qquad (5.40)$$

A conservative and more practical value for the determination of the maximum stresses of the slab is given by the relationship

$$s = E_c\,(DT_D \cdot a) \qquad (5.41)$$

where s is the value for the stresses and all the others as defined before. This value is constant at the slab centerline and it is added to the stresses due to friction along the slab.

As we can see, the model considers

(1) the relative effect of temperatures,
(2) friction,
(3) slab geometry, and
(4) the value of the soil support.

The flow of program PSCP2 in subroutine CURL with the installation of the model is in the following manner. First, the values for the average temperature gradients are determined and the maximum and minimum temperatures gradients for the cycle. Next, the program determines for each reading whether or not the slab is undergoing curling. If it is, the value for curling is determined for each time interval until the program detects a change in the gradient. Once the program establishes that the slab is experiencing a reversal in the temperature gradient, the program predicts the transition part of the cycle. That transition occurs when the slab is flattening. For each part of the process, the stresses that build up in the slab are computed after the displacements are calculated. Then, the command of the program returns to the main routine. Figure 5.4 shows a comparison of the vertical movement obtained at joint position 9S on July 25-26, 1988, with that predicted by PSCP2 for a typical summer day. Figure 5.5 shows a similar comparison for joint position 9N on January 21-22, 1989, with the model prediction for a typical winter day. In each case, the "actual and predicted" plots have been purposely separated (not normalized) for easier study. Note the vertical movement during the winter is significantly less than the vertical movement in the summer because of the different temperature characteristics during a 24-hour period.

Figures 5.6 and 5.7 show the relationship between the measured and predicted vertical movement for summer conditions for both the 240 and 440-foot slabs. Figures 5.8 and 5.9 reveal a similar plot for winter conditions. The winter conditions tend to be curvilinear; however, when considering the data scatter in comparison to the summer characteristics, a linear fit was used. These figures show a relatively strong association between the measured and predicted vertical movements. The R**2 values are about 90 and the relationship is approximately one-to-one. Typical input data and the results of the program may be found in Appendix A. A complete description of the calibration, program listing, and examples of program input and output are found in Research Report 556-3 (Ref 3).

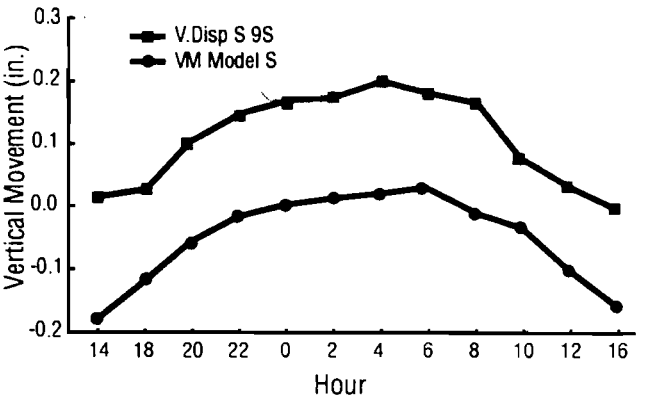

Fig 5.4. Comparison of vertical movement for summer: actual and model.

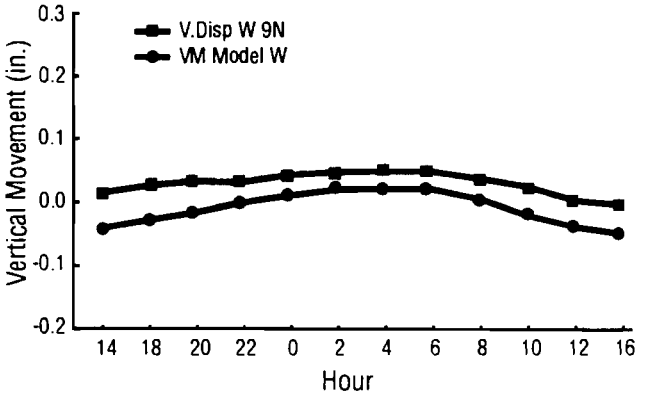

Fig 5.5. Comparison of vertical movement for winter: actual and model.

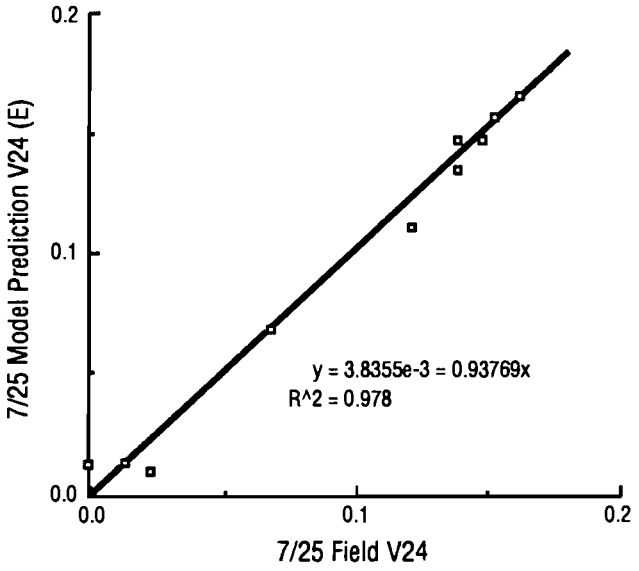

Fig 5.6. Degree of correlation between model and field vertical displacements predicted for a 240-foot slab for hot weather conditions.

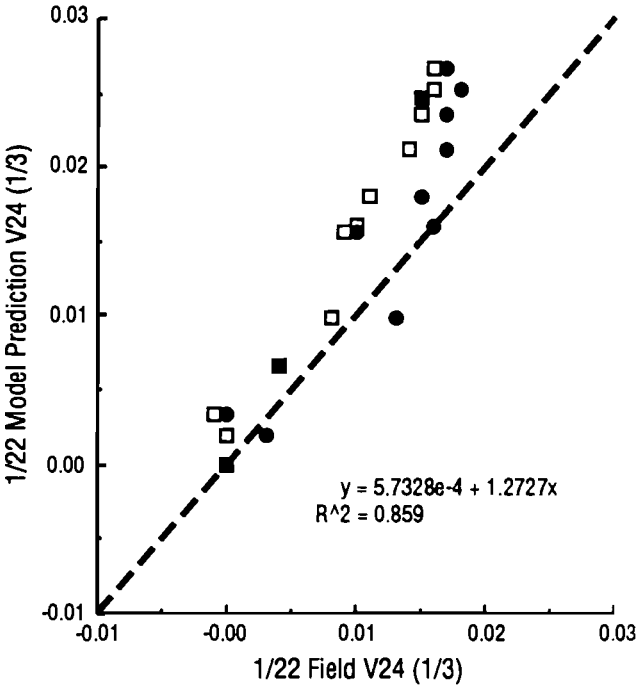

Fig 5.8. Degree of correlation between model and field vertical displacements predicted at first sixth of a 240-foot slab for hot weather conditions.

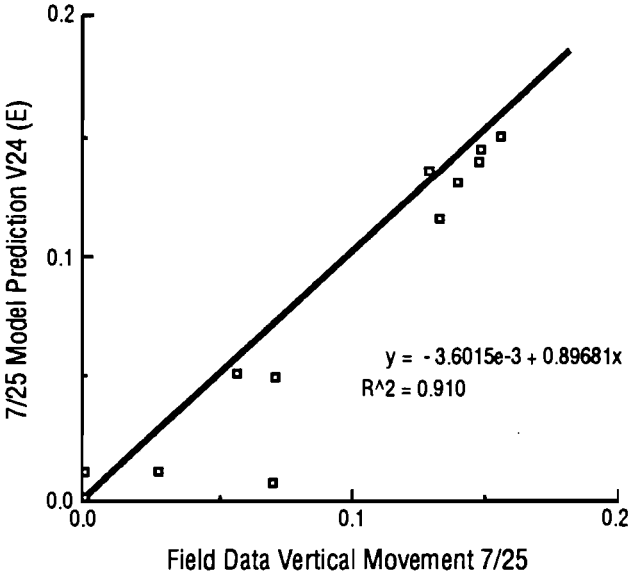

Fig 5.7. Degree of correlation between model and field vertical displacements predicted for a 440-foot slab for hot weather conditions.

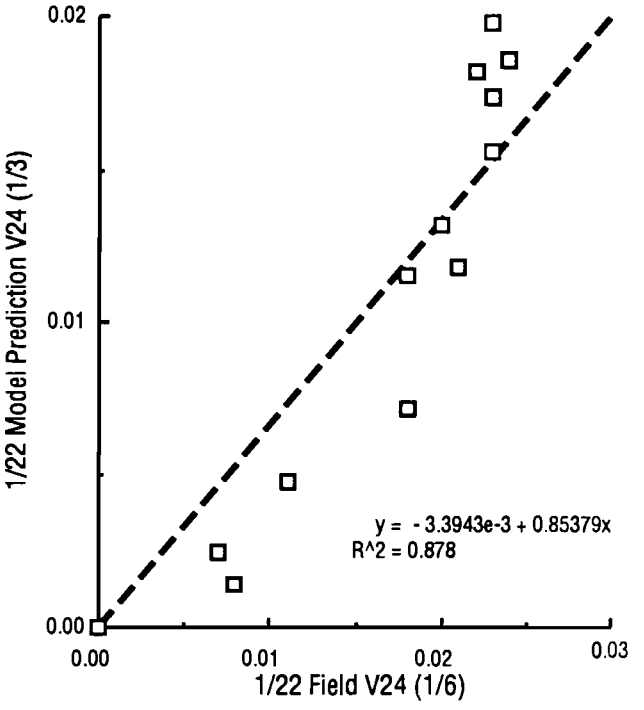

Fig 5.9. Degree of correlation between model and field vertical displacements predicted at first sixth of a 440-foot slab for hot weather conditions.

PHYSICAL PROPERTIES MODIFICATION

Recent work in Research Project 3-8 86-422, "Evaluation of Pavement Concrete Using Texas Coarse Aggregates," studied the physical properties of concrete used in concrete paving. The physical properties, such as the compressive modulus, compressive strength, tensile strength, shrinkage, and thermal coefficient, were obtained at various ages. The mixes were prepared using a variety of coarse aggregate types. The aggregate sources studied in the project included most of the commercial sources used in concrete paving in Texas (Ref 53). As a result of this study, models were developed which predicted the physical properties as a function of time. It was decided to include the properties which were pertinent to the program input to the models in the PSCP2 program. Therefore, if a granite aggregate was to be used in PCP, selection of the physical properties of the granite would be input in PSCP2. This would be accomplished by the selection of the granite module in the input portion of the program, etc. If the models of the physical properties obtained in Research Project 3-8-86-422 are not desired, the program reverts to the input procedures used in PSCP1. Examples of the aggregate types available may be found in the PSCP2 portion of the input shown in Appendix A.

FINITE ELEMENT MODEL

A finite element model for PCP that gives horizontal slab displacements and resulting principal stresses for any set of specified changes in slab temperature has been developed.

BACKGROUND

Although the most significant horizontal displacements for the McLennan County PCP occur in the longitudinal direction, there are several indications that thermal stresses in both the longitudinal and transverse directions are important parameters for the characterization of the behavior of the pavement.

Prestressing of the PCP was applied in both the longitudinal and transverse directions. Figure 5.10 shows the actual locations of longitudinal and transverse tendons for a typical 240 and 440-foot slab. The major purpose of the longitudinal prestress was to prevent cracking of the pavements slabs due to tensile stress caused by friction forces. Transverse prestress was applied primarily to prevent longitudinal cracking caused by flexural action resulting from wheel loads. Regardless of the role of the transverse stressing, however, the state of stress in the pavement as a result of thermal movements becomes complex if the transverse force components are considered. The orientation of principal planes (planes of stress in which pure tension or compression exists with no shear stress) could change from transverse to diagonal. This would result in different magnitudes of maximum tensile stress than when precompression was applied in the longitudinal direction only.

Furthermore, the prestressing method used for the PCP produces a two-dimensional state of stress in the slabs. The technique involved the stressing of tendons from internal locations in the slabs. When the slabs were constructed, tendons were anchored near the joints while blockouts were used to form empty pockets around the ends of the tendons (in the middle region of the slabs) while concrete was placed. As the concrete gained strength, the tendons were stressed from the pocket locations in two stages. The first stage of stressing was applied before the concrete could crack during the first cooling cycle, which occurred during the first night after concrete placement. After the concrete developed its design strength, a second stage of stressing completed final tensioning of the tendons. Several days later, the pockets were filled with concrete. Figure 5.10 (Ref 18) also shows the general locations of the stressing pockets. The significance of the pockets in terms of two-dimensional states of stress is indicated by the presence of cracks in the slabs (Ref 1). Typical cracks were observed to propagate diagonally from the corners of the pockets. Apparently, the pockets were causing the maximum tensile stress (the principal stress) to occur on principal planes that were not transverse. This state of stress warrants an investigation of slab behavior that considers two-dimensional effects.

The finite element method was chosen for analysis of the PCP. This method is performed through the discretization of a continuum into connected elements to which material and geometric properties are given. The overall operation of the continuum is accomplished by the transfer of material action from one element to another through connecting nodes. If correct material and geometric properties are assigned to the elements, the method can simulate true two-dimensional prototype behavior with a high degree of accuracy. The finite element model developed in this chapter incorporates the most important material actions of the PCP into a format that is useful for the analysis of specialized problems. The model has a wide range of capabilities for the application of special problems associated with PCP because elements can have different geometric orientations and different material properties, and because tendon forces can be applied at many locations in varying magnitudes and directions. In addition, the model is versatile in that a variety of effects that are not presently included can be easily adapted to the presented formulation.

The finite element model is not intended to be a design model; the input-output aspects of the computer code for the model require that the user be extremely meticulous in order to avoid time-consuming errors. The model presented in the previous portion of this chapter is better for use in a design setting. The subject model is

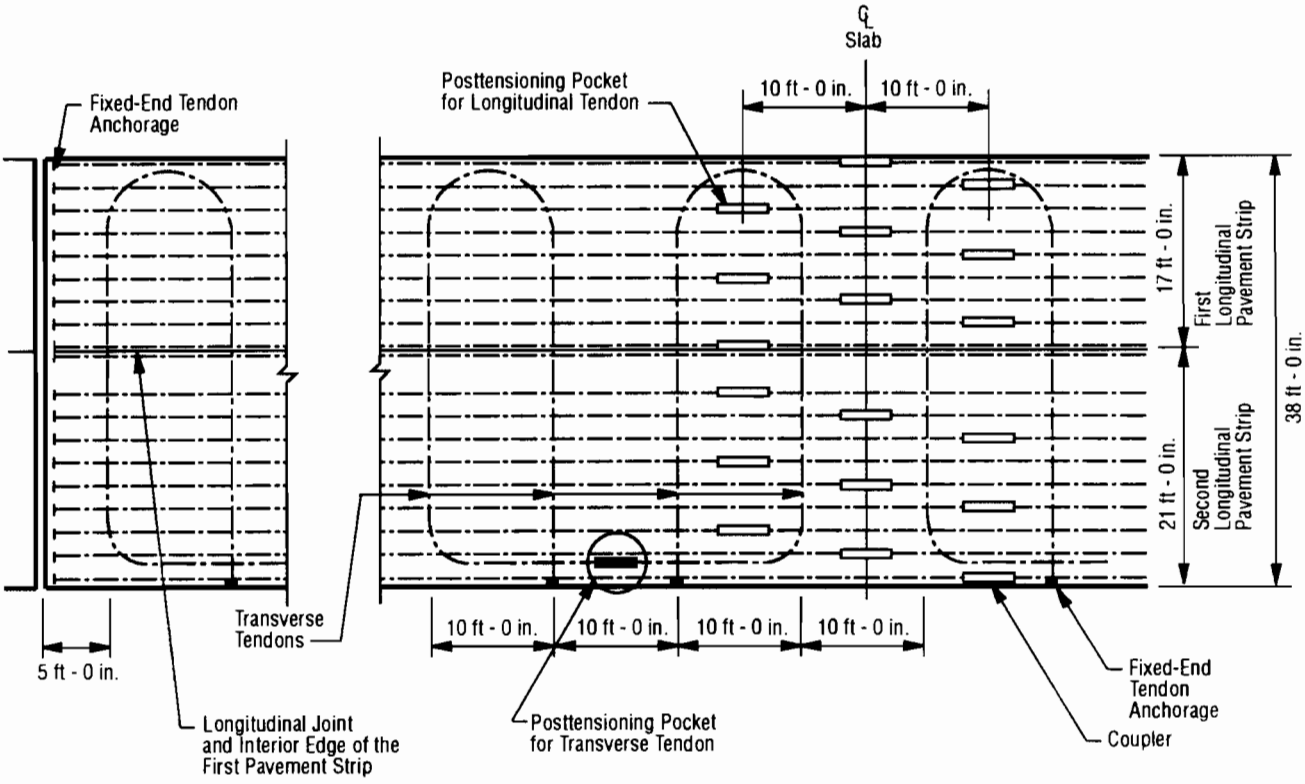

Fig 5.10. Layout of a typical PCP slab.

intended for the specialized analysis of complex problems that may occur with PCP.

FINITE ELEMENT MODEL DEVELOPMENT

The model developed for PCP is based on a stiffness formulation. Stiffness can be defined as the ability to resist deformation. This concept is best illustrated by a linear-elastic spring mechanism. Spring action is described by the equation F = kx, where k is the stiffness of the spring, F is the force exerted on the spring, and x is the resulting displacement of the spring. The same basic relationship also applies to PCP. The stiffness equation is more complex for the pavement than for a spring, however, because for PCP several forces are applied simultaneously on a body that has several materials and therefore several components of stiffness. Furthermore, the forces are applied on several boundaries, both in discrete and continuous manners.

In order to develop a finite element model for PCP, it was first necessary to characterize the stiffnesses of all of the material components that make up the pavement. This was done by establishing the force-deformation relationship that exists in concrete, in prestressing tendons, and in subbase friction under a rigid slab.

MATERIAL STIFFNESSES

The force-deformation characteristics of concrete are based on curves that result from breaking typical 6-inch by 12-inch cylinders. A typical concrete stress-strain curve is shown in Fig 5.11. If concrete deformations are considered to be completely linear and elastic, the modulus of elasticity, E_c, (material stiffness) of concrete for highway pavements constructed in Texas can be estimated by the equation $E_c = A(2\text{-}e^{-BT}\text{-}e^{-CT})$, where A, B, and C are experimentally determined coefficients and T is the age of the concrete in days (Ref 56). The shear modulus of the concrete, G, quantifies resistance to shear deformations and is equal to $E_c/2(1+u)$, where u is the Poisson ratio for concrete (about 0.2). The stress-strain curve of a typical prestressing tendon is shown in Fig 5.12. The tendons in PCP remain in the linear elastic range of deformation. The modulus of elasticity (E_s) of the tendons used in the McLennen County PCP is 28,000,000 psi (Ref 11 from report 2). The axial stiffness of a tendon is E_sA_s/L where A_s is the cross sectional area of a tendon, and L is the tendon length.

The force-deformation characteristics of subbase friction under a rigid slab have been determined to follow a non-linear hysteretic function. This has been reported

by Stott as a result of a comprehensive experimental investigation of the frictional behavior of several materials under a slab (Ref 36). A typical force-deformation curve obtained in the study is shown in Fig 5.13. This figure shows how, for one location on a long pavement slab, the curve is steep when a movement reversal first occurs but gradually becomes more shallow as the magnitude of displacement increases. This behavior has been simplified for the finite element model in this study. The frictional behavior has been assumed to follow a bilinear function, as shown in Fig 5.1. This pattern of the force-displacement characteristics for subbase friction divide the type of restraint into two types: elastic friction, as represented by the steep portions of the curve in Fig 5.1, and inelastic friction, as represented by the flat portions of the curve. The elastic limit of force and displacement shown in Fig 5.1 models the results of experiments performed at The University of Texas at Austin in 1986 in which the frictional force-displacement characteristics of a rigid slab on several friction reducing mediums were determined (Ref 21).

One layer of polyethylene sheeting was used as the friction reducing medium for the McLennan County PCP. As a slab expands and contracts, every point on the slab cycles through a characteristic friction curve like the curve in Fig 5.1. Slab locations that are far from the centerline go through a larger displacement with inelastic friction than do locations that are closer to the centerline. The cyclic behavior of subbase friction for different locations on a slab is shown in Fig 5.14. One daily temperature cycle is shown in 7 steps. These steps are indicated on the force-displacement curve for three different slab locations. The point closest to the centerline (point A) goes through a cycle of elastic displacements, whereas points B and C experience increasing amounts of inelastic behavior.

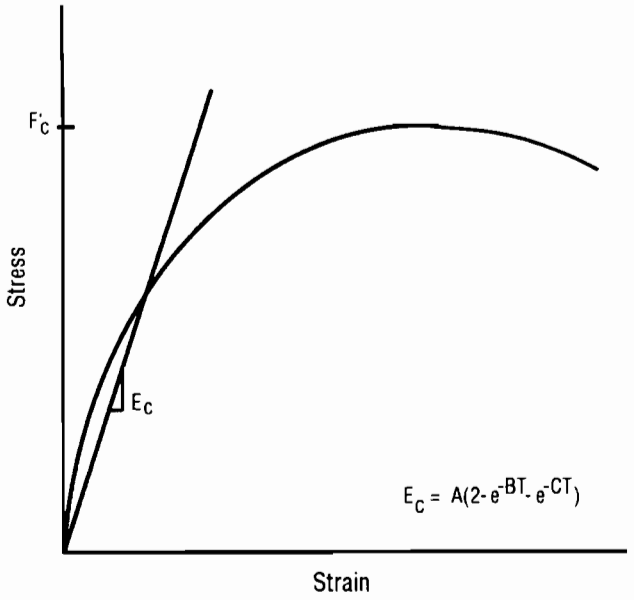

Fig 5.11. Typical stress-strain curve for concrete.

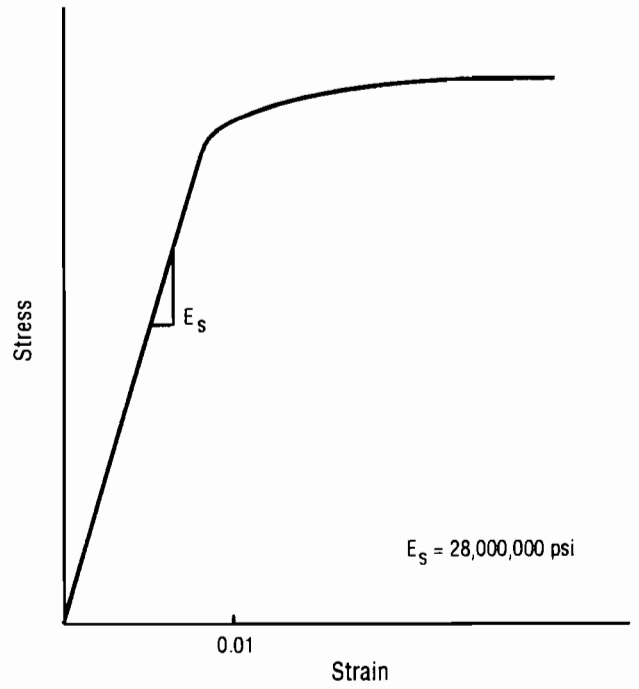

Fig 5.12. Typical stress-strain curve for a prestressing tendon.

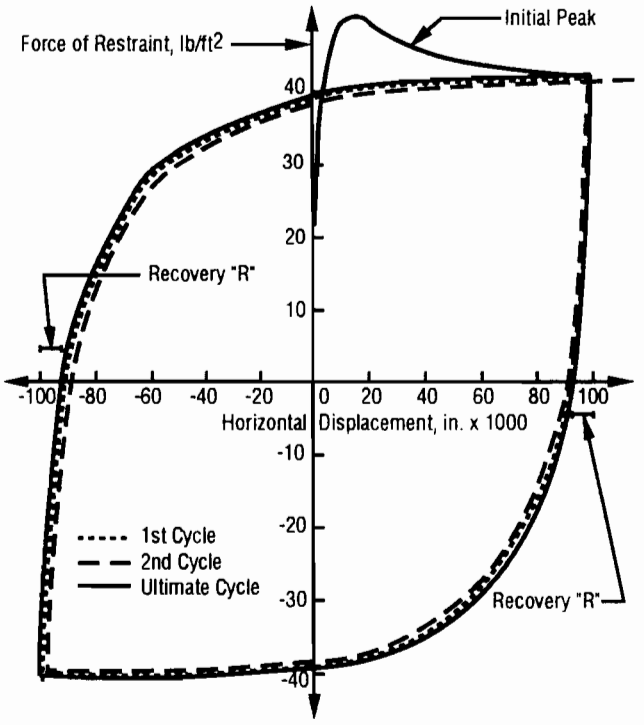

Fig 5.13. Force displacement behavior for subbase friction determined by Stott (Ref 19).

THE FINITE ELEMENT METHOD FOR PCP

The application of the finite element method to PCP involves the discretization of the pavement into elements that are connected by nodes. The element used for the PCP model is isoparametric and has 8 nodes and 9 integration points. An isoparametric element is one in which the functions that describe the geometry of the element describe displacements as well. Because these functions are the same, the element can be distorted to assume any octolateral shape (as long as the general-length-to-general-width ratio of the elements does not exceed a value of about 1.75). The 8-node isoparametric element is a common element that is known to give accurate results for elastic problems (although there is inelastic friction in the PCP problem, the elements themselves always remain elastic; friction is applied as an external force). Figure 5.15 shows the element used for this study.

The element's nodes perform several functions: they define the geometry of the elements, they connect the elements, and they serve as readout points for displacements and stresses. The element's integration points allow for the numerical integration of properties through the element. Each integration point is weighted according to its location in the element; when the numerical integration is carried out, the whole element assumes the property in a continuous manner. The integration points allow the elements to assume the properties of a continuum and to maintain the properties for any geometric orientation.

Stiffnesses and loads for the PCP must be applied at the proper boundaries in the finite element model in order for the behavior of the model to simulate prototype behavior. The concrete stiffness is a function of E_c and u. This stiffness is applied at the integration points so that the body of elements has the stiffness of concrete. The tendon stiffnesses and forces are applied as discrete forces at nodes that correspond with tendon anchor locations in the prototype. Since the tendons are unbonded, all of the tendon stiffness is applied at the node. The subbase frictional stiffnesses and frictional forces are applied at the integration points. This insures that the friction is "felt" by the elements as if they were in surface contact with the subbase. Finally, temperature changes are applied at the integration points. This allows each element to undergo a volumetric change that corresponds with the coefficient of thermal expansion of the concrete, a, and the geometry of the element. In this manner, slab displacements in the model due to changes in temperature are a function of the accumulation of the volumetric changes of all elements.

Once stiffnesses and forces are given to the model, a stiffness relationship similar to that for the linear spring, kx=F, can be formed. Equation 5.42 describes the total stiffness relationship for PCP:

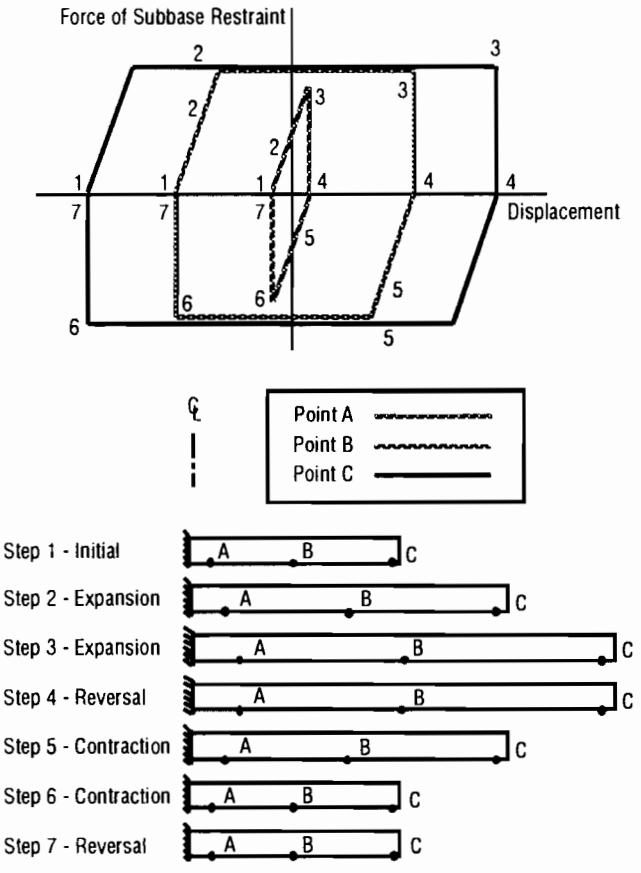

Fig 5.14. Cyclic behavior of subbase friction for different locations on a slab.

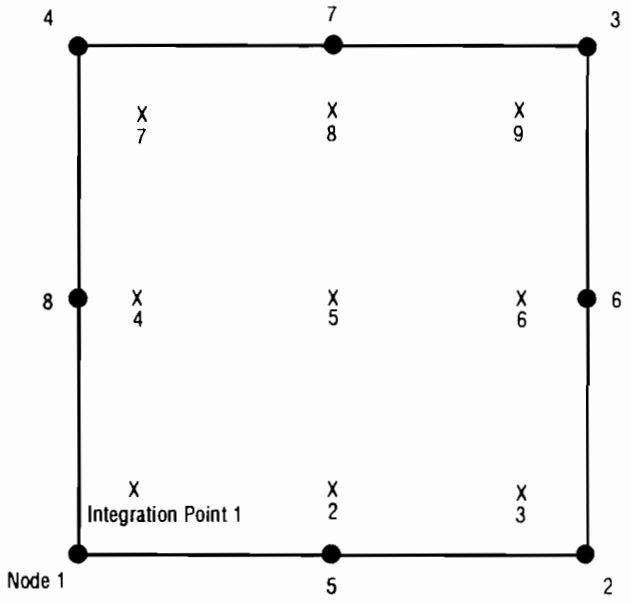

Fig 5.15. Typical 8-node isoparametric element with 9 integration points.

$$\left\{ [K_c]_{ip} + [K_s]_{ip} + [K_p]_n \right\} [U] = \left\{ [P_s]_{ip} + [P_p]_n + [P_{\Delta T}]_{ip} \right\} \quad (5.42)$$

where

[Kc]ip = concrete stiffness applied at the integration points,

[Ks]ip = subbase frictional stiffness applied at the integration points,

[Kp]n = tendon stiffness applied at nodes corresponding to anchor points,

[Ps]ip = subbase frictional forces applied at the integration points,

[Pp]n = tendon forces applied at nodes corresponding to anchor points,

[PΔT]ip = force corresponding to temperature change applied at the integration points (actually a change in strain, applied on the right-hand side of the equation), and

[U] = displacements of nodes.

This equation is the basis for the implementation of the finite element procedure into a computer code. A more detailed derivation of the relationships described by Eq 5.42 is presented in Ref 2. The derivation is based on energy methods and includes all algebraic relationships that were necessary to write the computer program. Figure 5.16 shows the physical system described by Eq 5.42. The tendon forces and stiffnesses are represented by springs at the right end of the model; these springs are applied at discrete points and are governed by the force-displacement characteristics described by the elastic portion of the curve in Fig 5.12. The subbase stiffness and forces are represented by a bed of horizontal springs; the effects of these springs are integrated over the surface of every element and are governed by the force-displacement characteristics described by the curve in Fig 5.1. Concrete stiffness is applied at the integration points of all elements and is governed by the force-displacement characteristics of the elastic behavior of concrete illustrated in Fig 5.11. The basic procedure of the program is to form all stiffnesses, apply all loads, and solve for displacements, [U]. Then, the displacements are used to calculate strains $\varepsilon=B[U]$, where B is the strain displacement matrix, as defined in Ref 55. The strains are then used to calculate stresses $\sigma=D\varepsilon$, where D represents a matrix of material properties for concrete. A more specific description of the calculations is presented in Ref 2.

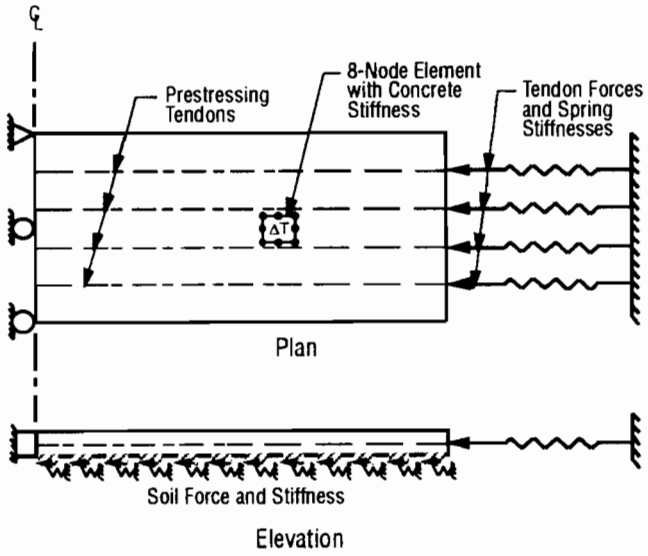

Fig 5.16. General components of the finite element model for PCP.

The boundary conditions for the model can be specified to allow displacements in either the longitudinal or transverse direction, or to completely fix displacements. The conditions are applied by assigning a displacement equal to 0.0 at specified nodes in the longitudinal or transverse directions, or in both directions. If the geometry of a PCP slab is symmetrical, boundary conditions can be applied so that only a fraction of the prototype is modelled. This saves both computation time and user effort. Typical boundary conditions are shown in Fig 5.16 at the left side of the body. They are applied at the centerline since the actual slabs are anchored at their centerlines and therefore behave symmetrically. The uppermost symbol represents a completely fixed condition and the lower symbol represents fixed longitudinal displacements but free transverse displacements. Because there is an interdependency between displacements and subbase frictional force, the computer program would normally require an iterative algorithm. However, since the elastic soil stiffness applies only to a very small amount of displacement (0.002 inch), actual soil friction is almost entirely inelastic for any practical range of slab movement. Therefore, the program operates under the assumption that all slab displacements result in inelastic friction. This assumption causes minor changes to Fig 5.1; the diagonal portions of the force-displacement curve become vertical. This simplifying assumption still allows for very close prediction of slab movements.

MODEL IMPLEMENTATION

The use of the computer model for PCP (PCPFEL1) is described in Ref 2, and user guidelines are outlined there as well. The model is implemented in three studies: a determination of finite element mesh fineness requirements, calibration of the model to the measured response of the PCP prototypes, and an analysis of stress concentrations around central stressing blockouts. The method of analysis is presented in Ref 2 for each study along with the results.

PROGRAM CALIBRATION

The computer program has been calibrated to the field data collected from the McLennan County PCP. The calibrated model allows for the prediction of displacements and stresses for future investigations into PCP. The calibrated model also allows for the back-calculation of material properties of PCP for which displacements have been measured.

The first step in the program calibration was to define which material properties were to be considered as "fixed" or "known" and which properties "unknown." The modulus of elasticity of the concrete was considered to be known, since material tests were performed on concretes of similar mix design (Ref 56). A value of 3958 ksi for the modulus of elasticity of concrete was used for calibration. The modulus of elasticity of the tendons was considered to be fixed at 28,000,000 psi, and the Poisson's ratio of the concrete was considered to be fixed at 0.2. The coefficient of thermal expansion had been determined to be equal to 5.44 x 10^{-6} inch/inch/°F for concrete that contained a similar coarse aggregate (Ref 57), but the displacements measured in the field could not be duplicated by the model using this value. This value for the thermal coefficient requires a subbase frictional force of restraint that is not physically possible in order for the measured displacements to be matched. Therefore the coefficient of thermal expansion was considered to be unknown and was expected to be slightly lower than the value determined in (Ref 57). The subbase frictional force of restraint, although measured experimentally in (Ref 21), was considered to be inherently variable and was therefore considered to be unknown.

Since the only two unknowns for program calibration were the coefficient of thermal expansion and the force of frictional restraint, there was a direct interdependency between these two parameters. An infinite number of combinations of these values (within bounds) could be used to achieve equality between measured and calculated values of displacements at the end of the slabs. Only one of these combinations of values, however, could give a best fit between the measured and calculated values for displacements at the third and sixth points in addition to the ends of the slabs. The method of calibration was based on this principle.

Calibration of the model was performed on the 44-element mesh shown in Fig 5.17. Equivalent nodal forces were used at the right end of the mesh to represent longitudinal tendon forces: 11 tendons at 39.5 kips. Transverse tendon forces of 39.5 kips were applied on the lower boundary of the mesh at locations that produce the same stress as that of the prototype slabs (even though these forces were not expected to affect calibration). The regression equations calculated in Chapter 3 of Reference 2 (Table 3.1) were used as the basis for calibration. Average slopes from these equations were used to determine the average measured changes in slab displacements for the joint, sixth point, and third point locations. The procedure followed for calibration involved solving for the values of the thermal coefficient and the frictional force that would allow the model to reproduce displacements produced by the average regression slopes. The final fit of the calibrated model output to the field data is shown in Fig 5.18.

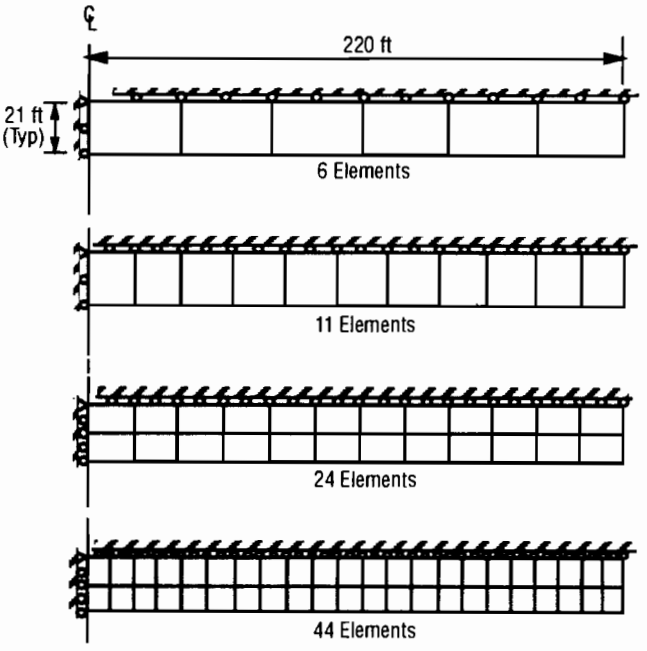

Fig 5.17. Meshes used for the determination of fineness requirements.

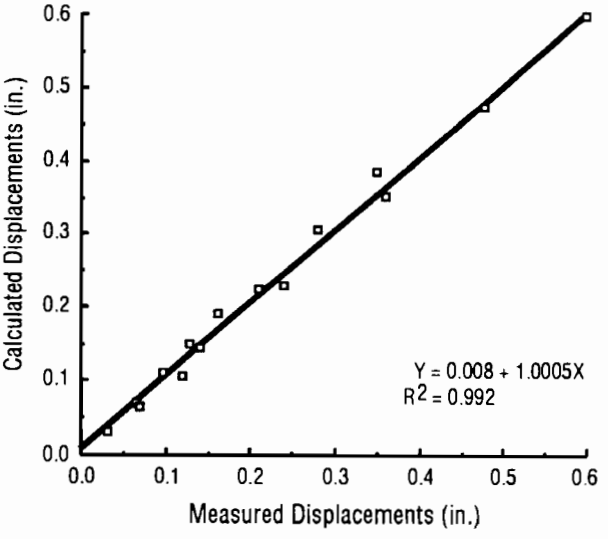

Fig 5.18. Calculated displacements produced by the calibrated model versus measured displacements.

The thermal coefficient of expansion that corresponds to the best data fit is 4.59 x 10^{-6} inch/inch/°F. The corresponding value of force of frictional restraint gives a coefficient of friction, μ, of 0.2. This value is significantly lower than the values of 0.45 and 0.4, which were determined through push-off experiments (Ref 21). However, it is exactly the same as the value determined in Ref 19 through back-calculation from previous measurements of displacements for the McLennan County PCP. A possible justification for the lower value is that the pushoff experiments in Ref 21 were conducted on small test slabs for which the only displacements occurred during the experimental procedure, whereas displacements of the actual PCP occurred on a daily basis. Abrasion between the pavement and the subbase might have caused the coefficient of friction to decrease over time. For design purposes, it would be conservative to use the higher coefficient of friction for the determination of expected stresses. The lower coefficient of friction also influences the determination of expected displacements (higher friction coefficients produce lower displacements). This should be taken into account when predicting slab displacements.

STRESS CONCENTRATIONS

An investigation of stress concentrations was carried out in response to cracking that was observed in the field. Cracking had occurred around the pocket locations that were used for stressing the tendons. Typical observed cracking patterns are shown in Fig 5.19, and a close-up view of representative cracks is shown in Figs 5.20 and 5.21. The exact cause of the cracking is not immediately apparent; this study is based on the hypothesis that one cause may be that the interruptions in the tension field in the center region of the slabs caused by the pockets has created tensile stress concentrations. The computer model has been used to simulate and analyze this situation.

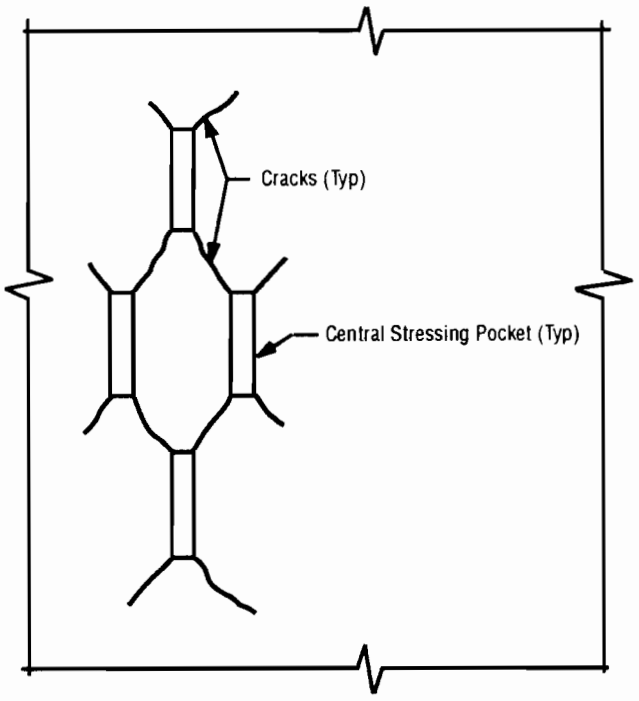

Fig 5.19. Typical cracking patterns observed around central stressing pockets.

The analysis had to consider the stress history of a slab since material properties were rapidly changing during the period of post-tensioning (the first three days of the life of the pavement). Therefore, the investigation was carried out in five stages, reflecting the staged stressing procedure used during construction. Table 5.1 lists and describes the stages of analysis. Tendon forces shown take into account an assumed 15 percent loss of prestress (Refs 20 and 58). Figure 5.22 shows the types of stresses that were calculated by the program (shown as positive). The longitudinal and transverse stresses are labelled σ_x and σ_y respectively, and the principal stresses are σ_1 and σ_2. The orientation of the principal plane is θ_p and is also shown as positive in Fig 5.22.

Table 5.2 lists the results of the analysis. The stresses for the full mesh are for a node that is located 3.5 feet from the centerline of the pavement. The stresses for the reduced mesh are at the upper right corner of a pocket (the pocket location is shown in Fig 5.23). The values of the concrete modulus of elasticity (E_c) and tensile strength (f_t) are listed for their appropriate magnitudes at the particular stage of analysis (Ref 56).

The maximum principal tensile stress has not exceeded the tensile capacity of the concrete according to this analysis. Only the second stage of the analysis exhibits tensile stress in the concrete, but the magnitude is less than half of the tensile capacity of the concrete (61.88 psi tensile stress versus 223 psi tensile capacity). Accordingly, no cracks around the pockets were reported to occur during stressing operations. The principal plane at the second stage of analysis is close to the crack orientations observed in the field (26.99° calculated versus about 30° observed in the field). The orientations of the principal plane and the observed crack angle are shown in Fig 5.24. The maximum principal stress at a location 17 inches away from the pocket corner (but close to the principal plane of 26.99°) was +18.22 psi acting on the principal plane of 24.21°. These results seem to indicate that the stress concentrations due to the pockets might contribute to the cause of the cracks but that other factors are probably involved. These factors might be (but are not limited to) the result of a combination of the following situations:

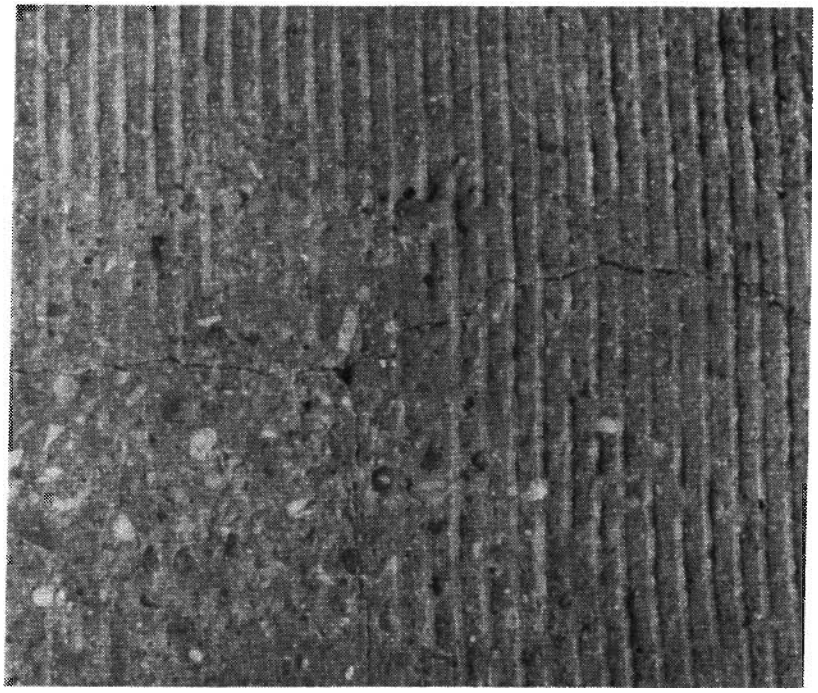

Fig 5.20. Crack propagating from the corner of a pocket.

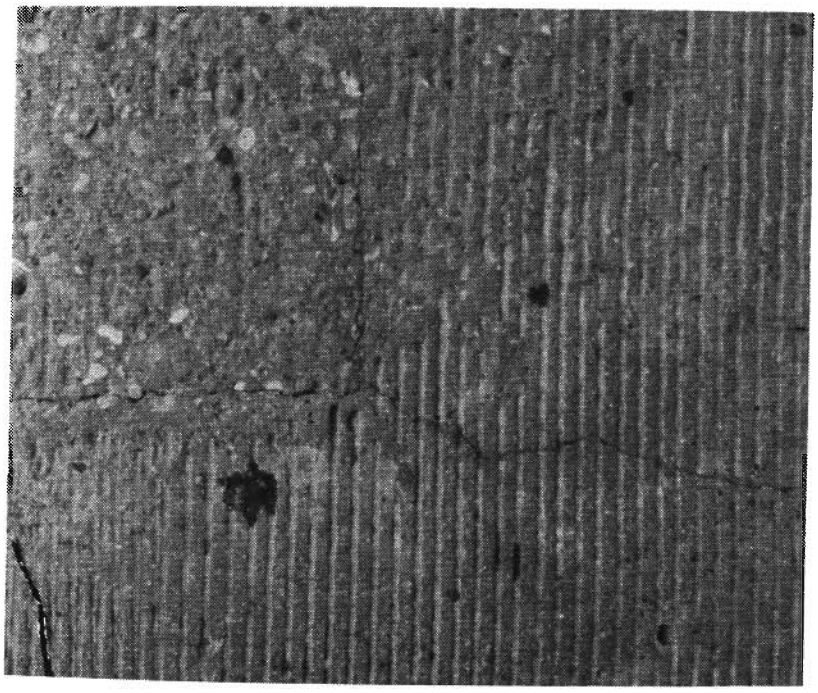

Fig 5.21. Crack propagating from the corner of a pocket.

TABLE 5.1. ANALYSIS STAGES FOR STRESS CONCENTRATION INVESTIGATION

Stage of Analysis	Description
1	Analysis of stresses for the first level of stressing: 14.0 kips per tendon (low level tensioning on 12-hour-old concrete; open pockets)
2	Analysis of stresses during the first cooling cycle: temperature decrease of 50°F (open pocket), 14.0 kips per tendon
3	Analysis of stresses for the final level of stressing: 39.5 kips per tendon (full tensioning on 60-hour-old concrete; open pockets)
4	Analysis of stresses during the third cooling cycle: temperature decrease of 50°F (open pocket), 39.5 kips per tendon
5	Analysis of stress for the current material conditions (filled pockets), 39.5 kips per tendon

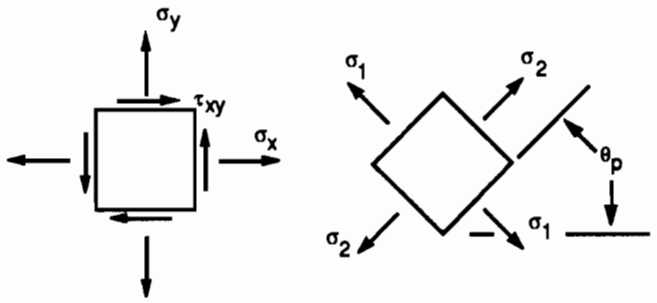

Fig 5.22. Postive stresses, principal stresses and principal plane for program output.

TABLE 5.2. RESULTS OF STRESS CONCENTRATION ANALYSIS

Mesh (Fig 5.7)	Stage of Analysis (Table 5.2)	Time (hours)	E_c (psi)	f_t (psi)	σ_x (psi)	σ_y (psi)	τ_{xy} (psi)	σ_1 (psi)	σ_2 (psi)	θ_p (degrees)
Full	1	12	2590	188	–101.9	–19.4	0.0	–19.4	–101.9	0.0
Full	2	17	2785	223	+1.3	–19.6	0.0	+1.3	–19.6	0.0
Full	3	60	3645	312	–287.4	–54.9	0.0	–54.9	–287.4	0.0
Full	4	65	3690	317	–184.2	–55.0	0.0	–55.0	–184.8	0.0
Full	5	10,000	3960	484	–183.1	–55.0	0.0	–55.0	–183.1	0.0
Reduced	1	12	2590	188	–529.9	–149.7	–227.1	–43.6	–636.0	25.0
Reduced	2	17	2785	223	+6.7	–151.0	+108.4	+61.9	–206.2	27.0
Reduced	3	60	3645	312	–1494.3	–422.4	–641.0	–122.9	–1793.9	25.1
Reduced	4	65	3690	317	–957.8	–423.8	–642.7	–15.3	–1386.7	33.7
Reduced	5	10,000	3960	484	–955.9	–423.4	–642.4	–25.8	–1385.0	33.7

(1) Several pockets are closely spaced in the center region of the slab. Actual stress concentrations may be due to a combined effect of more than one pocket.
(2) Wheel load stresses are subject to the same stress concentrations as thermal stresses. The effect of wheel loads is not simulated by the model.
(3) The combination of fatigue and stress concentration effects might be important. A condition survey of the experimental section (Ref 1) has revealed that the most cracking occurs in the right traffic lane, the lane with the heaviest use.
(4) Both the material properties of the concrete, and the physical parameters in the model (frictional resistance) are variable. This model is based on average or assumed values; actual field conditions may be less favorable.

The analysis of stress concentrations clearly shows that a higher tensile stress exists in a slab with pockets than in one without pockets (+61.88 psi with pockets vs. +1.28 psi without). This is supported by field observation; no cracking has occurred in the center region of the slabs except at the pocket locations. Since the maximum tensile stress at the pocket corners never exceeds the tensile capacity of the concrete, the influence of fatigue and wheel loads on crack development is validated. It should be noted that the cracks are not structurally significant at this time; they have not caused any further distress, and do not affect the serviceability of the pavement. Additionally, the transverse prestressing has been crucial to the control of the extent of cracking. Without the transverse tendons, the cracks would have been wider and could have triggered further damage.

With respect to the cracking observed in the field, it is recommended that steel reinforcement be used as the corners of the pockets (crossing potential crack paths) for any future PCP that uses the central stressing technique. The recommended placement of the reinforcement around the pockets is shown in Fig 5.25, where L_d is the development length of a reinforcing bar. Since an exact numerical value for the tensile stress that is causing the cracks was not determined from this analysis, the amount of steel should be based on conservative engineering judgement. Corner bars of this type are often used at the corners of openings in slabs, and they are quite effective in the control of cracks. Bars of No. 4 or No. 5 size in the position shown in Fig 5.25 should be satisfactory for a 6-inch slab.

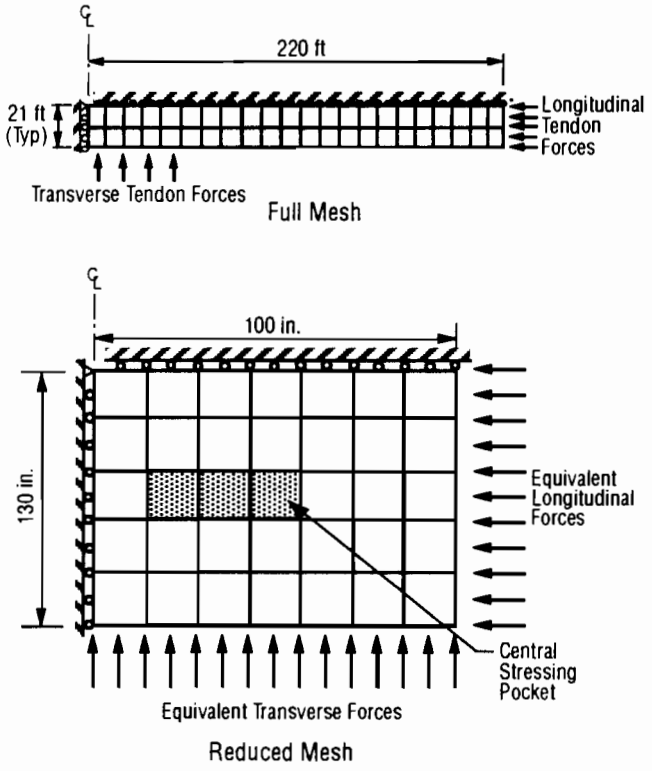

Fig 5.23. Meshes used for stress concentration analysis.

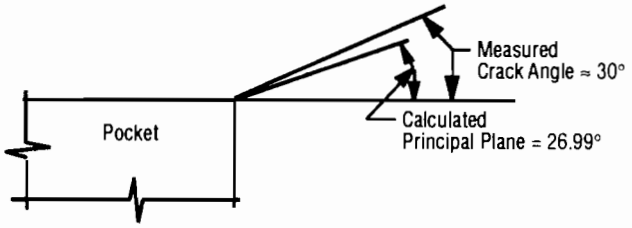

FIg 5.24. Orientation of calculated principal plane and observed crack angle.

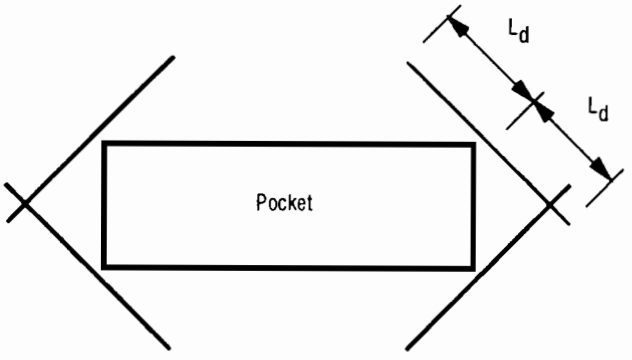

Fig 5.25. Recommended placement of reinforcement around pocket.

CHAPTER 6. DISCUSSION OF RESULTS

This chapter provides a summary discussion of the results developed from a study of the data collected for this report. The discussion is organized into five topics: instrumentation, slab movement, modelling, deflection, and condition surveys.

INSTRUMENTATION

The instrumentation program for this study was very successful. The collected data indicated trends that were in direct parallel with expected results. The buried anchors supported the instrumentation well, disturbance from extraneous sources was not detected, and the final data exhibited a high degree of consistency. The use of both LVDT's and dial gauges permitted a verification of the data. The embedded thermocouples at three depths in the slab provided a wealth of interesting temperature information. Even though much of the data collection was automated, the use of the dial gauges provided researchers with sufficient manual processing to allow an inherent "feel" for the pavement condition while at the same time ensuring the accuracy of the incoming data.

SLAB MOVEMENT

Slab movements are significant, since measurements indicate that entire slabs are moving. Maximum joint widths range from about 1.5 inches to 3 inches. The slab movements correlated well with the concrete temperatures at mid-depth of the slab. Regression equations predicting horizontal slab movement were developed for two lengths of slabs. The joints between the 240-foot slabs may close when the temperature rises above about 107 °F; however, the original decision to construct the "summer time" paving with the joints closed seems valid and the equations will assist PCP designers. Vertical movements are much larger than expected. The vertical movement seems associated with the differential temperature between the top and the bottom of the slab. The rate of vertical movement seems slower when the surface of the slab is cooling and moves at a faster rate when the surface begins to receive solar heat.

MODELLING

A finite element model was developed and a mechanistic design model, previously developed, was calibrated. The finite element model for PCP gives stresses and displacements due to changes in temperature and prestress. User guidelines have been presented as well as input output requirements. The finite element model may be used in specialized studies of PCP and was used to study the stress around the stressing pocket leave-outs. The study indicated the cracking reported in the condition surveys was not caused by thermal stresses alone but by a combination of effects. These effects are possibly due to a superposition of thermal stress and fatigue. The design model, PSCP2, was revised and calibrated to better predict the vertical movement. In addition, the design model was revised to permit the inclusion of the physical properties of a variety of concretes.

DEFLECTION

Deflection information was obtained on the old pavement prior to overlay, just before the addition of the PCP, and after the PCP overlay in both the summer and winter seasons. The deflection information indicates the PCP strengthened the pavement structure. However, the subbase and soil conditions in the winter seem stronger than the summer conditions. This result was unexpected and unexplained. The reason for the unexplained deflection could be the result of the PCP construction. The use of a sheet of plastic as a bond breaker is an unusual construction practice in Texas. This type of bond breaker has obviously permitted the pavement freedom to move both longitudinally and vertically. As a result of the possible vertical movement, even in the interior of the slab, the measurement of deflection could yield unusual data.

CONDITION SURVEYS

Condition surveys were conducted on two occasions. The first survey was performed after about two years and the second survey occurred when the paving had been in service about three years. The surveys indicate the pavement is in excellent condition. The fact that there are only two transverse cracks in the one-mile length indicates the initial prestressing followed by the final stressing is beneficial. Some longitudinal cracking, which seems to have initiated at the corners of the leave-out pockets, has occurred. The finite element program was used to verify the stress and a corrective technique was developed for future construction. It should be noted that the cracks are not structurally significant. The cracks have not caused further distress and do not affect the serviceability of the pavement. Transverse stressing appears to be warranted. The armored joints have performed well and there has been no unusual distress near the joints.

CHAPTER 7. EXAMPLE APPLICATION OF THE MODELS

This chapter discusses the input and output information and provides examples using the mechanistic model. Examples of input and output data are included in the appendix. A prediction of the stresses for the initial period has been selected to show the use of the program in design.

PSCP2 INPUT DATA

The input data to PSCP2 consist of the problem definition data, the concrete properties, compressive strength data, the slab-base friction properties, the stiffness of slab support, and the steel properties. The input also includes the sequence of temperature data for the initial period, the sequence of post-tensioning applications, and the temperature data for subsequent periods.

PROBLEM DEFINITION

The problem definition data are concerned with the slab dimensions and the statistical requirements of the program. The data consist of the slab length, the slab effective width, the slab thickness, the number of increments, the maximum number of iterations, and the relative closure tolerance.

CONCRETE PROPERTIES

The format for inputting concrete properties permits the user to use available data, default to PCI data, or select a coarse aggregate for which the physical properties are known. The data include the thermal coefficient, the total shrinkage, the unit weight, Poisson's ratio, creep coefficient, and Young's modulus. An aggregate type may be input by selecting the appropriate number assigned to the aggregate.

COMPRESSIVE STRENGTH

The compressive strength data are based on an age/strength relationship from the U.S. Bureau of Reclamation. The strength at various early ages of the concrete is developed from the 28-day compressive strength input by the user.

SLAB-BASE FRICTION PROPERTIES

Three types of slab-base friction relationships are available: linear, exponential, and multilinear. After the user selects the type of relationship, the origin or initial position of the slab should be input along with the movement at which sliding occurs and the maximum friction coefficient.

STIFFNESS OF THE SLAB SUPPORT

The stiffness of the slab support is the modulus of reaction at the top of the supporting layer of the slab, or the K Value in pci. Note that, when subbase or improved layers are used over the subgrade, the modulus of reaction is at the "top of the supporting layer of the slab." A composite K Value will be needed.

STEEL PROPERTIES

The steel properties are concerned with the physical properties and positioning of the steel strands. The input includes the percent reinforcement, strand spacing, nominal area, yield strength, elastic modulus, and thermal coefficient.

TEMPERATURE AND POST-TENSIONING DATA

The "sequence of temperature data for the initial period" requires input of the number of temperature sequences to be considered during the initial period, the hour of the day when the concrete set up, the mid-depth temperature when the concrete set up, and the mid-depth and top/bottom temperature differentials at each of the temperature sequence periods. Note that the temperature sequence period is set at two-hour intervals.

The "sequence of post-tensioning applications during the initial period" includes input on the number of stages in which the total post-tensioning force will be applied, the partial amount of prestress to be applied per strand, and the time since setting (hours) when the partial post-tensioning will be applied.

The "temperature data for subsequent periods" requires the time (days) that has elapsed since the concrete set up and the 12 pairs of mid-depth and top/bottom temperature differentials (for the 24-hour cycle) of the period for which the output data are desired.

PSCP2 OUTPUT DATA

The PSCP2 output basically consists of (1) an echo print of the input data and (2) a listing of longitudinal movements, friction coefficients, prestress/friction restraint stresses, curling movement, and curling stresses. The output information is listed at periodic distances from mid-slab to the slab ends. A listing is developed for each of the two-hour increments requested by the user in the input data.

A sample run of PSCP2 showing both input and output information is included in Appendix A.

CHAPTER 8. CONCLUSIONS AND RECOMMENDATIONS

This chapter presents the conclusions developed from an analysis of the collected data. After a review of initial research efforts, the design and construction of the experimental sections, and the analyses developed in this project, recommendations are offered which may be helpful in future work with PCP.

CONCLUSIONS

(1) The instrumentation techniques used in this project worked well. The supports were stable and provided a reliable foundation for the equipment. The method of measuring displacements furnished excellent information. Both the dial gages and LVDT's gave consistent and identical results.The two hour time increment between measurements was sufficient to characterize movements but permitted time to gather a large amount of data. The thermocouples produced accurate and consistent temperatures and can be used in the future if necessary. The method of measuring joint widths also worked well. The dial calipers were easy to use and the data produced joint widths that closely corresponded to measured horizontal movements of the slabs.

(2) The regression analysis of horizontal slab movements with temperature show the displacements can be described by a linear equation. The equations for the horizontal displacements measured at the joints, the sixth points, and the third points vary, but at a linear rate, indicating almost the entire slab moves horizontally on a daily basis. Maximum and minimum joint widths were 1.40 and 0.26 inch for the 240-foot slabs and 3.20 and 0.98 inches for the 440-foot slabs. Vertical movements tend to have a faster rate when the slab surface is heating as compared to when the surface begins to cool. The vertical movement seems related to the temperature differential from the top and the bottom of the slab. Relationships between the vertical movement and the temperature differential produce a curvilinear or exponential fit. The analysis did not show a strong trend for different moisture conditions. This may have been because the slabs were not completely saturated.

(3) The new model for vertical displacements in program PSCP2 represents an improvement in the model, providing the functional relationship between the vertical displacements and temperature, friction, slab geometry, and road bed strength. Again, the temperature gradient is the prime driving force for curling. The results from the new model showed good accuracy for the prediction of vertical movements at the edge and the intermediate point movements. The model used for horizontal displacements in programs PSCP1 and PSCP2 showed a good level of accuracy in the prediction of edge and intermediate point movements. The use of PSCP2 should be helpful in optimization of design and the achievement of economical design values. The finite element model (PCPFEL2) provides a two-dimensional technique for modelling PCP that can perform a detailed analysis of displacements and stresses. Results of an analysis of stress concentrations around the stressing pockets indicate the longitudinal cracking is not due to thermal effects alone. Other causes of the cracks are likely to be related to fatigue effects of wheel loads.

(4) The PCP has performed well. Several design features developed from a literature search and from research were recommended and used in design. Conclusions from the observations of these features follow:

(a) Joint Width Setting - The joint opening was set at zero during the hot weather construction. This setting has worked very well. Use of the equations developed to predict the longitudinal movement should be helpful to designers using different weather conditions.

(b) One layer of Plastic Sheet as a Bond Breaker - The use of a single plastic sheet under the PCP as a bond breaker seems adequate. In this project a transverse row of vertical dowels was embedded in the old jointed concrete at the center of each slab to restrict movement of the slab at the center. The longitudinal movement seems to occur along the entire length of the slab, beginning at the center. Thus a combination of the single sheet and dowels has performed adequately.

(c) Interior Stressing Pockets - The plans and construction incorporated small, rectangular, full-depth leave-out pockets placed near the center of the span. The pockets were constructed transversely along the width of the lane and were centered over the strands. The longitudinal strands were anchored at each end of the slab and stressed in the leave-out pockets. After stressing, the pockets were filled with concrete. During construction, the pockets were serviceable and permitted adequate space for stressing.

As noted previously, the small longitudinal cracking seems to originate near the corners of the leave-out pockets. The finite element model (PCPFEL1) results indicate the

addition of steel near the corners of the pockets would be helpful in reducing the corner stress.

(d) Transverse Prestressing - The PCP paving was accomplished with a slipform paver in two passes and on different days. Since transverse prestressing was to be used, the first pass consisted of setting one line of "in-place" forms and placing the transverse steel strands through the forms. The tracks of the slipform paver straddled the in-place forms, and the exterior portion of the transverse strands were draped along the exterior edge of these forms. Then, before the concrete was placed in the second pass, the transverse strands were moved to the correct position and the small rectangular forms for the stressing pockets were installed. The transverse prestressing was constructed without problems and in a satisfactory manner. Even though some longitudinal cracking is evident, the crack width is very small and the transverse stressing has aided the overall performance.

(e) Partial Prestressing - After initial placement, when the concrete had gained sufficient strength, the steel strands of the PCP received a partial prestress force. Testing of the paving concrete was necessary to determine the timing and extent of the partial stress. This technique has functioned very well, as evidenced by the fact that only two transverse cracks were found during the condition survey of the one-mile length of test sections.

(f) Armor Joints - The reinforced channel tupe joints previously described have performed in an excellent manner. The joints appear to be structurally sound, provide a sufficient anchor for the steel strands, and have prevented accelerated distress in the concrete normally found near the joint. The neoprene boot which spans the joint opening does collect debris and has been punctured when the joint closes; however, the neoprene has prevented much of the debris from entering the joint and at present the boot and joint are in good condition.

(g) Roughness - Pavement roughness was not measured in this project because of the unavailability of the measuring equipment. However, roughness values were reported in Project 401 and these values were low (Serviceability Index = 3.1 to 3.2), indicating the PCP was rougher than that normally experienced in the PC pavement construction. It is believed the roughness has not changed significantly since construction because an estimated Serviceability Rating performed by the authors produced values similar to those reported in Project 401. It is probable that the unusual roughness was produced because of the experimental nature of the construction project. That is, attention was directed to the strands, joints, etc,. rather than to the finishing and straight edge operations, as in normal construction procedures. SDHPT officials believe that they and the contractor could achieve a much smoother roadway surface on the next job.

RECOMMENDATIONS

(1) The exact effect of moisture level on magnitudes of displacement was not quantified in this study. Future instrumentation programs that investigate environmental effects on pavement should consider the importance of measuring moisture level at different depths in the concrete.

(2) A large sampling of material specimens (cylinders, test beams, etc.) should be collected at the time of construction so that material properties for long-term investigations can be determined directly.

(3) Computer program PCPFEL1 analyzes thermal effects on PCP. The model serves as a basis for other in-depth analyses. Due to the inherent complexities of finite element analysis, the program developed in this study, PCPFEL1, should be used only by those who have received at least cursory training in the finite element technique.

(4) It is recommended that the equations developed to predict the longitudinal movement be considered in joint design. The closed joint opening for summertime construction worked well for the PCP slabs. However, a more conservative approach using a slightly larger opening (0.5 inch) may be considered. After considering the above and studying the movement predicted from the equations, the designer should select the opening depending on the season and the temperature during construction.

(5) If PCP construction similar to that used in the experimental sections is anticipated, one layer of plastic sheet is recommended as a bond breaker. Consideration may also be given to pinning the slab in the center to prevent movement at the slab center (that is, prevent the entire slab from moving or being shoved).

(6) The interior stressing pockets have performed reasonably well and are recommended for those desiring this type of prestress. With respect to the observed cracking around the central stressing pockets, reinforcement should be placed around the pockets for any future PCP that uses the central stressing technique. This reinforcement would provide additional tensile capacity at the pocket corners and should prevent the cracking. Attention should be given to the placement and filling of the stressing pockets in order to prevent excessive roughness.

(7) The transverse prestressing technique used in the experimental sections consisted of a system where the strands were looped through the two slabs which were placed at different times. The strain was applied through stressing pockets similar to those used with the longitudinal strands. The strain applied to the transverse strands tends to bind the slabs together internally as well as along the longitudinal construction joint. Some longitudinal cracking has occurred; however, the cracks are very tight and the PCP seems to be performing well. It is believed the transverse prestressing is needed and the technique used is recommended.

(8) Partial prestressing is recommended as is the procedure for applying the strain as soon as possible after the concrete has taken the initial set and has gained sufficient strength. Preliminary testing of the concrete is necessary to establish the stress to be applied and the approximate application time. However, tests should be performed at periodic times after placement using samples of concrete obtained during placement to establish the actual time of stressing.

(9) It is recommended that armor joints similar to those used in the experimental sections be considered for use with PCP. Much debris is prevented from entering the joint, and once a foreign object is in the joint the point force is dissipated transversely along the joint. The joints are relatively costly but the reduced number of joints in PCP construction tends to make the armor joints cost effective.

REFERENCES

1. Mandell, Elliott, Jose Tena-Colunga, and Kenneth Hankins, "Performance Tests on a Prestressed Concrete Pavement-Presentation of Data," Research Report 556-1, Center for Transportation Research, The University of Texas at Austin, January, 1989.
2. Mandell, Elliott, Ned H. Burns, and B. F. McCullough, "Prestressed Concrete Pavement: Instrumentation, In Situ Behavior, and Analysis," Research Report 556-2, Center for Transportation Research, The University of Texas at Austin, August, 1989.
3. Tena-Colunga, José, B. F. McCullough, and Ned H. Burns, "Calibration of a Model for Prestressed Concrete Pavement Overlays," Research Report 556-3, Center for Transportation Research, The University of Texas at Austin, August, 1989.
4. ACI Committee 325, "Recommended Practice for Design of Concrete Pavements Prestressed with Post-tensioned Steel Tendons," Proposed Report for Committee Consideration, October 30, 1979.
5. ACI Committee 325, "Proposed Design for Experimental Prestressed Pavement Slab, and Restrained Temperature Movements in Long Slabs," ACI Journal, Proceedings, Vol 64, No. 4, April 1968.
6. Friberg, B. F., "Investigation of Prestressed Concrete for Pavements," HRB Bulletin 332, Highway Research Board, 1962.
7. Mendoza-Diaz, A., B. F. McCullough, and Ned H. Burns, "Design of the Texas Prestressed Concrete Pavement Overlays in Cooke and McLennan Counties and Construction of the McLennan County Project," Research Report 556-1, Center for Transportation Research, The University of Texas at Austin, February 1986.
8. Netter, M., "The Prestressed Concrete Runway at Orly," Annales de l'Institut Technique du Batiment et deus Travaux Publics (Paris), No. 5, January 1948.
9. Melville, Philip L., "Review of French and British Procedures in the Design of Prestressed Pavements," HRB Bulletin 179, Highway Research Board, May 1958.
10. ACI Committee 325, Subcommittee VI, "Prestressed Pavement. A World View of Its Status," ACI Journal, Proceedings, Vol 30, No. 8, February 1959.
11. Friberg, B. F., and T. J. Pasko, "Prestressed Concrete Highway Pavement at Dulles International Airport. Research Program Report to 100 Days," FHWA-RD/DP/17-1, August 1973.
12. Brunner, R. J., "Prestressed Pavement Demonstration Project," TRB Record 535, Transportation Research Board, 1975.
13. Albritton, G., "Prestressed Concrete Pavement Near Brookhaven, Mississippi," Mississippi Department of Transportation, 1976.
14. Morris, G. R., and H. C. Emergy, "The Design and Construction of Arizona's Prestressed Concrete Pavement," Arizona Department of Transportation, October 1977.
15. "Prestressed Pavement Performance in Four States - A Panel Report," FHWA/RD-82/169, Final Report; September 1983.
16. "Prestressed Pavement, Vol. 2, Thickness Design," FHWA/RD-82/091, Final Report; June 1983.
17. O'Brien, J. S., N. H. Burns, and B. F. McCullough, "Very Early Post-tensioning of Prestressed Concrete Pavements," Research Report 401-1, Center for Transportation Research, The University of Texas at Austin, July 1985.
18. Cable, N. D., Ned H. Burns, and B. F. McCullough, "New Concepts in Prestressed Pavements," Research Report 401-2, Center for Transportation Research, The University of Texas at Austin.
19. Mendoza-Diaz, A., B. F. McCullough, and Ned H. Burns, "Behavior of Long Prestressed Pavement Slabs and Design Methodology" Research Report 401-3, Center for Transportation Research, The University of Texas at Austin, September 1986.
20. Maffei, J., Ned H. Burns, and B. Frank McCullough, "Instrumentation for Monitoring PCP Behavior," Research Report 401-4, Center for Transportation Research, The University of Texas at Austin, September 1986.
21. Chia, W.S., Ned H. Burns, and B. F. McCullough, "Field Evaluation of Subbase Friction Characteristics" Research Report 401-5, Center for Transportation Research, The University of Texas at Austin, September, 1986.

22. Dunn, B. W.,Ned H. Burns, and B. F. McCullough, "Friction Losses in Unbonded Post-Tensioning Tendons," Research Report 401-6, Center for Transportation Research, The University of Texas at Austin, November 1986.

23. B. F. McCullough, and Ned H. Burns, "Prestressed Concrete Pavement Design-Design and Construction of Overlay Applications" Research Report 401-8F, Center for Transportation Research, The University of Texas at Austin, November 1986.

24. Neville, A. M., Properties of Concrete, Pitman Publishing Limited, London, 1978.

25. Ramachandran, V. S., R. F. Feldman and J. J. Beaudoin, "Concrete Science," Hetdeb & Son Ltd.,1981.

27. Teller, L. W., and E. C., Sutherland, "The Structural Design of Concrete Pavements," Public Road Administration, Reprints from Public Roads; Part I, October 1935; Part II, November 1935; Part III, December 1935; Part IV, September/October 1936; Part V, April/May/June 1943.

28. Sargious, M., and S. K. Wang, "Economical Design of Prestressed Concrete Pavements," Journal of the Prestressed Concrete Institute, Vol 16, No. 4, July/August 1971.

29. Sargious, M., and S. K. Wang, "Design of Prestressed Concrete Airfield Pavements Under Dual and Dual-Tandem Wheel Loadings, Journal of the Prestressed Concrete Institute, Vol 16, No. 6, November/December 1971.

30. Barenberg, E. J., "Fundamentals of Prestressed Pavement Design," paper presented at the Annual Meeting of the ACI, Chicago, Ill., October 1985.

31. "Revised AASHTO Guide for Design of Pavement Structures," prepared for National Cooperative Highway Research Program and AASHTO Joint Task Force, ARE, Inc., 1986.

32. "Thickness Design for Concrete Highway and Street Pavements," Portland Cement Asssociation, Skokie, Illinois, 1984.

34. Kelley, E. F., "Application of the Results of Research to the Structural Design of Concrete Pavements," Public Roads, August 1939.

35. Friberg, B. F., "Frictional Resistance Under Concrete Pavements and Restraint Stresses in Long Reinforced Slabs," Proceedings, Highway Research Board, Vol 33, 1954.

36. Stott, J. P., "Tests on Materials for Use as Sliding Layers Under Concrete Road Slabs," Civil Engineering, 56, 1961.

37. Mandel, E.D., "Instrumentation for the PCP Overlay", Tech Memo 556-17, Center for Transportation Research, The University of Texas at Austin, February 1, 1989.

38. Mandel, E.D., "Data Acquisition System Set-Up", Tech Memo 556-18, Center for Transportation Research, The University of Texas at Austin, February 1, 1989.

39. Mandel, E.D., "Record of Field Work", Tech Memo 556-19, Center for Transportation Research, The University of Texas at Austin, February 1, 1989.

40. Concrete Manual, Seventh Edition, United States Department of the Interior, Bureau of Reclamation, Denver, Colorado, 1966.

41. "American Concrete Institute Standards," 1966.

42. Hansen, T. C., and A. H. Mattock, "Influence of Size and Shape of Member on the Shrinkage and Creep of Concrete," Journal of the American Concrete Institute, Proceedings, Vol 63, No. 2, February 1966.

43. Wittmann, F. and J. Lucas, "Mag. Concr. Res." Vol. 26, No.191,1974.

44. Gamble, B. R., "Creep: Problems and approaches involving the metastability of hardened cement paste," Proceedings of the Conference on Cement Production and Use, New Hampshire, pp. 163-171, 1979.

45. Neville, A. M., "Creep of Concrete: Plain, Reinforced and Prestessed," North-Holland, Amsterdam, 1970.

46. Feldman, R. F., "Cem. Concr. Res.",Vol.2, No. 521, 1972.

47. "Designing for Effects of Creep, Shrinkage and Temperature in Concrete Structures," ACI Special Publication Sp-27, ACI Journal, 1971.

48. Nilson, A. H., Design of Prestressed Concrete, John Wiley & Sons, 1978.

49. McCullough, B. F., A., Abou-Ayyash, W. R. Hudson, and J. P. Randall, "Design of Continuously Reinforced Concrete Pavements for Highways," NCHRP 1-15, Center for Transportation Research, The University of Texas at Austin, 1975.

50. Rivero-Vallejo, F., and B. F. McCullough, "Drying Shrinkage and Temperature Drop Stresses in Jointed Reinforced Concrete Pavements," Research Report 177-1, Center for Transportation Research, The University of Texas at Austin, August 1975.

52. Westergaard, H. M., "Analysis of Stresses in Concrete Roads Caused by Variations of Temperature, Public Roads, May 1927.

53. Castedo, Humberto, "Summary of Laboratory Test Results", Tech Memo 422-17, Center for Transportation Research, The University of Texas at Austin, February 1, 1989.

55. Zienkiewicz, O.C., "The Finite Element Method", 3rd Edition, McGraw-Hill, Ltd., Londin, 1977.

56. Lu, J. "Recommendations for a Model Based on Various Criteria", Tech Memo 422-40, Center for Transportation Research, The University of Texas at Austin, September 19, 1988.

57. Castedo, Humberto, "Summary of Laboratory Test Results-Phase I and II", Tech Memo 422-47, Center for Transportation Research, The University of Texas at Austin, January 16, 1989.

58. Hankins, Kenneth, "Visit to Waco to Obtain Prestressed Paving Information", Tech Memo 556-8, Center for Transportation Research, The University of Texas at Austin, September 19, 1988.

59. Klunker, F., "Prestressed Concrete Pavements," Dykerhoff and Wildman AG Co. Munich, Federal Republic of Germany,1988.

60. Concrete Construction, "Pavement Cost Comparisons," Concrete Construction , May 1986.

APPENDIX

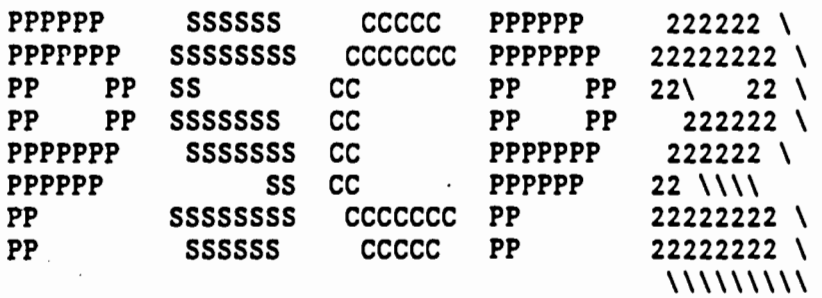

****

*

* ANALYSIS OF PRESTRESSED CONCRETE PAVEMENTS *

* CONSIDERING THE INELASTIC *

* NATURE OF THE SLAB-BASE FRICTION FORCES *

* (VERSION 2, APRIL 1989) *

*

* CENTER FOR TRANSPORTATION RESEARCH *

* THE UNIVERSITY OF TEXAS AT AUSTIN *

*

****

```
*--**--**--**--**--**--**--**--**--**--**--**--**--**--*

*--*ANALYSIS OF PRESTRESSED PVMT SLABS: REPORT 556-3*--*

*--*           ECHO-PRINT OF GENERAL DATA           *--*

*--**--**--**--**--**--**--**--**--**--**--**--**--**--*
```

****
* PROBLEM DEFINITION *
****

SLAB LENGTH (FT)	=	240.0
SLAB EFFECTIVE WIDTH(FT)	=	12.0
SLAB THICKNESS (IN)	=	6.0
NO.OF INCREMENTS	=	50
MAX. NO. OF ITERATIONS	=	100
REL. CLOSURE TOLERANCE	=	.5

****
* CONCRETE PROPERTIES *
****

THERMAL COEFFICIENT	=	.500E-05
TOTAL SHRINKAGE	=	.300E-03
UNIT WEIGHT (PCF)	=	150.0
POISSON RATIO	=	.15
CREEP COEFFICIENT	=	2.10
AGGREGATE TYPE	=	.00
YOUNG'S MODULUS PROVIDED	=	.00

0=NOT SPECIFIED ;1=GRANITE ;2=DOLOMITE ;3=VEGA ;4=BDG/TT;
5=W-T ;6=FERRIS;7=LIMESTONE;8=SILICEOUS RIVER GRAVEL

****
* COMPRESSIVE *
* STRENGTH DATA *
****

THE FOLLOWING STRENGTH RELATIONSHIP WAS DEVELOPED BASED ON THE RECOMMENDATION GIVEN BY THE U.S. BUREAU OF RECLAMATION AND THE 28TH DAY COMPRES. STRENGTH PROVIDED BY USER

AGE (DAYS)	COMPRESSIVE STRENGTH
.0	.0
1.0	450.0
3.0	1140.0
5.0	1590.0
7.0	1890.0
14.0	2460.0
21.0	2820.0
28.0	3000.0

****
* SLAB-BASE FRICTION PROPERTIES *
* Z-U RELATIONSHIP *
****

TYPE OF FRICTION CURVE IS A MULTILINEAR CURVE

Z(I)	U(I)
.000	.000
.001	.250
.002	.400
.003	.500
.004	.625
.007	.740
.020	.960

****
* STIFFNESS OF SLAB SUPPORT *
****

K-VALUE OF SUPPORT(PCI) = 500.00

****
* STEEL PROPERTIES *
****

PERCENT REINFORCEMENT	=	.113
STRAND SPACING (IN)	=	32.00
NOMINAL AREA (SQ.IN)	=	.216
YIELD STRENGTH (KSI)	=	270.00
ELASTIC MODULUS (PSI)	=	.300E+08
THERMAL COEFFICIENT	=	.700E-05

*--**--**--**--**--**--**--**--**--**--**--**--**--**--*

*--*ANALYSIS OF PRESTRESSED PVMT SLABS: REPORT 556-3*--*

*--*PREDICTION PAVEMENT STRESSES FOR INITIAL PERIOD*--*

*--**--**--**--**--**--**--**--**--**--**--**--**--**--*

SETTING TEMP. (DEG.F) = 90.00

HOUR OF DAY	TEMP. AT MID-DEPTH (DEG.F)	TEMP. DIFF. (DEG.F)	PRESTRESS PER STRAND (KSI)
4 P.M.	95.0	12.5	.0
6 P.M.	87.0	-.5	.0
8 P.M.	78.0	-6.4	.0
10 P.M.	70.0	-6.4	.0
12 MIDNIGHT	65.0	-5.8	46.4
2 A.M.	62.0	-5.1	46.4
4 A.M.	60.0	-5.3	46.4
6 A.M.	57.0	-5.1	46.4
8 A.M.	57.0	-2.5	46.4
10 A.M.	65.0	1.8	46.4
12 NOON	80.0	17.4	46.4
2 P.M.	90.0	20.4	215.0
4 P.M.	95.0	12.5	215.0
6 P.M.	87.0	-.5	215.0
8 P.M.	78.0	-6.4	215.0
10 P.M.	70.0	-6.4	215.0
12 MIDNIGHT	65.0	-5.8	215.0
2 A.M.	62.0	-5.1	215.0

HOUR = 4 P.M.

DISTANCE FROM MID SLAB(ft)	MOVEMENT (in)	COEFF OF FRICTION (psi)	PRST+FRICT STRESS (psi)	CURLING DEFLECTION (in)	BOT.CURL STRESS (psi)
.00	.00000	.00000	-69.56	.00000	.00
4.80	.00023	-.02864	-69.42	-.00047	.00
9.60	.00046	-.08661	-68.99	-.00077	.00
14.40	.00071	-.14663	-68.25	-.00105	.00
19.20	.00097	-.21005	-67.20	-.00128	.00
24.00	.00125	-.26548	-65.88	-.00149	.00
28.80	.00156	-.31136	-64.32	-.00166	.00
33.60	.00189	-.35994	-62.52	-.00181	.00
38.40	.00227	-.40638	-60.49	-.00194	.00
43.20	.00267	-.44782	-58.25	-.00205	.00
48.00	.00312	-.49218	-55.79	-.00214	.00
52.80	.00361	-.54670	-53.05	-.00222	.00
57.60	.00415	-.60405	-50.03	-.00229	.00
62.40	.00474	-.64202	-46.82	-.00236	.00
67.20	.00538	-.66532	-43.50	-.00243	.00
72.00	.00608	-.69057	-40.04	-.00250	.00
76.80	.00683	-.71784	-36.45	-.00258	.00
81.60	.00764	-.74096	-32.75	-.00267	.00
86.40	.00850	-.75717	-28.96	-.00278	.00
91.20	.00943	-.77221	-25.10	-.00290	.00
96.00	.01043	-.78839	-21.16	-.00305	.00
100.80	.01149	-.80580	-17.13	-.00322	.00
105.60	.01263	-.82457	-13.01	-.00342	.00
110.40	.01385	-.84483	-8.79	-.00365	.00
115.20	.01517	-.86669	-4.45	-.00392	.00
120.00	.01658	-.89033	.00	-.00423	.00

HOUR = 6 P.M.

DISTANCE FROM MID SLAB(ft)	MOVEMENT (in)	COEFF OF FRICTION (psi)	PRST+FRICT STRESS (psi)	CURLING DEFLECTION (in)	BOT.CURL STRESS (psi)
.00	.00000	.00000	60.36	.00000	.00
4.80	.00017	.00723	60.32	.00328	.00
9.60	.00034	.02248	60.21	.00545	.00
14.40	.00051	.04015	60.01	.00738	.00
19.20	.00067	.06204	59.70	.00906	.00
24.00	.00083	.09003	59.25	.01050	.00
28.80	.00098	.12602	58.62	.01174	.00
33.60	.00111	.17192	57.76	.01279	.00
38.40	.00123	.22738	56.62	.01368	.00
43.20	.00132	.28097	55.22	.01444	.00
48.00	.00138	.33362	53.55	.01509	.00
52.80	.00141	.39172	51.59	.01567	.00
57.60	.00141	.44813	49.35	.01618	.00
62.40	.00136	.51184	46.79	.01667	.00
67.20	.00126	.58898	43.85	.01716	.00
72.00	.00111	.64564	40.62	.01766	.00
76.80	.00090	.67988	37.22	.01822	.00
81.60	.00063	.71850	33.63	.01886	.00
86.40	.00030	.74931	29.88	.01960	.00
91.20	-.00011	.77087	26.03	.02046	.00
96.00	-.00057	.79441	22.05	.02149	.00
100.80	-.00111	.82040	17.95	.02269	.00
105.60	-.00173	.84898	13.71	.02410	.00
110.40	-.00242	.88035	9.31	.02574	.00
115.20	-.00319	.91470	4.73	.02764	.00
120.00	-.00405	.94633	.00	.02983	.00

HOUR = 8 P.M.

DISTANCE FROM MID SLAB(ft)	MOVEMENT (in)	COEFF OF FRICTION (psi)	PRST+FRICT STRESS (psi)	CURLING DEFLECTION (in)	BOT.CURL STRESS (psi)
.00	.00000	.00000	108.01	.00000	.00
4.80	-.00161	.18784	107.07	.00667	.00
9.60	-.00325	.48221	104.66	.01107	.00
14.40	-.00493	.63831	101.47	.01500	.00
19.20	-.00668	.71940	97.87	.01842	.00
24.00	-.00849	.76861	94.03	.02136	.00
28.80	-.01036	.80477	90.00	.02387	.00
33.60	-.01231	.84256	85.79	.02601	.00
38.40	-.01433	.88212	81.38	.02782	.00
43.20	-.01643	.92358	76.76	.02937	.00
48.00	-.01861	.95240	72.00	.03069	.00
52.80	-.02088	.96000	67.20	.03186	.00
57.60	-.02323	.96000	62.40	.03291	.00
62.40	-.02567	.96000	57.60	.03390	.00
67.20	-.02821	.96000	52.80	.03489	.00
72.00	-.03084	.96000	48.00	.03592	.00
76.80	-.03357	.96000	43.20	.03706	.00
81.60	-.03640	.96000	38.40	.03835	.00
86.40	-.03934	.96000	33.60	.03985	.00
91.20	-.04238	.96000	28.80	.04161	.00
96.00	-.04554	.96000	24.00	.04369	.00
100.80	-.04880	.96000	19.20	.04614	.00
105.60	-.05218	.96000	14.40	.04900	.00
110.40	-.05567	.96000	9.60	.05235	.00
115.20	-.05927	.96000	4.80	.05622	.00
120.00	-.06299	.96000	.00	.06067	.00

HOUR = 10 P.M.

DISTANCE FROM MID SLAB(ft)	MOVEMENT (in)	COEFF OF FRICTION (psi)	PRST+FRICT STRESS (psi)	CURLING DEFLECTION (in)	BOT.CURL STRESS (psi)
.00	.00000	.00000	113.99	.00000	.00
4.80	-.00382	.31346	112.43	.00896	.00
9.60	-.00769	.69317	108.96	.01486	.00
14.40	-.01161	.79475	104.99	.02013	.00
19.20	-.01561	.86611	100.66	.02472	.00
24.00	-.01969	.93108	96.00	.02866	.00
28.80	-.02385	.96000	91.20	.03204	.00
33.60	-.02809	.96000	86.40	.03491	.00
38.40	-.03242	.96000	81.60	.03734	.00
43.20	-.03683	.96000	76.80	.03941	.00
48.00	-.04132	.96000	72.00	.04119	.00
52.80	-.04591	.96000	67.20	.04275	.00
57.60	-.05059	.96000	62.40	.04416	.00
62.40	-.05536	.96000	57.60	.04549	.00
67.20	-.06024	.96000	52.80	.04682	.00
72.00	-.06522	.96000	48.00	.04821	.00
76.80	-.07031	.96000	43.20	.04973	.00
81.60	-.07552	.96000	38.40	.05147	.00
86.40	-.08085	.96000	33.60	.05348	.00
91.20	-.08631	.96000	28.80	.05585	.00
96.00	-.09189	.96000	24.00	.05864	.00
100.80	-.09761	.96000	19.20	.06192	.00
105.60	-.10346	.96000	14.40	.06577	.00
110.40	-.10945	.96000	9.60	.07025	.00
115.20	-.11556	.96000	4.80	.07544	.00
120.00	-.12179	.96000	.00	.08142	.00

HOUR = 12 MIDNIGHT

DISTANCE FROM MID SLAB(ft)	MOVEMENT (in)	COEFF OF FRICTION (psi)	PRST+FRICT STRESS (psi)	CURLING DEFLECTION (in)	BOT.CURL STRESS (psi)
.00	.00000	.00000	63.51	.00000	.00
4.80	-.00615	.35800	61.72	.01003	.00
9.60	-.01234	.77709	57.84	.01665	.00
14.40	-.01861	.89328	53.37	.02255	.00
19.20	-.02495	.95418	48.60	.02769	.00
24.00	-.03138	.96000	43.80	.03211	.00
28.80	-.03789	.96000	39.00	.03589	.00
33.60	-.04448	.96000	34.20	.03910	.00
38.40	-.05116	.96000	29.40	.04183	.00
43.20	-.05793	.96000	24.60	.04415	.00
48.00	-.06478	.96000	19.80	.04614	.00
52.80	-.07173	.96000	15.00	.04789	.00
57.60	-.07877	.96000	10.20	.04947	.00
62.40	-.08591	.96000	5.40	.05096	.00
67.20	-.09316	.96000	.60	.05245	.00
72.00	-.10053	.96000	-4.20	.05400	.00
76.80	-.10802	.96000	-9.00	.05571	.00
81.60	-.11563	.96000	-13.80	.05766	.00
86.40	-.12338	.96000	-18.60	.05991	.00
91.20	-.13126	.96000	-23.40	.06256	.00
96.00	-.13929	.96000	-28.20	.06569	.00
100.80	-.14746	.96000	-33.00	.06936	.00
105.60	-.15576	.96000	-37.80	.07367	.00
110.40	-.16421	.96000	-42.60	.07870	.00
115.20	-.17279	.96000	-47.40	.08451	.00
120.00	-.18149	.96000	-52.20	.09121	.00

HOUR = 2 A.M.

DISTANCE FROM MID SLAB(ft)	MOVEMENT (in)	COEFF OF FRICTION (psi)	PRST+FRICT STRESS (psi)	CURLING DEFLECTION (in)	BOT.CURL STRESS (psi)
.00	.00000	.00000	63.86	.00000	.00
4.80	-.00701	.37202	62.00	.01055	.00
9.60	-.01407	.80577	57.97	.01750	.00
14.40	-.02121	.91375	53.40	.02371	.00
19.20	-.02842	.96000	48.60	.02911	.00
24.00	-.03572	.96000	43.80	.03376	.00
28.80	-.04310	.96000	39.00	.03774	.00
33.60	-.05057	.96000	34.20	.04112	.00
38.40	-.05812	.96000	29.40	.04398	.00
43.20	-.06576	.96000	24.60	.04642	.00
48.00	-.07349	.96000	19.80	.04852	.00
52.80	-.08132	.96000	15.00	.05036	.00
57.60	-.08926	.96000	10.20	.05202	.00
62.40	-.09730	.96000	5.40	.05359	.00
67.20	-.10546	.96000	.60	.05515	.00
72.00	-.11374	.96000	-4.20	.05679	.00
76.80	-.12216	.96000	-9.00	.05858	.00
81.60	-.13071	.96000	-13.80	.06063	.00
86.40	-.13941	.96000	-18.60	.06300	.00
91.20	-.14826	.96000	-23.40	.06579	.00
96.00	-.15726	.96000	-28.20	.06907	.00
100.80	-.16641	.96000	-33.00	.07294	.00
105.60	-.17571	.96000	-37.80	.07747	.00
110.40	-.18514	.96000	-42.60	.08275	.00
115.20	-.19471	.96000	-47.40	.08887	.00
120.00	-.20441	.96000	-52.20	.09590	.00

HOUR = 4 A.M.

DISTANCE FROM MID SLAB(ft)	MOVEMENT (in)	COEFF OF FRICTION (psi)	PRST+FRICT STRESS (psi)	CURLING DEFLECTION (in)	BOT.CURL STRESS (psi)
.00	.00000	.00000	64.00	.00000	.00
4.80	-.00759	.37693	62.12	.01084	.00
9.60	-.01523	.82050	58.02	.01799	.00
14.40	-.02295	.92357	53.40	.02437	.00
19.20	-.03075	.96000	48.60	.02992	.00
24.00	-.03863	.96000	43.80	.03469	.00
28.80	-.04659	.96000	39.00	.03878	.00
33.60	-.05464	.96000	34.20	.04225	.00
38.40	-.06278	.96000	29.40	.04520	.00
43.20	-.07100	.96000	24.60	.04770	.00
48.00	-.07931	.96000	19.80	.04986	.00
52.80	-.08773	.96000	15.00	.05175	.00
57.60	-.09624	.96000	10.20	.05345	.00
62.40	-.10487	.96000	5.40	.05506	.00
67.20	-.11361	.96000	.60	.05667	.00
72.00	-.12247	.96000	-4.20	.05835	.00
76.80	-.13147	.96000	-9.00	.06020	.00
81.60	-.14061	.96000	-13.80	.06230	.00
86.40	-.14989	.96000	-18.60	.06474	.00
91.20	-.15932	.96000	-23.40	.06760	.00
96.00	-.16890	.96000	-28.20	.07097	.00
100.80	-.17864	.96000	-33.00	.07495	.00
105.60	-.18851	.96000	-37.80	.07960	.00
110.40	-.19853	.96000	-42.60	.08503	.00
115.20	-.20869	.96000	-47.40	.09132	.00
120.00	-.21897	.96000	-52.20	.09855	.00

HOUR = 6 A.M.

DISTANCE FROM MID SLAB(ft)	MOVEMENT (in)	COEFF OF FRICTION (psi)	PRST+FRICT STRESS (psi)	CURLING DEFLECTION (in)	BOT.CURL STRESS (psi)
.00	.00000	.00000	64.23	.00000	.00
4.80	-.00846	.38426	62.30	.01120	.00
9.60	-.01697	.84252	58.09	.01858	.00
14.40	-.02555	.93825	53.40	.02517	.00
19.20	-.03422	.96000	48.60	.03090	.00
24.00	-.04297	.96000	43.80	.03583	.00
28.80	-.05181	.96000	39.00	.04005	.00
33.60	-.06073	.96000	34.20	.04363	.00
38.40	-.06974	.96000	29.40	.04668	.00
43.20	-.07885	.96000	24.60	.04927	.00
48.00	-.08805	.96000	19.80	.05149	.00
52.80	-.09735	.96000	15.00	.05344	.00
57.60	-.10677	.96000	10.20	.05520	.00
62.40	-.11631	.96000	5.40	.05687	.00
67.20	-.12597	.96000	.60	.05853	.00
72.00	-.13577	.96000	-4.20	.06026	.00
76.80	-.14572	.96000	-9.00	.06217	.00
81.60	-.15582	.96000	-13.80	.06434	.00
86.40	-.16608	.96000	-18.60	.06686	.00
91.20	-.17650	.96000	-23.40	.06981	.00
96.00	-.18707	.96000	-28.20	.07330	.00
100.80	-.19780	.96000	-33.00	.07740	.00
105.60	-.20868	.96000	-37.80	.08221	.00
110.40	-.21969	.96000	-42.60	.08782	.00
115.20	-.23084	.96000	-47.40	.09431	.00
120.00	-.24211	.96000	-52.20	.10178	.00

HOUR = 8 A.M.

DISTANCE FROM MID SLAB(ft)	MOVEMENT (in)	COEFF OF FRICTION (psi)	PRST+FRICT STRESS (psi)	CURLING DEFLECTION (in)	BOT.CURL STRESS (psi)
.00	.00000	.00000	64.23	.00000	.00
4.80	-.00846	.38432	62.31	.01120	.00
9.60	-.01698	.84268	58.09	.01858	.00
14.40	-.02557	.93836	53.40	.02517	.00
19.20	-.03425	.96000	48.60	.03090	.00
24.00	-.04301	.96000	43.80	.03583	.00
28.80	-.05185	.96000	39.00	.04005	.00
33.60	-.06078	.96000	34.20	.04363	.00
38.40	-.06979	.96000	29.40	.04668	.00
43.20	-.07890	.96000	24.60	.04927	.00
48.00	-.08811	.96000	19.80	.05149	.00
52.80	-.09742	.96000	15.00	.05344	.00
57.60	-.10684	.96000	10.20	.05520	.00
62.40	-.11639	.96000	5.40	.05687	.00
67.20	-.12606	.96000	.60	.05853	.00
72.00	-.13587	.96000	-4.20	.06026	.00
76.80	-.14583	.96000	-9.00	.06217	.00
81.60	-.15593	.96000	-13.80	.06434	.00
86.40	-.16620	.96000	-18.60	.06686	.00
91.20	-.17662	.96000	-23.40	.06981	.00
96.00	-.18720	.96000	-28.20	.07330	.00
100.80	-.19793	.96000	-33.00	.07740	.00
105.60	-.20882	.96000	-37.80	.08221	.00
110.40	-.21984	.96000	-42.60	.08782	.00
115.20	-.23099	.96000	-47.40	.09431	.00
120.00	-.24227	.96000	-52.20	.10178	.00

HOUR = 10 A.M.

DISTANCE FROM MID SLAB(ft)	MOVEMENT (in)	COEFF OF FRICTION (psi)	PRST+FRICT STRESS (psi)	CURLING DEFLECTION (in)	BOT.CURL STRESS (psi)
.00	.00000	.00000	-86.33	.00000	.00
4.80	-.00876	.03824	-86.52	.01003	.00
9.60	-.01754	.10911	-87.07	.01665	.00
14.40	-.02632	.16625	-87.90	.02255	.00
19.20	-.03513	.20682	-88.94	.02769	.00
24.00	-.04395	.23051	-90.09	.03211	.00
28.80	-.05279	.23727	-91.27	.03589	.00
33.60	-.06165	.22691	-92.41	.03910	.00
38.40	-.07053	.19901	-93.40	.04183	.00
43.20	-.07942	.15300	-94.17	.04415	.00
48.00	-.08834	.08811	-94.61	.04614	.00
52.80	-.09728	.00344	-94.63	.04789	.00
57.60	-.10624	-.10219	-94.12	.04947	.00
62.40	-.11522	-.22018	-93.02	.05096	.00
67.20	-.12423	-.32921	-91.37	.05245	.00
72.00	-.13327	-.42009	-89.27	.05400	.00
76.80	-.14234	-.51138	-86.71	.05571	.00
81.60	-.15144	-.60218	-83.70	.05766	.00
86.40	-.16057	-.66471	-80.38	.05991	.00
91.20	-.16972	-.71011	-76.83	.06256	.00
96.00	-.17889	-.74758	-73.09	.06569	.00
100.80	-.18807	-.77419	-69.22	.06936	.00
105.60	-.19724	-.80188	-65.21	.07367	.00
110.40	-.20639	-.83246	-61.05	.07870	.00
115.20	-.21549	-.86613	-56.72	.08451	.00
120.00	-.22452	-.90308	-52.20	.09121	.00

HOUR = 12 NOON

DISTANCE FROM MID SLAB(ft)	MOVEMENT (in)	COEFF OF FRICTION (psi)	PRST+FRICT STRESS (psi)	CURLING DEFLECTION (in)	BOT.CURL STRESS (psi)
.00	.00000	.00000	-163.61	.00000	.00
4.80	-.00578	-.23430	-162.44	.00600	.00
9.60	-.01152	-.57478	-159.57	.00995	.00
14.40	-.01721	-.72206	-155.96	.01348	.00
19.20	-.02282	-.78900	-152.01	.01655	.00
24.00	-.02837	-.84201	-147.80	.01919	.00
28.80	-.03385	-.89767	-143.32	.02144	.00
33.60	-.03925	-.94309	-138.60	.02337	.00
38.40	-.04456	-.96000	-133.80	.02500	.00
43.20	-.04981	-.96000	-129.00	.02638	.00
48.00	-.05498	-.96000	-124.20	.02757	.00
52.80	-.06009	-.96000	-119.40	.02862	.00
57.60	-.06514	-.96000	-114.60	.02956	.00
62.40	-.07014	-.96000	-109.80	.03045	.00
67.20	-.07510	-.96000	-105.00	.03134	.00
72.00	-.08001	-.96000	-100.20	.03227	.00
76.80	-.08489	-.96000	-95.40	.03329	.00
81.60	-.08974	-.96000	-90.60	.03445	.00
86.40	-.09455	-.96000	-85.80	.03580	.00
91.20	-.09932	-.96000	-81.00	.03738	.00
96.00	-.10406	-.96000	-76.20	.03925	.00
100.80	-.10874	-.96000	-71.40	.04145	.00
105.60	-.11335	-.96000	-66.60	.04402	.00
110.40	-.11789	-.96000	-61.80	.04702	.00
115.20	-.12235	-.96000	-57.00	.05050	.00
120.00	-.12669	-.96000	-52.20	.05450	.00

HOUR = 2 P.M.

DISTANCE FROM MID SLAB(ft)	MOVEMENT (in)	COEFF OF FRICTION (psi)	PRST+FRICT STRESS (psi)	CURLING DEFLECTION (in)	BOT.CURL STRESS (psi)
.00	.00000	.00000	-329.29	.00000	.00
4.80	-.00578	-.23428	-328.12	.00196	.00
9.60	-.01152	-.57476	-325.24	.00325	.00
14.40	-.01721	-.72204	-321.63	.00440	.00
19.20	-.02283	-.78899	-317.69	.00540	.00
24.00	-.02837	-.84200	-313.48	.00626	.00
28.80	-.03385	-.89767	-308.99	.00700	.00
33.60	-.03924	-.94309	-304.28	.00763	.00
38.40	-.04456	-.96000	-299.48	.00816	.00
43.20	-.04980	-.96000	-294.68	.00861	.00
48.00	-.05496	-.96000	-289.88	.00900	.00
52.80	-.06006	-.96000	-285.08	.00934	.00
57.60	-.06508	-.96000	-280.28	.00965	.00
62.40	-.07004	-.96000	-275.48	.00994	.00
67.20	-.07495	-.96000	-270.68	.01023	.00
72.00	-.07980	-.96000	-265.88	.01054	.00
76.80	-.08459	-.96000	-261.08	.01087	.00
81.60	-.08933	-.96000	-256.28	.01125	.00
86.40	-.09403	-.96000	-251.48	.01169	.00
91.20	-.09866	-.96000	-246.68	.01221	.00
96.00	-.10324	-.96000	-241.88	.01281	.00
100.80	-.10875	.00133	-240.10	.01353	.00
105.60	-.11346	.01448	-240.17	.01437	.00
110.40	-.11818	.04897	-240.42	.01535	.00
115.20	-.12290	.10571	-240.94	.01649	.00
120.00	-.12762	.18609	-241.88	.01779	.00

HOUR = 4 P.M.

DISTANCE FROM MID SLAB(ft)	MOVEMENT (in)	COEFF OF FRICTION (psi)	PRST+FRICT STRESS (psi)	CURLING DEFLECTION (in)	BOT.CURL STRESS (psi)
.00	.00000	.00000	-331.94	.00000	.00
4.80	-.00439	-.31397	-330.37	-.00047	.00
9.60	-.00873	-.69455	-326.90	-.00077	.00
14.40	-.01301	-.79768	-322.91	-.00105	.00
19.20	-.01721	-.87203	-318.55	-.00128	.00
24.00	-.02134	-.93493	-313.88	-.00149	.00
28.80	-.02538	-.96000	-309.08	-.00166	.00
33.60	-.02934	-.96000	-304.28	-.00181	.00
38.40	-.03322	-.96000	-299.48	-.00194	.00
43.20	-.03701	-.96000	-294.68	-.00205	.00
48.00	-.04073	-.96000	-289.88	-.00214	.00
52.80	-.04437	-.96000	-285.08	-.00222	.00
57.60	-.04794	-.96000	-280.28	-.00229	.00
62.40	-.05143	-.96000	-275.48	-.00236	.00
67.20	-.05486	-.96000	-270.68	-.00243	.00
72.00	-.05822	-.96000	-265.88	-.00250	.00
76.80	-.06151	-.96000	-261.08	-.00258	.00
81.60	-.06475	-.96000	-256.28	-.00267	.00
86.40	-.06792	-.96000	-251.48	-.00278	.00
91.20	-.07103	-.96000	-246.68	-.00290	.00
96.00	-.07409	-.96000	-241.88	-.00305	.00
100.80	-.05402	-.96000	-261.08	-.00322	.00
105.60	-.05758	-.96000	-256.28	-.00342	.00
110.40	-.06103	-.96000	-251.48	-.00365	.00
115.20	-.06437	-.96000	-246.68	-.00392	.00
120.00	-.06759	-.96000	-241.88	-.00423	.00

HOUR = 6 P.M.

DISTANCE FROM MID SLAB(ft)	MOVEMENT (in)	COEFF OF FRICTION (psi)	PRST+FRICT STRESS (psi)	CURLING DEFLECTION (in)	BOT.CURL STRESS (psi)
.00	.00000	.00000	-187.92	.00000	.00
4.80	-.00560	-.02203	-187.81	.00328	.00
9.60	-.01121	-.06110	-187.51	.00545	.00
14.40	-.01682	-.08788	-187.07	.00738	.00
19.20	-.02242	-.09925	-186.57	.00906	.00
24.00	-.02803	-.09360	-186.10	.01050	.00
28.80	-.03364	-.06945	-185.76	.01174	.00
33.60	-.03925	-.02559	-185.63	.01279	.00
38.40	-.04486	.03908	-185.82	.01368	.00
43.20	-.05049	.12587	-186.45	.01444	.00
48.00	-.05614	.22682	-187.59	.01509	.00
52.80	-.06183	.32339	-189.20	.01567	.00
57.60	-.06757	.40879	-191.25	.01618	.00
62.40	-.07336	.49467	-193.72	.01667	.00
67.20	-.07922	.58752	-196.66	.01716	.00
72.00	-.08516	.65583	-199.94	.01766	.00
76.80	-.09117	.69969	-203.44	.01822	.00
81.60	-.09728	.73913	-207.13	.01886	.00
86.40	-.10348	.76805	-210.97	.01960	.00
91.20	-.10977	.79476	-214.95	.02046	.00
96.00	-.11617	.82416	-219.07	.02149	.00
100.80	-.12344	.85466	-223.34	.02269	.00
105.60	-.12989	.88465	-227.76	.02410	.00
110.40	-.13653	.91609	-232.34	.02574	.00
115.20	-.14336	.94631	-237.08	.02764	.00
120.00	-.15038	.96000	-241.88	.02983	.00

HOUR = 8 P.M.

DISTANCE FROM MID SLAB(ft)	MOVEMENT (in)	COEFF OF FRICTION (psi)	PRST+FRICT STRESS (psi)	CURLING DEFLECTION (in)	BOT.CURL STRESS (psi)
.00	.00000	.00000	-135.28	.00000	.00
4.80	-.00730	.16384	-136.09	.00667	.00
9.60	-.01463	.42040	-138.20	.01107	.00
14.40	-.02201	.58439	-141.12	.01500	.00
19.20	-.02945	.69061	-144.57	.01842	.00
24.00	-.03696	.74620	-148.30	.02136	.00
28.80	-.04455	.78472	-152.23	.02387	.00
33.60	-.05221	.82176	-156.34	.02601	.00
38.40	-.05995	.86141	-160.64	.02782	.00
43.20	-.06777	.90374	-165.16	.02937	.00
48.00	-.07567	.94279	-169.88	.03069	.00
52.80	-.08368	.96000	-174.68	.03186	.00
57.60	-.09178	.96000	-179.48	.03291	.00
62.40	-.09999	.96000	-184.28	.03390	.00
67.20	-.10832	.96000	-189.08	.03489	.00
72.00	-.11676	.96000	-193.88	.03592	.00
76.80	-.12532	.96000	-198.68	.03706	.00
81.60	-.13401	.96000	-203.48	.03835	.00
86.40	-.14283	.96000	-208.28	.03985	.00
91.20	-.15178	.96000	-213.08	.04161	.00
96.00	-.16086	.96000	-217.88	.04369	.00
100.80	-.17086	.96000	-222.68	.04614	.00
105.60	-.18006	.96000	-227.48	.04900	.00
110.40	-.18947	.96000	-232.28	.05235	.00
115.20	-.19910	.96000	-237.08	.05622	.00
120.00	-.20893	.96000	-241.88	.06067	.00

HOUR = 10 P.M.

DISTANCE FROM MID SLAB(ft)	MOVEMENT (in)	COEFF OF FRICTION (psi)	PRST+FRICT STRESS (psi)	CURLING DEFLECTION (in)	BOT.CURL STRESS (psi)
.00	.00000	.00000	-128.31	.00000	.00
4.80	-.00949	.29457	-129.79	.00896	.00
9.60	-.01903	.66890	-133.13	.01486	.00
14.40	-.02864	.78188	-137.04	.02013	.00
19.20	-.03833	.84954	-141.29	.02472	.00
24.00	-.04811	.91972	-145.89	.02866	.00
28.80	-.05797	.95773	-150.68	.03204	.00
33.60	-.06792	.96000	-155.48	.03491	.00
38.40	-.07796	.96000	-160.28	.03734	.00
43.20	-.08809	.96000	-165.08	.03941	.00
48.00	-.09831	.96000	-169.88	.04119	.00
52.80	-.10863	.96000	-174.68	.04275	.00
57.60	-.11906	.96000	-179.48	.04416	.00
62.40	-.12960	.96000	-184.28	.04549	.00
67.20	-.14026	.96000	-189.08	.04682	.00
72.00	-.15105	.96000	-193.88	.04821	.00
76.80	-.16198	.96000	-198.68	.04973	.00
81.60	-.17305	.96000	-203.48	.05147	.00
86.40	-.18426	.96000	-208.28	.05348	.00
91.20	-.19563	.96000	-213.08	.05585	.00
96.00	-.20715	.96000	-217.88	.05864	.00
100.80	-.21960	.96000	-222.68	.06192	.00
105.60	-.23128	.96000	-227.48	.06577	.00
110.40	-.24318	.96000	-232.28	.07025	.00
115.20	-.25532	.96000	-237.08	.07544	.00
120.00	-.26768	.96000	-241.88	.08142	.00

HOUR = 12 MIDNIGHT

DISTANCE FROM MID SLAB(ft)	MOVEMENT (in)	COEFF OF FRICTION (psi)	PRST+FRICT STRESS (psi)	CURLING DEFLECTION (in)	BOT.CURL STRESS (psi)
.00	.00000	.00000	-126.91	.00000	.00
4.80	-.01091	.33429	-128.58	.01003	.00
9.60	-.02188	.73275	-132.24	.01665	.00
14.40	-.03293	.84228	-136.46	.02255	.00
19.20	-.04406	.92381	-141.08	.02769	.00
24.00	-.05528	.96000	-145.88	.03211	.00
28.80	-.06659	.96000	-150.68	.03589	.00
33.60	-.07798	.96000	-155.48	.03910	.00
38.40	-.08947	.96000	-160.28	.04183	.00
43.20	-.10105	.96000	-165.08	.04415	.00
48.00	-.11272	.96000	-169.88	.04614	.00
52.80	-.12450	.96000	-174.68	.04789	.00
57.60	-.13639	.96000	-179.48	.04947	.00
62.40	-.14839	.96000	-184.28	.05096	.00
67.20	-.16053	.96000	-189.08	.05245	.00
72.00	-.17279	.96000	-193.88	.05400	.00
76.80	-.18521	.96000	-198.68	.05571	.00
81.60	-.19777	.96000	-203.48	.05766	.00
86.40	-.21050	.96000	-208.28	.05991	.00
91.20	-.22339	.96000	-213.08	.06256	.00
96.00	-.23644	.96000	-217.88	.06569	.00
100.80	-.25043	.96000	-222.68	.06936	.00
105.60	-.26366	.96000	-227.48	.07367	.00
110.40	-.27712	.96000	-232.28	.07870	.00
115.20	-.29082	.96000	-237.08	.08451	.00
120.00	-.30474	.96000	-241.88	.09121	.00

HOUR = 2 A.M.

DISTANCE FROM MID SLAB(ft)	MOVEMENT (in)	COEFF OF FRICTION (psi)	PRST+FRICT STRESS (psi)	CURLING DEFLECTION (in)	BOT.CURL STRESS (psi)
.00	.00000	.00000	-126.38	.00000	.00
4.80	-.01178	.35081	-128.13	.01055	.00
9.60	-.02361	.76387	-131.95	.01750	.00
14.40	-.03552	.87881	-136.35	.02371	.00
19.20	-.04752	.94575	-141.08	.02911	.00
24.00	-.05961	.96000	-145.88	.03376	.00
28.80	-.07179	.96000	-150.68	.03774	.00
33.60	-.08406	.96000	-155.48	.04112	.00
38.40	-.09641	.96000	-160.28	.04398	.00
43.20	-.10886	.96000	-165.08	.04642	.00
48.00	-.12141	.96000	-169.88	.04852	.00
52.80	-.13405	.96000	-174.68	.05036	.00
57.60	-.14681	.96000	-179.48	.05202	.00
62.40	-.15969	.96000	-184.28	.05359	.00
67.20	-.17269	.96000	-189.08	.05515	.00
72.00	-.18583	.96000	-193.88	.05679	.00
76.80	-.19911	.96000	-198.68	.05858	.00
81.60	-.21255	.96000	-203.48	.06063	.00
86.40	-.22615	.96000	-208.28	.06300	.00
91.20	-.23991	.96000	-213.08	.06579	.00
96.00	-.25383	.96000	-217.88	.06907	.00
100.80	-.26870	.96000	-222.68	.07294	.00
105.60	-.28279	.96000	-227.48	.07747	.00
110.40	-.29713	.96000	-232.28	.08275	.00
115.20	-.31170	.96000	-237.08	.08887	.00
120.00	-.32649	.96000	-241.88	.09590	.00